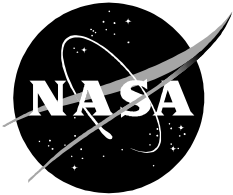# Second International Conference on Near-Field Optical Analysis: Photodynamic Therapy & Photobiology Effects

Proceedings of the Second International Conference on NOA

Houston, Texas, USA

May 31 – June 1, 2001

October 2002

The NASA STI Program Office . . . in Profile

Since its founding, NASA has been dedicated to the advancement of aeronautics and space science. The NASA Scientific and Technical Information (STI) Program Office plays a key part in helping NASA maintain this important role.

The NASA STI Program Office is operated by Langley Research Center, the lead center for NASA's scientific and technical information. The NASA STI Program Office provides access to the NASA STI Database, the largest collection of aeronautical and space science STI in the world. The Program Office is also NASA's institutional mechanism for disseminating the results of its research and development activities. These results are published by NASA in the NASA STI Report Series, which includes the following report types:

- TECHNICAL PUBLICATION. Reports of completed research or a major significant phase of research that present the results of NASA programs and include extensive data or theoretical analysis. Includes compilations of significant scientific and technical data and information deemed to be of continuing reference value. NASA's counterpart of peer-reviewed formal professional papers but has less stringent limitations on manuscript length and extent of graphic presentations.

- TECHNICAL MEMORANDUM. Scientific and technical findings that are preliminary or of specialized interest, e.g., quick release reports, working papers, and bibliographies that contain minimal annotation. Does not contain extensive analysis.

- CONTRACTOR REPORT. Scientific and technical findings by NASA-sponsored contractors and grantees.

- CONFERENCE PUBLICATION. Collected papers from scientific and technical conferences, symposia, seminars, or other meetings sponsored or cosponsored by NASA.

- SPECIAL PUBLICATION. Scientific, technical, or historical information from NASA programs, projects, and mission, often concerned with subjects having substantial public interest.

- TECHNICAL TRANSLATION. English-language translations of foreign scientific and technical material pertinent to NASA's mission.

Specialized services that complement the STI Program Office's diverse offerings include creating custom thesauri, building customized databases, organizing and publishing research results . . . even providing videos.

For more information about the NASA STI Program Office, see the following:

- Access the NASA STI Program Home Page at *http://www.sti.nasa.gov*

- E-mail your question via the Internet to help@sti.nasa.gov

- Fax your question to the NASA Access Help Desk at (301) 621-0134

- Telephone the NASA Access Help Desk at (301) 621-0390

- Write to:
  NASA Access Help Desk
  NASA Center for AeroSpace Information
  7121 Standard
  Hanover, MD 21076-1320
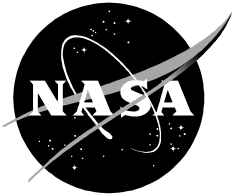
Second International Conference on Near-Field Optical Analysis: Photodynamic Therapy & Photobiology Effects

Proceedings of the Second International Conference on NOA

Houston, Texas, USA

May 31 – June 1, 2001

October 2002

Second International Conference on Near-Field Optical Analysis: Photodynamic Therapy & Photobiology Effects

Chairmen

Dennis R. Morrison, Ph.D.
Senior Biotech Project Scientist
Biological Systems Office
NASA Johnson Space Center

Kurt Henry, Ph.D.
Program Manager
Biological Warfare Defense
Advanced Consequence Mgmt
DARPA Defense Sciences Office

Harry T. Whelan, M.D.
Professor of Neurology
Medical College of Wisconsin
Diving Medical Officer
Naval Special Warfare Group-2

Andrei P. Sommer, Ph.D.
ENSOMA Laboratory
University of Ulm
Germany

Edited by   Debra L. Bulgher, M.S., NASA Johnson Space Center

Available from:

NASA Center for AeroSpace Information
7121 Standard
Hanover, MD 21076-1320

National Technical Information Service
5285 Port Royal Road
Springfield, VA 22161

This report is also available in electronic form at http://techreports.larc.nasa.gov/cgi-bin/NTRS

PREFACE

The Second International Conference on Near-Field Optical Analysis: Photodynamic Therapy & Photobiology Effects (2nd NOA), held May 31 to June 1, 2001, at the Center for Advanced Space Studies (CASS) in Houston, Texas, demonstrated where low-level laser therapy (LLLT), respectively low-intensity light-activated biostimulation (LILAB) and nanotechnological applications employing photobiomodulation techniques, will presumably go in the next ten years. The conference was a continuation of the First International Conference on Near-Field Optical Analysis (1st NOA) organized by Andrei Sommer (ENSOMA Lab, University of Ulm, Germany) and held in November 2000 at Castle Reisensburg, Germany. Starting with a group of ten scientists from eight different countries – Brazil, Denmark, Germany, Finland, Hungary, Israel, Saudi Arabia and the United States – the 1st NOA conference was cosponsored by the American Chemical Society (Attila Pavláth, president) for "its objective of evaluating the molecular mechanism of accelerated and normal wound healing processes."

The 2nd NOA conference, cosponsored by the Defense Advanced Research Projects Agency (DARPA), NASA Johnson Space Center (JSC), and the Medical College of Wisconsin, was organized by Harry Whelan (Medical College of Wisconsin), Andrei Sommer (University of Ulm), Kurt Henry (DARPA), and Dennis Morrison (NASA-JSC).

Despite the unusually short time between the events, the 2nd NOA conference was regarded as a very successful meeting, with 40 international LLLT/LILAB and photobiology experts from universities, research institutes, agencies, and the industry attending.

The multidisciplinary group of researchers focused on LLLT/LILAB applications under extreme conditions expected to have beneficial effects, particularly in space (microgravity), on submarines (no solar irradiation, modified atmospheric conditions), and under severe battlefield conditions on Earth (hostile and low hygienic environment: wounds; burns; and chemical, biological, and radioactive hazards). Following the spirit of the 1st NOA conference, novel technologies were highlighted, investigating the interaction of light with biological systems, molecular mechanisms of wound healing, bone regeneration, nerve regeneration, pain modulation, as well as biomineralization and biofilm formation processes induced by nanobacteria.

The scientific presentations and discussions emphasised results of clinical and in vitro biology studies demonstrating the dramatic therapeutic effects of LLLT and LILAB. Near-infrared in wavelengths between 630-1100 nm has been used successfully to: 1) increase the rate of repair of open epidermal and connective tissue lesions, 2) treat severe mouth ulcers in immunologically compromised children following radiotherapy, 3) treat superficial cuts and severe abrasions in submariners, 4) increase the rate of bone regeneration surrounding dental implants, and 5) eliminate dental hypersensitivity (pain) associated with exposed dentin. LILAB has direct effects on mitochondrial functions and cytochromes. Studies on cultured nerve cells indicate that LLLT stimulates regeneration of neurites in damaged retinal cells. The materials published here are expected to become milestones, forming a novel platform in biomedical photobiology.

These proceedings, together with the proceedings of the 1st NOA conference published in 2001 (Journal of Clinical Laser Medicine & Surgery, vol. 19, pp.109-112), demonstrate the synergistic interplay and complementary output of a coherent approach to interrelated scientific questions of excessive clinical relevance, offering results beyond any previous expectation. The 3rd NOA conference is scheduled for 2002, in Brazil.

Contents

Thursday, May 31

Session 1:

Registration
Welcome and Introductions
Harry Whelan, Kurt Henry,
Dennis Morrison

Session 2:

Friday, June 1

Session 1:

Session 2:

Closing Remarks

FOREWORD

Significance to NASA, DARPA, and Potential New Biomedical Treatments

NASA has a keen interest in microgravity-induced alterations of cellular mechanisms of wound healing, especially those that may involve tissue repair following traumatic injuries, compound fractures and infections, and remote medical care on long-term space missions. NASA also has a critical path goal to develop pharmaceutical countermeasures to offset any major retardation of cellular repair of radiation damage, immune cell dysfunction, and increased virulence or antibiotic resistance of infectious organisms.

Astronaut and cosmonaut experiences have indicated that normal healing of superficial skin wounds is retarded similar to the delayed healing observed during long-term submerged operations on submarines. Photodynamic therapy using near infrared (NIR) light has been shown to enhance wound repair via several molecular mechanisms, involving absorption by cytochrome C in the mitochondria, enhancement of intracellular signalling, gene expression and subsequent cytokine secretions. NASA intends to evaluate NIR light therapy as a potential countermeasure to accelerate healing processes, especially since the 600- to 1000-nm wavelengths can penetrate 10-20 cm of tissue. Much of the research into photodynamic mechanisms has been studied with high-intensity lasers and fiber optic illuminators. NASA has recently developed handheld light-emitting diode (LED) devices that emit the appropriate NIR light, which can be used for photodynamic therapy without side effects to adjacent tissues.

Wound healing is a complex interaction involving clotting mechanisms, local acute inflammation, various immune cell functions, recruitment of mesenchymal cells, proliferation of epithelial cells and connective tissue fibroblasts, re-vascularization, generation of granulation tissues, and remodelling to rebuild the tensile strength and functional capabilities of the pre-wounded tissues. Each of the four major phases of wound repair involves extensive interplay between different cells at critical stages, multiple cytokines, and extracellular matrix formation.

Microgravity experiments and randomized gravity experiments in rotating bioreactors on Earth have shown significant effects on enhanced Interferon α & γ production, decreased TNF-α, reduced T-cell activation, increased production of critical Interleukins, increased production of vascular endothelial growth factor, fibroblast growth factor, and matrix molecules such as ICAM & VCAMs. Thus, it would appear that many critical stages of wound repair, especially inflammation, will be altered in microgravity. Ground-based research, using NASA rotating bioreactors, can be used to investigate the intracellular mechanisms of the combined effects of altered gravity and NIR on molecular mechanisms of wound healing, bone regeneration, nerve regeneration, pain modulation, and biofilm formation processes. Important changes can then be confirmed with microgravity experiments on the International Space Station. Deciphering changes in cell functions, up- and down-regulation of certain cytokines, and matrix proteins during

spaceflight will likely lead to new countermeasures that could be enhanced by low-level laser therapy (LLLT) and photodynamic therapy.

The Johnson Space Center has additional interest in this research because of its development of technology for microencapsulating photodynamic therapy drugs for new cancer treatments. The Center has been studying the combined effects of radioprotectants, cytokine inducers, and model microgravity effects on various immune cell functions in randomized gravity experiments using the horizontal rotating bioreactors. Now it is a logical extension to use these cellular models to evaluate the potential benefit of NIR–LLLT to enhance wound healing or increase the effectiveness of pharmaceutical countermeasures to the adverse physiological effects of microgravity.

The Defense Advanced Research Projects Agency (DARPA) is interested in innovative research and development of technologies to enable the combatant to administer self-aid for minor to moderate injuries without relying on outside support. This would allow a combatant to overcome injuries that make up a majority of casualties in the battlefield, thereby significantly reducing the requirements for medic support and/or evacuation. Specific objectives include: 1) a tenfold increase in the number of combatants using self-aid techniques in the battlefield, 2) a fivefold increase in the rate of tissue repair, 3) a major reduction of the number of minor injury evacuations from the battlefield, 4) a physically functional combatant 96 hours post-injury, resulting in a decrease in convalescent leave, and 5) control of pain and initiating treatment within 5 minutes of injury for more rapid stabilization.

Accomplishing DARPA's goals requires exploiting the human body's innate capabilities to accelerate the healing process in acute incapacitating minor tissue injury, acute non-compressible hemorrhage, and acute intractable pain. For acute incapacitating minor tissue injury, DARPA seeks to initiate the development of a new generation of novel noninvasive therapeutic technologies such as low-level energy therapy (including electromagnetic, NIR, visible, thermal, acoustic, and vibratory fields) to accelerate in vivo tissue repair and the regeneration of tissue, including retinal, corneal, epidermal, dermal, musculoskeletal, neuronal, cartilage, ligaments, and tendons.

The conference participants achieved general consensus that several areas of research need to be pursued in order to establish the foundation for more widespread use of LLLT and special applications in spaceflight and undersea environments. We also voiced a need to establish several model systems as reference standards for future work and comparisons in biophysical and biological studies. Areas for further study include:

Biophysical characteristics of photodynamic molecules and design of new photosensitizers. a) <u>Biophysics of photosensitizing molecules</u>. High priorities include: (1) characterizing the absorption spectra for maximum effect on cytochrome oxidase and other photosensitive molecules in the mitochondria; (2) comparing multiple-wavelength LLLT vs. dose and optimum timing for maximum photostimulation of rhodopsin, hemo-

globin derivatives (prophrin rings), and myoglobin; and (3) developing new strategies for designing photostimulation drugs. b) <u>Strategies for design of new photosensitizers</u>. Recommendations included: (1) screening potential photosensitizers using tissue culture models, randomized gravity bioreactors, and several reference cell systems; (2) determining the effect on immune cell function vs. regeneration of epithelial and connective tissues; and (3) characterizing the changes in cytokine mechanisms caused by the LLLT and then designing adjuvant drugs that will enhance those same changes that stimulate critical phases of the wound healing process.

Determination of specific cellular and cytokine mechanisms of photostimulation of the wound healing process. a) <u>Characterize</u> the LLLT effects on inflammatory cytokines, including PGE2, Leukotriene 4, and other prostaglandins. b) <u>Determine the effects</u> on inflammatory cell invasion, local secretions, cellular, and systemic immune responses. c) <u>Determine the effects</u> on gene expression and protein secretions, especially for regulation of cell proliferation. d) <u>Study stimulation</u> effect on neuritis regeneration following nerve transection or high-energy laser damage (retina).

Clinical applications of LLLT for stimulation of wound healing. There are many clinical studies showing that LLLT can dramatically increase the healing of difficult wounds. Unfortunately, since the doses, dose rate, and temporal details of the treatment are not standardized, it is difficult to compare the LLLT efficacy for different types of wounds and for stimulation of healing in different types of tissues. Hence, several recommendations were made regarding issues that needed further study: a) <u>Standardization of exposures</u>. There needs to be a standard reference as to intensity (dose rate at different wavelengths), light energy (wavelength), total exposure (J/cm^2), and total exposure area (vs. area of wound) that is cited in each study. b) <u>Optimization of therapy</u>. LLLT therapeutic regimens must be customized for special tissue healing, including: (1) bone regeneration – determine optimum therapy timeline to achieve maximum long-term benefits of enhanced healing; (2) skin wounds – different course of healing from fire, radiation, chemical, and severe lacerations; and (3) dental tissues have special requirements and exposure to oral organisms. c) <u>Time course of LLLT effect</u>. In some cases, daily treatment with LLLT appears beneficial, however, in other cases, such as superficial abrasions and cuts, one dose every three days appears adequate to stimulate healing. Standardized studies are needed to determine the most effective frequency and total duration of treatment. d) <u>LLLT for pain</u>. It appears that LLLT can reduce pain, as already demonstrated in treatment of dentin to reduce dental pain for hypersensitive teeth. However, studies are needed to compare the effectiveness of LLLT on acute local pain vs. chronic pain and the potential for LLLT to reduce the requirements for narcotics, especially in terminally ill cancer patients.

Potential bacteriostatic effect. It appears that LLLT has a local bacteriostatic action, although the mechanism is unknown. Even if the effect is indirect rather than actual

sterilization, one should explore LLLT as a potential treatment for battlefield wounds, fungal infections, and perhaps applications during long-term space missions.

Combined effects of LLLT and photosensitizers. a) <u>Multiple LLLT fields</u>. Initial studies used lasers to illuminate with NIR light, but now that the LED sources are available commercially, it is important to evaluate the use of the non-thermal LEDs and to determine the effective beam penetration of different wavelengths in various tissues. b) <u>Time-course</u>. Since healing stimulation has different effects at various wavelengths, and since the longer wavelengths (> 720 nm) have a greater effect on cell proliferation, it appears logical to study combined field effects at different time-courses. c) <u>Combined field effects.</u> Studies should determine the molecular mechanisms and then use strategies whereby combinations of LLLT and electric fields or magnetic fields can be used to potentiate the photostimulation effects of the LLLT alone.

Understanding these molecular mechanisms could also lead to the development of new photosensitizers that can enhance wound healing and regeneration of certain tissues for medical therapies on Earth. NASA-developed LED systems using NIR light (600 to 1000 nm) and the new photodynamic therapy drug strategies are expected to have potential new biomedical applications in space, on submarines, and under extreme battlefield conditions.

PHOTO-OXIDATIVE STRESS DOWN-MODULATES THE ACTIVITY OF NF-KB VIA INVOLVEMENT OF BCL-2 AND CASPASE-1, LEADING TO APOPTOSIS OF PHOTORECEPTOR CELLS

Neeraj Agarwal, Raghu R Krishnamoorthy, Matthew J Crawford

Department of Pathology and Anatomy
University of North Texas Health Science Center,
North Texas Eye Research Institute
Fort Worth, Texas, USA

Introduction

Light has been extensively used as an initiator of photoreceptor cell death in a number of in vivo and in vitro experimental conditions (1-3). In vivo studies have also shown that exposure of rats to constant light results in apoptosis of photoreceptor cells (4-9). Production of lipid hydroperoxides has been observed in light exposed retinas (10). The retina has been shown to be susceptible to lipid peroxidation (11,12) despite having high levels of antioxidants (13-15). Since photoreceptor cells in the retina are constantly exposed to light and retina is one of the highest oxygen-consuming tissues in the body, it has a high risk to oxidative damage.

Methods, Results and Discussion

In an effort to understand the visible light-induced oxidative changes, we have been using cultured retinal photoreceptor cells, 661W. In the present report, we show that visible light exposure of mouse cultured 661W photoreceptor cells at 4.5 mwatt/cm^2 caused a significant increase in oxidative damage of 661W cells leading to apoptosis of these cells. These cells show constitutive expression of NF-κB and light exposure of photoreceptor cells, resulting in lowering of NF-κB levels in both the nuclear and cytosolic fractions in a time-dependent manner. Immunoblot analysis of IκBα and p50, and p65 (RelA) subunits of NF-κB, suggested that photo-oxidative stress results in their depletion. Immunocytochemical studies using antibody to RelA subunit of NF-κB further revealed the presence of this subunit constitutively both in the nucleus and cytoplasm of the 661W cells. Upon exposure to photo-oxidative stress, we observed a depletion of the cytoplasmic and nuclear RelA subunit. The depletion of NF-κB appears to be mediated through involvement of caspase-1. Further, transfection of these cells with a dominant negative mutant IκBα greatly enhanced the kinetics of down-modulation of NF-κB, resulting in a faster photo-oxidative stress-induced apoptosis.

To further delineate the mechanism of visible light-induced photoreceptor cell death, we sought to determine the effects of Bcl-2 over-expression on cell survivability. We transfected wild-type 661W cells with the plasmid construct pSFFV-neo-Bcl-2 and isolated several clones. All clones demonstrated increased Bcl-2 mRNA and protein levels, with the B4 clone exhibiting the greatest enhancement. On exposure to visible light, the B4 cells were protected from undergoing apoptosis when compared with the mock trans-

1

fected cells, as ascertained by TUNEL apoptosis assay and formazan-based estimation of cell viability. The Bcl-2 over-expressing cells also maintained a higher Bcl-2/Bax ratio, suggesting that this ratio is important in protection from photo-oxidative stress. Electrophoretic mobility shift assays for NF-κB demonstrated higher activity in both nuclear and cytosolic fractions of the B4 photoreceptors as compared with the 661W wild type cells at all light exposure time points. The findings of the gel shift assays were corroborated by immunocytochemistry for NF-κB, which revealed that protein levels of the RelA subunit of NF-κB were protected in the nucleus as well as in the cytoplasm of Bcl-2 over-expressing B4 cells exposed to light compared to the 661W cells.

Conclusion

Taken together, these studies show that the presence of NF-κB RelA subunit in the nucleus is essential for protection of photoreceptor cells against apoptosis mediated by an oxidative pathway. Furthermore, these results also suggest that Bcl-2 over-expression protects NF-κB protein levels and activity in the nucleus, indicating that preservation of NF-κB binding activity in the nucleus may be essential for photoreceptor cells to survive photo-oxidative damage induced apoptosis.

References

1. Penn, J.S., Howard, A.G. and William, T.P. (1985) In: M.M. LaVail, J.G. Hollyfield and R.E. Anderson (eds) Retinal degenerations: experimental and clinical studies. Liss, New York. pp 439-447.

2. Rapp, L.M., Tolman, B.L. and Dhindsa, H.S. (1990) *Invest Ophthalmol Vis Sci* 31: 1186-1190.

3. Organisciak, D.T. and Winkler, B.S. (1994) *Progress in Retinal and Eye Res* 13: 1-29.

4. Abler, A.S., Chang, C.J., Fu, J. and Tso, M.O.M.. (1994) *Invest Ophthalmol Vis Sci* 35: 1517-1517.

5. Tso, M.O.M., Zhang, C., Abler, A.S., Chang, C.J., Wong, F., Chang, G.Q. and Lam, T.T. 1994. *Invest Ophthalmol Vis Sci* 35: 2693-2699.

6. Li, S., Chang, C.J., Abler, A.S., and Tso, M.O.M. (1995) In: Degenerative diseases of the Retina, editors: R.E. Anderson, M.M. LaVail, and J.G. Hollyfield (Plenum Press, NY) pp. 27-38.

7. Organisciak, D.T., Kutty, R.K., Leffak, M., Wong, P., Messing, S., Wiggert B., Darrow, R.M., and Chader, G.J. (1995) In: Degenerative diseases of the Retina, editors: R.E. Anderson, M.M. LaVail, and J.G. Hollyfield (Plenum Press, NY) pp. 9-17.

8. Reme, C.E., Weller, M., Szezesny, P., Munz, K., Hafezi, F., Reinboth, J.J. and Clausen, M. (1995) In: Degenerative diseases of the Retina, editors. R.E. Anderson, M.M. LaVail, and J.G. Hollyfield (Plenum, NY) pp. 19-25.

9. Noell, W.K., Walker, V.S., Kang, B.S. and Berman, S. (1966) *Invest Ophthalmol* 5: 450-473.

10. Kagan, V.E., Shvedova, A.A., Novikov, K.N. and Yu, P. (1973) *Biochem Biophy Acta* 330: 76-79.

11. Anderson, R.E., Kretzer, F.I., and Rapp, L.M. (1994) In: Free Radicals in Diagnostic Medicine, editors: D Armstrong, Plenum Press, NY pp73-86.

12. De La Paz, M., and Anderson, R.E. (1992) *Invest Ophthalmol Vis Sci* 33: 3497-3499.

13. Heath, H., Rutter, A.C. and Beck, T.C. (1962) *Vis Res* 2: 431.

14. Hall, M.O. and Hall, D.O. (1975) *Biochem Biophys Res Com* 67: 1199-1204.

15. Rapp, L.M., Naash, M.I., Weigand, R.D., Joel, C.D., Nielson, J.D., and Anderson, R.E. (1985) In: "Retinal Degenerations," M.M. LaVail ed., Alan R Liss, Inc., New York, pp. 421-431.

THE INTERFACE OF CELLS IN VITRO, OR TISSUES IN VIVO AND IMPLANT MATERIALS: AN EXTENDED STUDY MOTIVATING NEAR-FIELD OPTICAL ANALYSIS IN VITRO AND IN VIVO

Ralf-Peter Franke

University of Ulm, Dept. of Biomaterials,
ENSOMA Laboratory,
Ulm, Germany

Introduction

Integration of bioimplants in hard or soft body tissues requires histocompatibility of the biomaterials. Integration or non-integration of bioimplants is affected by the body's own cells, by the locotypical cells and by the so-called free cells, the leucocytes. For their proper function, both cell types need highly specific locotypical informations, which are supplied especially by the local extracellular matrix. The local extracellular matrix has to be regarded as a condensed, stored information supply of and for the cells. When cells bind to the locotypical extracellular matrix via specific receptors, the uptake of locotypical information starts and the cells enter certain differentiation routes. This interaction was presented at the 1st International NOA conference last November (Franke, 2001) and it is repeated now because it is fundamental for an understanding of the interaction between body foreign biomaterials and surrounding tissues.

Methods

Biomaterial surfaces so far do not provide the locotypical information, so that the cells brought into contact during the bioimplantation develop without the proper information and have no chance practically to integrate the implant into the regional tissues. According to our present knowledge, lymphocytes play an important role in the locotypical attachment of hard tissues at bioimplants. Relatively new is information on the selective attractivity, which means that the presence and the type of corrosive wear stemming from biomaterials determine local interfacial accumulation of lymphocytes/cells of monocytic origin at different stages of activation. We are presently attempting to evaluate the physico-chemical determinants of local corrosive tendencies via NOA. In addition, it is of particular importance to characterise decontamination mechanisms and routes (i.e. the transport of wear products out of the critical interfacial zone). The international scientific community is attempting to structurize the surfaces of bioimplants on a micro- and nano-level so that cells can bind to these surfaces specifically and enter locotypical differentiation routes. In vitro and in vivo investigation of the selective attractivity are in the focus of our research activities. Here, we expect access to the wear particle material/attracted cell and/or wear particle size/attracted cell and/or wear particle surface structure/attracted cell interaction.

Results and Discussion

Additional information is expected from the micro-/nanoscale inspection of loosened implants, compared to implants of the same material that did not become loose. A critical interface determining the local tissue reactions exists between soft tissues and contacting biomaterial surfaces (e.g. mucosal cells derived from the porcine gastrointestinal tract). Nanoscale structurization of biomaterial surfaces were shown to have a selective attractivity for neuronal cells. Bone marrow cultures have shown large differences in adhesion and differentiation of different subpopulations on similarly structured surfaces. The surface structurization of bio-implants can comprise geometrical, chemical and/or electrical structures (Fig. 1).
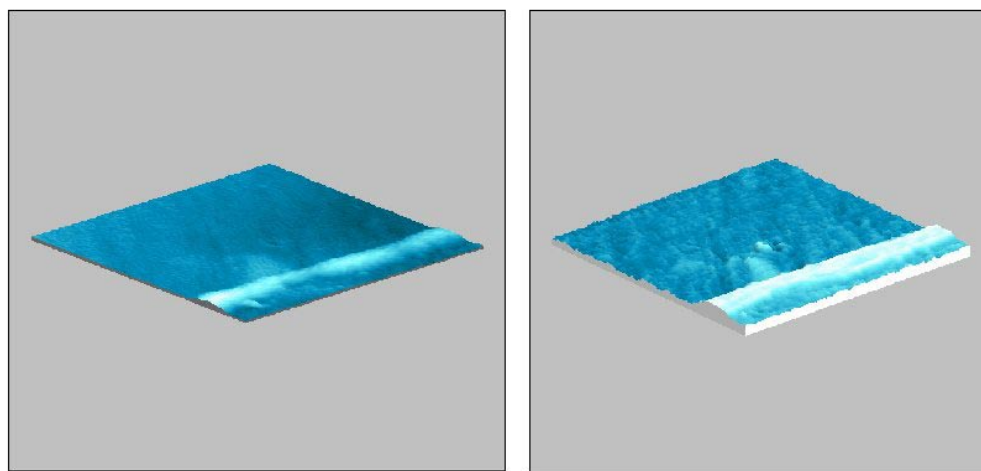
Figure 1: 8 x 8 μm scan of aluminum/copper-sample processed to isolevel topography (left). The whitish line shows diamond based polishing paste accumulated at the Al/Cu-interface. The scan on the right shows the differences in the optical properties of the materials (NOA).

Conclusion

A high-resolution analysis of surface structures and of the interaction between living cells/tissues and surface structures under physiological conditions (aqueous environment) are prerequisites for understanding tissue integration of bioimplants (Sommer and Franke, 2001). Confocal Scanning Laser Microscopy was the first advanced tool for analysis in an aqueous environment, but restricted to a resolution $\geq$ 150 nm and not yet able to reveal chemical components. NOA/NSOM allows a resolution down to 30 nm in an aqueous environment and has a potential to reveal different chemical constituents.

References

Franke, R.P., (2001); The Interface of Cells In Vitro or Tissues In Vivo and Implant Materials, Proc. 1st International Conference on Near-Field Optical Analysis, Castle Reisensburg, Germany, Nov. 4-7, 2000, Sommer, A.P., (ed), J. Clin. Laser Med. Surg., 19 (2), 111.

Sommer, A.P., and Franke, R.P., (2001), Hydrophobic Optical Elements for Near-Field Optical Analysis (NOA) in Liquid Environment – a preliminary study, Micron (accepted).

MITOCHONDRIA, CELL GROWTH, AND PYRIMIDINE SYNTHESIS

Robert K. Naviaux

The Mitochondrial and Metabolic Disease Center, School of Medicine
University of California at San Diego
San Diego, California, USA

Biochemical Background

Mitochondria are highly integrated, intracellular bioreactors that perform a diverse array of metabolic functions ranging from free radical production, oxygen consumption, water synthesis, ATP synthesis, fatty acid and amino acid oxidation, to pyrimidine nucleotide biosynthesis. The protein concentration of the mitochondrial matrix approaches 500 mg/ml. This is equivalent to the packing density and hydration state of a crystal of trypsin. The spatial packing of mitochondrial proteins in the matrix and in the inner mitochondrial membrane is highly conserved and regulated according to local environmental signals and physiologic need. This ensures that mitochondria can respond dynamically to changing cellular needs.

The synthesis, transport, and efficient interconversions of pyrimidines are essential for normal cell and organ function. Particularly heavy demands are placed on these pathways during growth stimuli in embryogenesis, wound healing, and cancer. All cellular pyrimidines are ultimately derived from the synthesis of uridine, which in turn, must be synthesized from orotic acid by condensation with phosphoribosyl pyrophosphate (PRPP) and decarboxylation. The fourth and potentially rate-limiting step in the synthesis of pyrimidines is catalyzed by dihydroorotate CoQ10 oxidoreductase (DHO-QO, EC 1.3.99.11; also called dihydroorotate dehydrogenase (DHOD, EC 1.3.3.1). This enzyme is located exclusively on the inner mitochondrial membrane and is coupled to the electron transport chain via coenzyme Q10 (ubiquinone). See Figure 1.

Essential Roles of Pyrimidines in Metabolism

The metabolic fates of uridine range from RNA, DNA, and protein synthesis, to cofactors and activated intermediates of carbohydrate, glycoprotein, glycolipid and phospholipid metabolism. UDP-glucose, UDP-galactose, and UDP-N-galactosamine are required for accurate post-translational modification for protein trafficking, membrane ion channel, receptor and intracellular glycoprotein and glycolipid synthesis. UDP-glucose is required for glycogen synthesis and the prevention of fasting hypoglycemia. UDP-glucuronate is required for drug, steroid, and bilirubin excretion by glucuronidation. In addition, uridine triphosphate is converted to cytidine triphosphate by glutamine-dependent amination catalyzed by CTP synthetase, and dUMP is converted to thymidine monophosphate by folate-dependent methylation catalyzed by thymidylate synthetase. Finally, CDP-choline and CDP-ethanolamine are essential precursors for all cell membrane and myelin phospholipid synthesis. Cardiolipin is a unique diphospholipid

that is essential for normal oxidative phosphorylation, and found exclusively in the inner mitochondrial membrane. One of the many effects cardiolipin is to stabilize the assembly of cytochrome c oxidase (COX, complex IV). Because cardiolipin is essential for normal oxidative phosphorylation, depletion will lead to reduced ATP synthesis, and restoration of normal cardiolipin synthesis will facilitate more normal cellular bioenergetics. Activated cytidine-diphosphate (CDP-lipid derived from uridine) is essential for all cardiolipin synthesis. See Figure 2 for a summary of the fates and functions of uridine in intermediary metabolism.
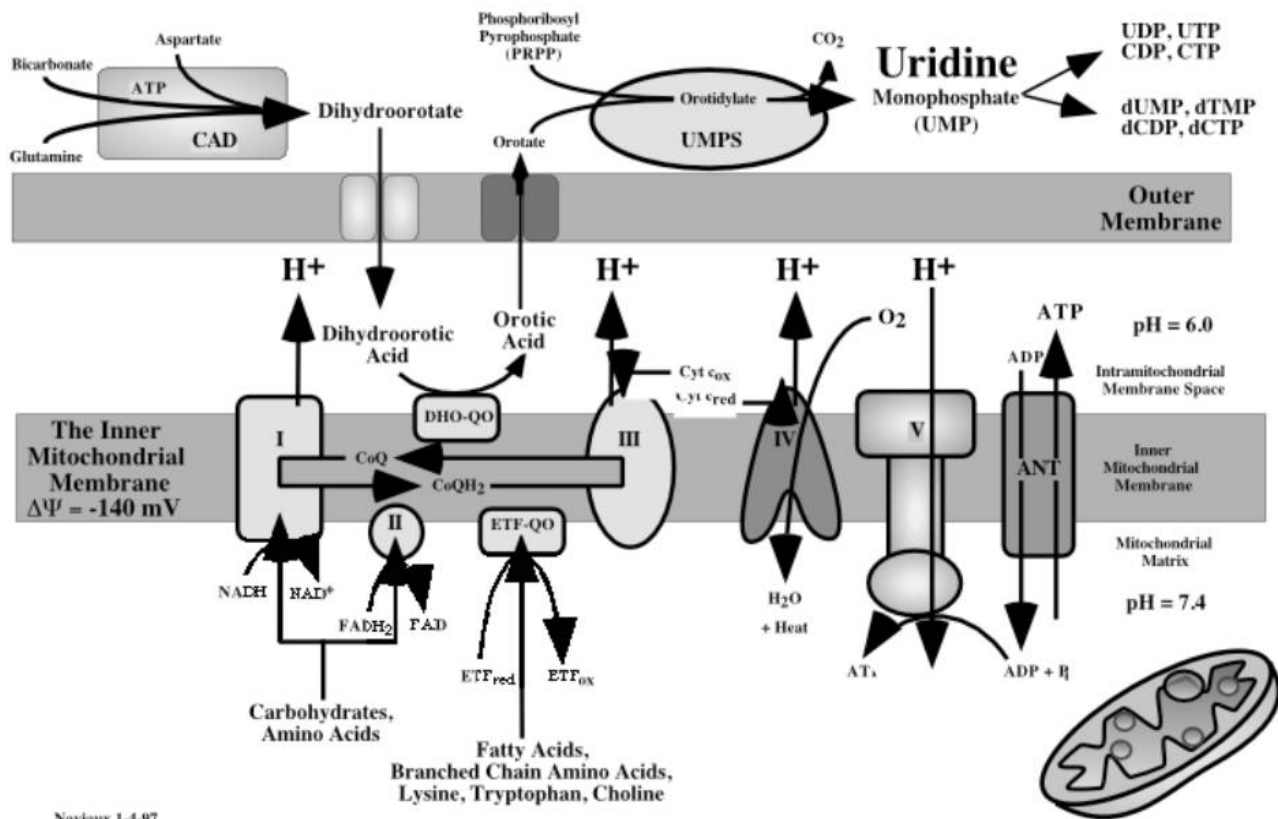
Figure 1: De novo pyrimidine synthesis is coupled to the mitochondrial electron transport chain.
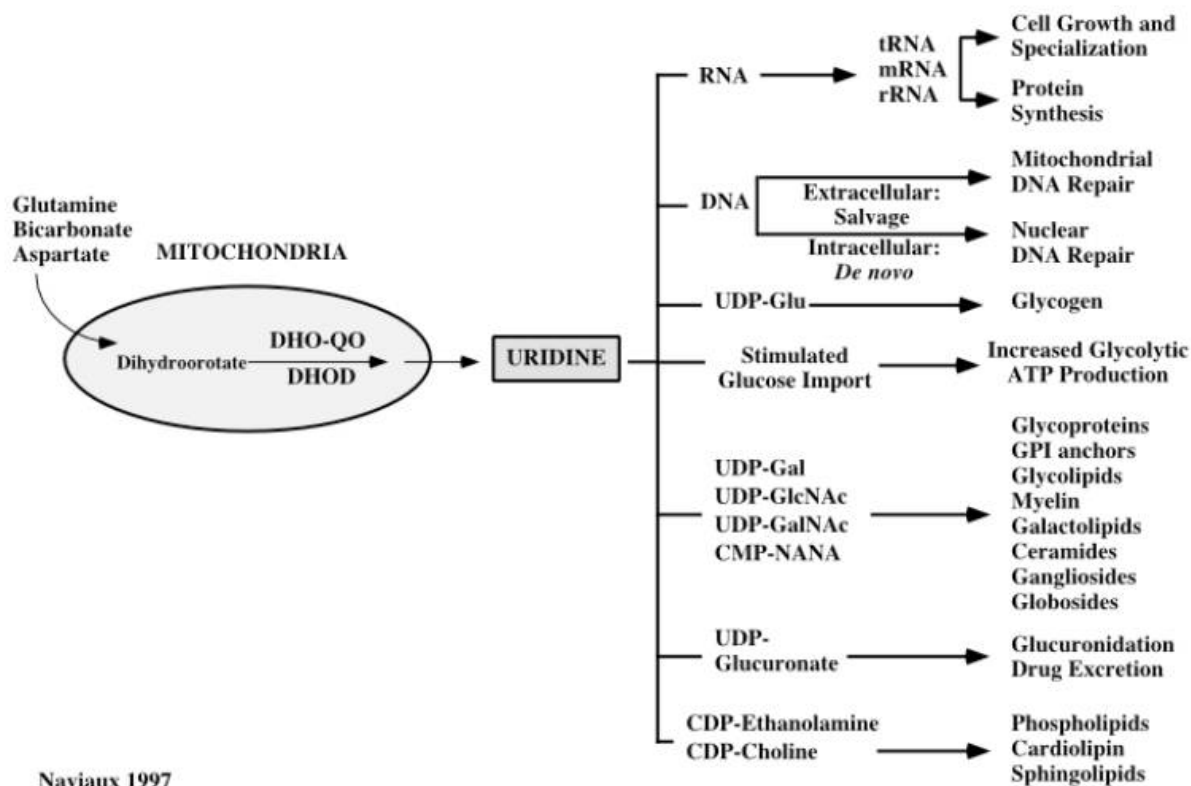
Figure 2: Metabolic fates and functions of uridine.

GC/MS Detection of DHO-QO Activity in Cells and Tissues

DHO-QO catalyzes the transfer of two electrons from dihydroorotate to CoQ10 in the mitochondrial respiratory chain. The product of this reaction is orotate, which differs from the parent dihydroorotate by 2 mass units (155 vs. 157 mu, respectively). Conventional spectrophotometric methods are not sufficiently sensitive to detect DHO-QO activity in samples containing less than about 100 milligrams of cells or tissues. We have developed a gas chromatography-mass spectrometric method that is 100 times more sensitive than previous analytical methods, and is capable of measuring DHO-QO activity in as little as 1 mg of cells or 1 µg of isolated mitochondria. Kinetic analysis of skeletal muscle mitochondrial DHO-QO showed typical Michelis-Menton kinetics and a K_m for dihydroorotate of 30 µM. This assay provides a useful method for measuring changes in mitochondrial pyrimidine synthesis that occur in response to proliferative stimuli, and other positive or negative modulators of mitochondrial function.

OPTICAL ACTUATION AND CONTROL OF BIOLOGICAL SYSTEMS: BASIC CONCEPTS AND MEDICAL AND TECHNOLOGICAL APPLICATIONS

Noah Lotan

Leonard & Diane Sherman Center for Research in Biomaterials
Dept. of Biomedical Engineering
Technion – Israel Institute of Technology
Haifa, Israel

Introduction

Chemical, physico-chemical and biological processes take place by overcoming an activation energy barrier. The higher this barrier is, the slower is the process. In principle, such processes can be facilitated, i.e., their rate increased, along two main routes: (a) by using chemical or biochemical catalysts, which perform their function upon lowering the activation energy barrier; (b) by providing to the system the entire activation energy required and this can be achieved upon using, for example, thermal, ultrasonic or optical means.

Methods

As part of our studies, we relied on the use of optical instrumentality in order to access the most novel and multi-disciplinary area of Molecular Bio-Electronics. In the systems considered, chemical and biochemical molecular elements, as well as electro-conducting polymers are integrated in multicomponent arrays. These are built to operate as molecular switches, logic elements and high-order assemblies, in order to perform complex tasks of information processing. These systems are activated and controlled by outside optical signals.

Results and Discussion

In the first stage of this program, we have used molecular engineering methodologies in order to design and experimentally implement enzyme-based molecular switching elements (ENMOSEs), based on specifically modified enzymes. In these elements the enzymic activity is switched ON and OFF by outside optical signals and, particularly, by irradiation at different wavelengths. Additional molecular switching elements (MOSEs), not enzyme-based but enzyme-related, were also considered. Such elements are enzyme substrates or inhibitors.

The second stage of the program addressed the development of enzyme-based logic gates (ENLOGs), operating under the rules of the Boolean algebra. These systems are made of two modified enzymes (ENMOSEs), or one modified enzyme (ENMOSE) and its inhibitor (MOSE), and perform logic operations such as OR, NOR, AND or NAND.

Upon expanding one of the OR gates, and relying on the Threshold Value concept, we have developed a multi-functional gate. This gate is capable of performing a variety of logic operations while using a single enzymic system.

The third stage of the program is concerned with the design, implementation, analysis and operation of higher-order arrays, assembled as biochemical neural networks (ENENETs). These systems are built of well-defined, enzyme-based repeating units (i.e., biochemical neurons), the latter being joined together in a particular connectivity. The information from one biochemical neuron to another is conveyed by transfer of molecular species, much the same as it actually occurs in the synapses between natural neurons. Using such nets we have shown that, for a given system input, the system output depends on which particular component is used as the monitoring element, on the operation rules of individual neurons, as well as on the particular connectivity established between the composing neurons.

Conclusions

The activity outlined herein has far-reaching implications in key areas of modern science and technology. Thus, for example, the molecular elements developed may serve as basic components towards the ultra-miniaturization of information processing and artificial intelligence devices. Being built on the novel principles presented above, these devices will be free of cross-talk interference and will not be limited by the heat dissipation capabilities of the system.

An additional area of application of these systems is in nanometric biomedical devices performing diagnostic or therapeutic tasks. Thus, for example, we can conceive very-low-weight, molecular-size assemblies that contain polymeric light-emitting diodes and act as electroluminescent devices for locally applied photodynamic therapy. And, in view of their very low energy requirements, such devices may be operated for very long periods of time. Other such devices may be built for targeted, controlled release of drugs, which will be operated and controlled by the status of the disease. Thus, upon interacting with specific elements in the physiological systems, these devices will gather the biochemical information required and, accordingly, will control and actuate the release of drug.

HOW IT ALL STARTED: DR. ENDRE MESTER'S PIONEERING WORK

Adam R. Mester[1] and Andrei P. Sommer[2]

[1]Semmelweis University, Faculty of Medicine,
Department of Diagnostic Radiology and Oncotherapy,
National Laser Therapy Centre, Peterfy Sandor Teaching Hospital,
Budapest, Hungary
[2]University of Ulm, Central Institute of Biomedical Engineering,
Department of Biomaterials, ENSOMA Laboratory,
Ulm, Germany

Introduction

Low level (low intensity) laser irradiation is accepted to induce an acceleration of wound healing processes, to reduce inflammations, to support neuro-regeneration, to promote vascular and lymphatic microcirculation, to stimulate the immune system and to reduce pain − nonthermal radio-biological therapeutic effects relevant for civilians, military personnel and astronauts.

Methods

Energy density: Photobiological surface effects were achieved in most cases at energy densities between 1 and 4×10^4 Jm^{-2}, e.g. in the therapy of ulcera cruris with 5-50 mW He/Ne-Lasers (Mester, 1981). This, and further experimental evidence, led to the establishment of one basic Arndt-Schultz-curve showing different modes of cell reaction at different energy density levels. At smaller levels, there were no observable clinical effects. Higher levels resulted in the transient inhibition of cellular functions. Smaller levels could, however, be effective in in-vitro experiments.

Intensity: While Mester and his group used from the beginning laser equipment with a minimum power of ~ 5 mW (Mester et al., 2001), many low level laser therapy (LLLT) groups disregarded the fundamental importance of the laser power and its implicit impact on the intensity of the irradiation acting on the tissue, respectively penetrating into the biological target volume − the principal source behind a large body of negative results in this field. With Mester's Arndt-Schultz relation, and the basic equation connecting the irradiation parameters energy density E and intensity I (E = I t), where t is the duration of the irradiation, it was tempting to try lasers with a power far below 5 mW in biostimulation, and to extend the irradiation of the biological target volume until the total energy density was in the correct $1 - 4 \times 104$ Jm^{-2} range. Unfortunately, the lower light intensity limits, below which no biological effects could be observed, were not quantified systematically for three decades. Following the hypothesis of photobiological intensity thresholds (Sommer, 1993), the influence of the light intensity on irradiated cells was verified in fibroblast cultures (Lubart et al., 1993). Observations in irradiated patients confirmed that thresholds of light intensity (presumably wavelength dependent) have to

11

be surpassed in order to realize reproducible biostimulatory effects. A protocol of the precise intensity thresholds was prior to our study (Sommer et al., 2001) lacking.

Results and Discussion

The central point in the present study is the quantitative explanation of the reproducible results in Mester's pioneering laser work. The biostimulative effect of laser irradiation (Mester et al., 1998) and light in general, depends on a set of at least four parameters, besides the wavelength of the light: a light intensity threshold I_o, the beam cross section a, the total irradiation time Δt_{tot} and the light energy density $(E/a)_{act}$ required for photo-activation in the biological target volume, where the effective intensity/dose-values could sensitively differ from values measured at the surface, because the photon density decreases with the penetration of the irradiation into the tissues. The variable biostimulation parameters relevant for activation are interrelated according to the low-intensity laser activated biostimulation LILAB-equation: $(E/a)_{act} = I_{stim} \cdot \Delta t_{tot}$, where intensities necessary for stimulation I_{stim} have to surpass the biological threshold intensity I_o. The majority of the published results with a negative outcome stem from ignoring the importance of the relation $I_{stim} \geq I_o$ in LLLT. Light intensities lower than the threshold values I_o could not produce biostimulatory effects – even under a prolongation of the irradiation time Δt_{tot}. The effective range of $(E/a)_{act}$ is determined by the particular Arndt-Schultz-curve. Although the LILAB equation is physically simple, its biological implications are in no way trivial. We suggest that LLLT studies should be accompanied by a transparent protocol of all the irradiation parameters entering the LILAB-equation (e.g. Figure 1).

Figure 1: Left side irradiated 60s per day, treatment area ~1cm^2, 670nm diode laser, beam cross section ~ 12.5mm^2, power 5mW, intensity 400Wm^{-2}, dose 2.4×10^4 Jm^{-2}.

Conclusion

The biophysical equation inter-relating the variable irradiation parameters in photostimulation is the LILAB-equation. Biologically, the parameters $(E/a)_{act}$ and I_{stim} are independent from each other – an important consideration for the medical applications of photobiological effects realized via lasers (including non-coherent light sources) at low intensity and low energy density levels.

References

Lubart, R., Friedmann, H., Peled, I., and Grossmann, N., (1993); Light Intensity Effect on Cell Proliferation, 5th Congress of the European Society for Photobiology, Marburg/Lahn, Germany, September 19-26.

Mester, A.R., Nagylucskay, S., and Mako, E.K., (2001); Nonthermal Biological Effects of Radiology-Based Laser Irradiation, Proc. 1st International Conference on Near-Field Optical Analysis, Castle Reisensburg, Germany, Nov. 4-7, 2000, Sommer, A.P., (ed), J. Clin. Laser Med. Surg., 19 (2), 110.

Mester, A.R., Nagylucskay, S., Mako, E., Hoffmann, G., and Serenyi, M., (1998); Experimental immunological study with radiological application of low power lasers, Laser in Medicine, Waidelich, W., (ed), Berlin, Heidelberg, New York: Springer, 502-512.

Mester, E., (1981); Über die stimulierende Wirkung der Laserstrahlung auf die Wundheilung, Der Laser: Grundlagen und klinische Anwendungen. Dinstl, K., and Fischer, P.L., (eds.), Berlin, Heidelberg, New York: Springer, 109-118.

Sommer, A.P., (2000); Beam distributor for lasers, Patent Nr. 4308474, Germany, March 1993.

Sommer, A.P., Pinheiro, A.L.B., Mester, A.R., Franke, R.P., and Whelan, H.T., (2001); Biostimulatory Windows in Low-Intensity Laser Activation: Lasers, Scanners, and NASA's Light-Emitting Diode Array System, J. Clin. Laser Med. Surg., 19 (1), 29-30.

BIOMODULATORY EFFECTS OF LLLT ON BONE REGENERATION

Antonio L.B. Pinheiro[1], Marilia G. Oliveira[2], Pedro Paulo M. Martins[3], Luciana Maria Pedreira Ramalho[4], Marcos A. Matos de Oliveira[5], Aurelício Novaes Silva Júnior[6] and Renata Amadei Nicolau[7]

[1]Professor of Oral and Maxillofacial Surgery, School of Dentistry, Department of Diagnostic and Therapeutics, Universidade Federal da Bahia, Salvador, BA, 40110-150, Brazil; Researcher, Institute of Research and Development (IP&D) Universidade Vale do Paraíba (UNIVAP) - São José dos Campos, SP, 12244-000, Brazil
[2]Professor of Oral and Maxillofacial Surgery, School of Dentistry, Post-Graduate Program on Oral and Maxillofacial Surgery, Pontifícia Universidade Católica do Rio Grande do Sul, Porto Alegre, RS, Brazil
[3]Associated Professor, School of Dentistry, University of Pernambuco, Camaragibe, 50000-000, Brazil
[4]Associate Professor of Oral Medicine, School of Dentistry, Department of Diagnostic and Therapeutics, Universidade Federal da Bahia, Salvador, BA, 40110-150, Brazil
[5]School of Dentistry, Laser Center, Universidade Federal da Bahia, Salvador, BA, 40110-150, Brazil
[6] Post-Graduate Program on Oral and Maxillofacial Surgery, Pontifícia Universidade Católica do Rio Grande do Sul, Porto Alegre, RS, 90619-900, Brazil
[7]Lecture, Institute of Research and Development (IP&D) Universidade Vale do Paraíba (UNIVAP) - São José dos Campos,SP, 12244-000, Brazil

Introduction

Tissue healing is a complex process with local and systemic responses. The process of wound healing involves several types of cells, enzymes, growth factors, and other substances. LLLT for wound healing has been shown effective in modulating both local and systemic responses. On soft tissues it has been shown that – depending on the wavelength, dose, and local conditions – LLLT has anti-inflammatory effects, reduces pain, quickens cell proliferation,[11,14-16,24] and, consequently, induces the healing process. Bone healing differs from that observed in soft tissue because of both morphology and composition. Usually the healing process of the bone is slower than that observed in soft tissues.[17] The natural course of bone healing is composed of consecutive phases and differs according to the type and intensity of the trauma and also the extension of the damage to the bone. Traumatic injuries are major sources of bone fractures. These injuries may occur in several different situations and usually impair patients' abilities in performing their normal daily activities, bringing about problems for both patient and employers as sufferers had their work capacity reduced for several weeks. Confining civilian or military activities such as petroleum platform work, space trips and submarine work, further make difficult the management of skeletal injuries. It is known that the lack of gravity and extremely high pressures may impair even more of the body's abilities to repair. The effects of LLLT on bone are still controversial as previous reports found elsewhere in the literature show different or conflicting results. It is possible that LLLT effect on bone regeneration depends not only on the total dose of

irradiation, but also on irradiation time and irradiation mode (CW or PLS). Most importantly, recent study has suggested that the threshold parameter energy density and intensity are biologically independent from each other. This independence accounts for the success and the failure of LLLT achieved at low-energy density levels as described previously by Sommer et al.[20] This paper reports recent observations on the effect of LLLT on bone healing.

Materials and Methods

We have evaluated morphometricaly the amount of newly formed bone after 830nm laser irradiation of surgical wounds created in the femur of rats. We divided 40 *Wistar* rats into 4 groups of 12 animals each: group A (12 sessions, 4.8J/cm^2 per session, observation time of 28 days); group C (3 sessions, 4.8 J/cm^2 per session, observation time of 7 days). Groups B and D acted respectively as non-irradiated controls. Experimental groups A and C defects were irradiated transcutaneously 48 hours after the surgery, with the hand piece perpendicularly positioned on the wound with an 830-nm diode laser (CW, 40 mW, $\phi \sim$ 1mm) with a total dose of 4.8 J/cm^2 (Laser Beam, Rio de Janeiro, Brazil). Irradiation was performed three times a week, resulting in 12 applications (57.6 J/cm^2) on Group A and three applications (14.4 J/cm^2) on group C. The animals were humanely killed with an overdose of general anesthetics at the end of the experimental periods and specimens were taken. The specimens were routinely processed to wax and cut at 6 μm thickness and stained with H&E. We performed computerized morphometry using specific software (Imagelab[®]) and selected the best sets of images of each specimen of each group for this analysis. We calibrated the computerized system for a relationship of 1 pixel = 6.5 mm. The software delimited and quantified the area measured (Fig.1).

In a second investigation, we verified LLLT effect on bone healing after inserting implants. It is known that dental implants need 4 to 6 months for fixation on the maxillae and on the mandible before receiving loading. Current literature has shown several reports on the effect of LLLT on healing soft tissue, a study assessed clinically and with SEM the efficacy of using 830-nm (40 mW) laser light at a dose of 4.8 J/cm^2 on bone healing after inserting dental implants on the dog's tibiae. Ten male and female dogs with an average weight of 14 kg in this study were divided into 2 groups. Each group's 5 animals received the implant. Three animals were irradiated and 2 were controls. The animals were sacrificed 45 and 60 days after surgery. The animals were irradiated 3 times a week for 2 weeks in contact mode with an 830-nm diode laser (CW, 40 mW, $\phi \sim$1mm) and a total dose of 4.8 J/cm^2 per session and a dose per point of 1.2 J/cm^2 (Laser Beam, Brazil). The animals were humanely killed with an intraperitonial overdose of general anesthetics at the end of the experimental periods. After the removal, the specimens were routinely prepared for SEM.

Results

Figures 2 and 3 show the histological aspect of irradiated and non-irradiated specimens at day 7 and 28. Table 1 shows the comparison between the mean areas of irradiated and non-irradiated subjects. Fig. 4 shows the results of the measurements obtained for

irradiated and non-irradiated specimens seven days after surgery. The Mann-Whitney test showed a significant difference between irradiated and non-irradiated groups (p=0.17, Table 2) and within this experimental group (p=0.01, Table 3). On the other hand, the Mann-Whitney test failed to demonstrate a significant difference between irradiated and non-irradiated defects 28 days after surgery (p=0.383, Table 4). The results of the measurements can be seen on Fig. 5.

Table 1: Comparison Between the Means of the Areas on Irradiated and Non-Irradiated Bone Defects at Both Experimental Periods

GROUP	TIME	AREA
IRRADIATED	07 days	2852629.12
	28 days	861794.15
NON-IRRADIATED	07 days	1561740.66
	28 days	655798.96

Table 2: Comparison Between Irradiated and Non-Irradiated Samples Seven Days After Surgery

GROUP	MEAN	SD	VARIATION COEFFICIENT	P
Irradiated	2852629.12	745985.83	26.15%	0.017
Non-Irradiated	1561740.66	248036.22	15.88%	

Table 3: Comparison Between Time and Area on Irradiated Subjects

TIME	MEAN	SD	P
7 days	2852629.12	745985.83	0.01
28 days	861794.15	470949.95	

Table 4: Comparison Between Irradiated and Non-Irradiated Samples 28 Days After Surgery

GROUP	MEAN	SD	VARIATION COEFFICIENT	P
Experimental	861794.15	470949.95	54.61%	0.383
Control	655798.96	298272.25	45.50%	

The second study showed no macroscopic differences between irradiated and non-irradiated subjects throughout the experimental period. SEM analysis showed a better quality of the bone on both times on irradiated and non-irradiated specimens (Figures 6-9).
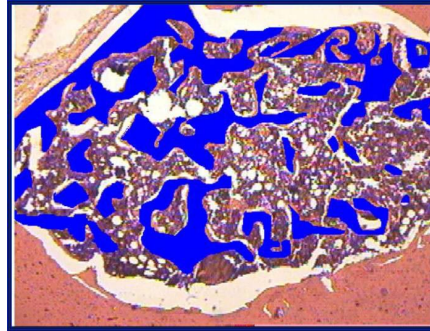
Figure 1: Delimitation of the area by the Imagelab®.

Figure 2: On the left, histological aspect of a non-irradiated specimen seven days after surgery. On the right, at the same experimental time, the aspect of an irradiated specimen (H&E, x4).

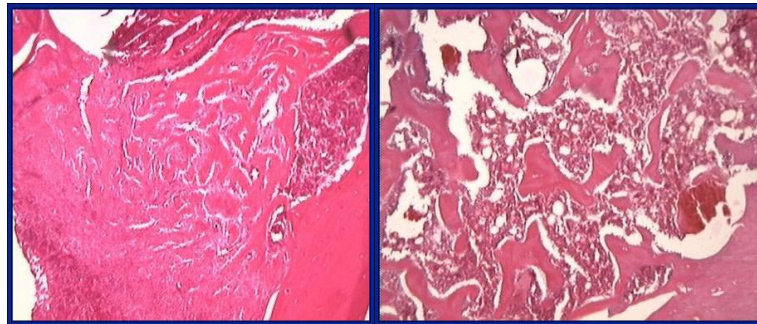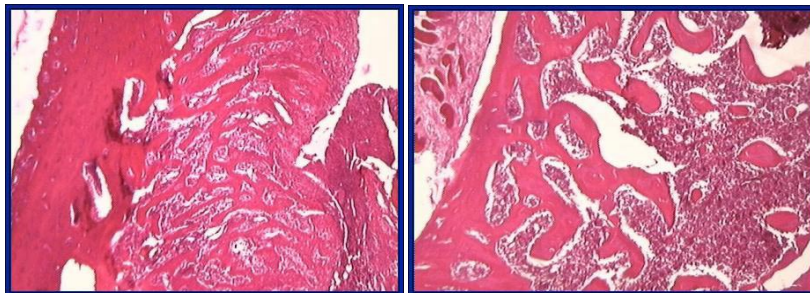**Figure 3**: On the left, histological aspect of a non-irradiated specimen 28 days after surgery. On the right, at the same experimental time, the aspect of an irradiated specimen (H&E, x4).
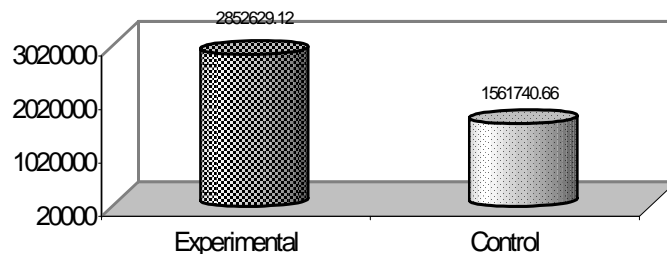
Figure 4: Comparison between experimental group experimental and control; period of observation 7 days.
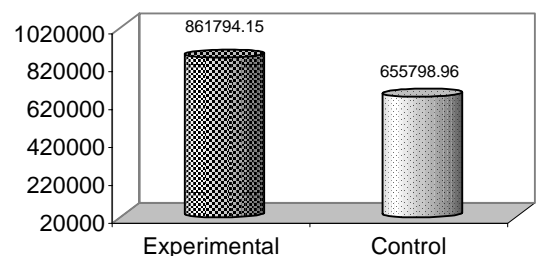
Figure 5: Comparison between group and control; period of observation 28 days.
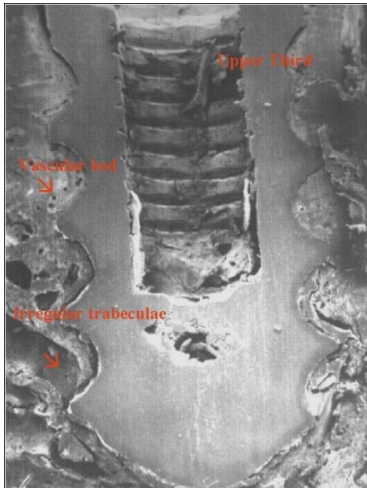
Figure 6: SEM of a non-irradiated specimen 45 days after implantation. Compact bone is observed on the upper third, presence of vascular beds. In the intermediate and lower thirds, irregular bone trabeculae limiting the cavities are observed (x12).
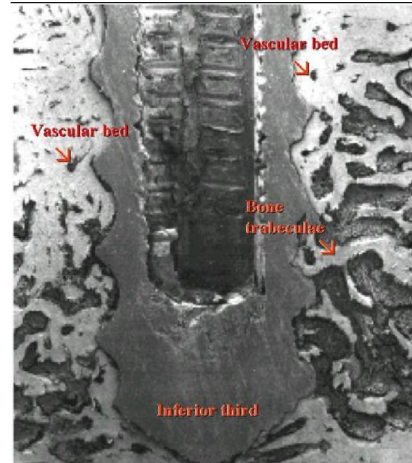
Figure 7: SEM of an irradiated specimen 45 days after implantation. There is a lamellar rearrangement, more pronounced at the bone/implant interface. Increased neovascularization is higher on the upper and intermediate thirds. There are also trabeculae on the lower third (x12).

Figure 9: SEM of non-irradiated specimen 60 days after implantation. Bone/implant interface shows an immature aspect (x100).

Figure 8: SEM of irradiated specimen 60 days after implantation. Presence of mature bone on the upper and intermediate thirds, good distribution of the vascular beds and lamellar arrangement of the bone on the implant/bone interface. On the lower third, the bone has a more immature aspect (x12).

Discussion

The results of the studies showed better bone healing after irradiation with the 830 nm diode laser. Although several groups have studied LLLT effects on soft-tissue, few works are on the effect of LLLT on bone. Some previous reports do recognize that LLLT has positive effects on bone.[18,19] These studies reflect the idea that non-differentiated mesenchymal cells could be biomodulated positively to osteoblasts that would more rapidly change to osteocytes.[18] This aspect may be corroborated by several previous studies in which LLLT was used in fractures,[10] bone defects,[26] tooth extraction[3,8,21] and after the placement of dental implants.[13] On the other hand, LLLT seems ineffective when used on normal tissues.[19] Biomodulating effects of LLLT to be observed demand some level of tissue deficiency.[14] We know that the osteogenic potential of mesenchymal cells depends on several genetic factors and also on systemic and local inducer factors.[7] LLLT may act as such an inducer factor. However, some reports[23] suggested that LLLT would improve bone matrix production due to improved vascularization and anti-inflammatory effects. These aspects would result in an increase of both the release of mediators and micro-vascularization, which would accelerate bone healing. It was suggested that PGE_2 activates wound healing[6] and the Mester group[12] observed an increased lev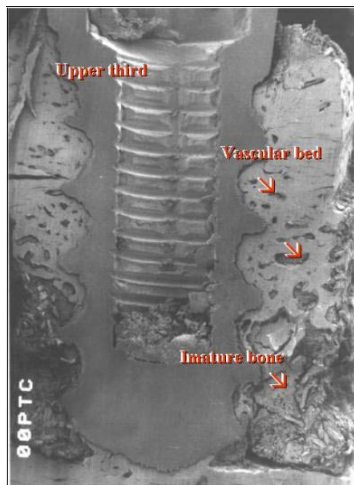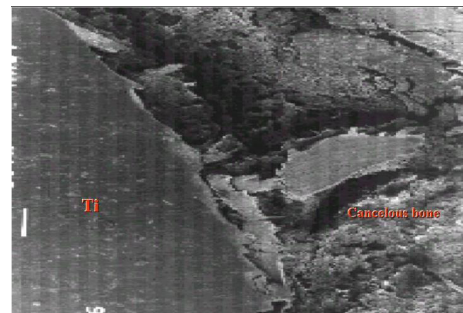el of PGE_2. There is evidence that osteoblasts also produce PGE_2 and that its effects may be therapeutic or adverse.[25] Another point to consider is that this kind of therapy may also be used in cases of fractures in which plates and screws are used for immobilization. IR laser light on these studies was chosen for its higher penetration on the tissues. The results observed on SEM are aligned with previous reports, which demonstrated increased vascularization, quick alveolar socket repair and increased osteoblast, condrocite and fibroblast activities.[2,21,22,27] Both studies kept low surface doses in accordance with the findings of previous studies that suggested doses ranging from 1-4 J/cm^2.[11] Although some studies recommended higher doses, our clinical results on the use of LLLT have recommended similar surface doses[15,16] to those suggested in several studies within the range of 1-5 J/cm^2.[19, 26,23] The session dose never exceeded 20 J/cm^2. Exposure time and intensity on these studies are in accordance to suggestions that the strongest biomodulatory effects are observed at exposures timing ranging from 30 to 120s.[24]

It is acknowledged that the controversy observed in the results found in the literature is due to different protocols used in which different wavelengths, association of wavelengths, different modes of emission and several doses were used in different animal or cell models. It is recognized that each method has its advantage and disadvantage. We tried to use reproducible methods of measurement or visual analysis on the present investigations. It is also recognized that tissue morphology and the shape and distribution of the trabeculae may differ on the samples that would lead to imprecise interpretation of the results found in these studies. We used serial cuts to prevent greater variation on the reading; in doing so, approximately the same serial cut of each specimen was used for the computerized analysis or SEM. The computerized analysis has been found effective on measuring the area of new-formed bone and confirmed the findings of a previous report that also

found increased bone proliferation after LLLT using a similar software and immunohisto-chemistry. This was not aligned with other research groups, which did not find positive effect of LLLT on healing bone[1,5] and others. It is important that some previous reports, which found no biomodulating effects of LLLT, presented some problem on the method used,[4] did consider the systemic effect of LLLT[23,26] and used contra-lateral procedures as controls. On the other hand, this investigation's findings are very close to a study that found intense activity and high numbers of osteoblasts 5-6 days after the procedure was performed on bone defects using the same model used in our study. Previous work using a 790-nm laser with a dose similar to that used in our investigation demonstrated a 10% increase in the amount of mineralized bone with the seven-day procedure on irradiated animals. A previous study verified the progress on bone consolidation with increased formation of trabecular bone and in the number of osteoblasts after the use of 632.8 nm He-Ne laser (1 mW, ϕ ~1.1 mm). In the previously mentioned study, the experimental period was that of seven days and doses per treatment of 3.15, 31.5 and 94.7 J/cm^2 were used for the treatment. Positive response was found at 31.5 and 94.7 J/cm^2 but not at lower doses. These values were higher than those used in this work (4.8 J/cm^2). These may indicate a more effective effect of 830 nm laser light in comparison to lasers emitting on 632.8 or 790 nm. This is probably due to a higher penetration of laser light with higher wavelength (Infrared) on the tissues.[9] We concluded that using LLLT at 830 nm significantly improved bone healing at early stages. Further studies are needed on the effects LLLT on growth factors, BMPs, prostaglandin and on bone forming genes to assess the possibility of further improvement on bone healing.

References

1. Anneroth et al. (1988). The effect of low-energy infrared laser radiation on wound healing in rats. Brit. J. Oral & Maxillofac. Surg.26, 12-17.

2. Bisht, D. et al. (1994). Effect of low laser radiation on healing of open skin wounds in rats. Indian J. Med. Res., 100, 43-46.

3. Freitas, A.C. (1998). Avaliação do efeito antiinflamatório do laser Diodo Infravermelho de 830nm através da monitorização da proteína C-Reativa. Recife: Universidade Federal de Pernambuco. 74p.

4. Gordjestani, M. et al. (1994). Infrared laser and bone metabolism: A pilot study. Int. J. Oral Maxillofac. Surg. 23, 54-56.

5. Hall, G. et al. (1994). Effect of low energy laser irradiation on wound healing. An experimental study in rats. Swed. Dent. J. 18, 29-34.

6. Hight, W.B. (1985) apud Trelles, M. A., Mayayo, E. (1987). Bone fracture consolidates faster with low-power laser. Lasers Surg. Med. 7, 36-45.

7. Katchburian, E., Arana-Chavez, V. E. (1999). Histologia e Embriologia Oral: Texto-Atlas Correlações Clínicas. São Paulo: Panamericana, 41-70.

8. Kucerová, H. et al. (2000) Low-level laser therapy after molar extraction. J.Clin. Laser Med. Surg. 18, 309-315.

9. Lizarelli, R.F.Z., Lamano,-Carvalho, T.L., Brenttegnani, L.G. (1999). Histometrical evaluation of the healing of the dental alveolus in rats after irradiation with a low-powered GaAlAs laser. Featherstone, J.D.B, Rechman, P. Fried, D. Lasers Dentistry V, Billingham: SPIE. 49-56.

10. Luger, E.J. et al. (1998). Effect of low-power laser irradiation on the mechanical properties of bone fracture healing in rats. Lasers Surg. Med. 22, 97-102

11. Mester, E. et al. (1971). Effect of rays on wound healing. Am. J. Surg.122. 532-535.

12. Mester, E., Mester, A.F., Mester, A. (1985). The biomedical effects of laser application. Lasers Surg. Med. 5, 31-39.

13. Oliveira, M. A. M. (1999). Efeito da Radiação Laser Não Cirúrgica na Bioestimulação Óssea Pós-Implante: Ánálise com Microscopia Eletrônica de Varredura. Monografia de Especial-zação; Recife: Faculdade de Odontologia da Universidade Federal de Pernambuco. 88p

14. Pinheiro, A.L.B, Nascimento, S.C, Vieira, .A. L.B et al. (2001). Effects of   LLLT on malignant Cells: Study in Vitro. Rechman, P., Fried, D, Haning, P. Lasers in Dentistry VII. Billingham: SPIE. 56-60.

15. Pinheiro A.L.B. et al. (1997). Low-level laser therapy in management of disorders of the maxillofacial region. J. Clin. Laser Med. Surg. 15, 81-183.

16. Pinheiro, A.L.B. et al. (1997). LILT in the treatment of disorders of the maxillofacial region. In Wigdor, H.A, Featherstone, J.D.B, Rechman, P. Lasers in Dentistry III. Bellingham: SPIE. 227-234.

17. Pinheiro, A. L. B. (1993). Comparison of tissue damage and healing in scalpel and CO_2 Laser mucosal wounds**.** Birmingham: University of Birmingham, PhD Thesis, 529 p.

18. Pinheiro; A. L. P, Frame, J. F. (1992). Laser em Odontologia: Seu Uso Atual e Perspectivas Futuras. RGO. 40, 327-332.

19. Saito, S., Shimizu, N. (1997). Stimulatory effects of low-power laser irradiation on bone regeneration in mid-palatal suture during expansion in the rat. Am. J. Orthod. Dentofac. Orthop. 111, 525-532.

20. Sommer, A.P., Pinheiro, A.L.B., Mester, A.R. Franke, R.P, Whelan, Whelan, H.T. (2001). Biostimulatory windows in low intensity laser activation: Lasers, Scanners and NASA's Light Emitting Diode Array System. J. Clin. Laser Surg. Med.19, 29-34.

21. Takeda, Y. (1988) Irradiation effect of Low-energy laser on alveolar bone after tooth extraction: Experimental study in rats. Int. J. Oral Maxillofac. Surg. 7, 388-391.

22. Tang X. M. Chai B.P. (1986) Effect of C02 laser irradiation on experimental fracture healing: a transmission electron microscopic study. Lasers Surg. Med., 6, 346-352.

23. Trelles, M. A., Mayayo, E. (1987). Bone fracture consolidates faster with low-power laser. Lasers Surg. Med. 7,36-45.

24. Tunér, J., Hode, L. (1999). Low level laser therapy (Clinical Practice and Scientific Background). Gängesberg: Prima Books.

25. Valcanaia, T.C. (1999). A Influência do Uso do Antiinflamatório não Hormonal, O Diclofenaco Potássico, No Reparo ósseo. Tese de Doutorado. Porto Alegre: Pontifícia Universidade Católica do Rio Grande do Sul.99p.

26. Yaakobi, T., Maltz, L., Oron, U. (1996). Promotion of bone repair in the cortical of the tibia in rats by low energy laser (He-Ne) irradiation. Calcif. Tiss. Intnl. 59, 297-300.

27. Yamada K. (1991). Biological effect of low power laser on clonal osteoblastic cells (MC3T3-E1). Nippon Seikeigeka Gakkai Zasshi, 787-799.

LLLT IN TREATING DENTINARY HYPERSENSIBILITY: A HISTOLOGIC STUDY AND CLINICAL APPLICATION

Aldo Brugnera Junior[1], Ana Eliza Garrini[2], Antonio Pinheiro[3], Dilma Helena Souza Campos[2], Elisângela Donamaria[2], Fábio Magalhães[2], Fatima Zanin[2], Jesus Djalma Pécora[4], Márcia Takamoto[2] and Thereza Christinna Ladalardo[2]

[1]Professor and Chairman of the Laser Department, School of Dentistry, Universidade Camilo Castelo Branco, São Paulo, SP, Brazil; Researcher of the Endodontic Laboratory – FORP USP, Ribeirão Preto, SP, Brazil; Researcher of the Laser Center, Universidade Federal da Bahia, Salvador, BA, 40110-150, Brazil
[2]Professor of the Laser Department, School of Dentistry, Universidade Camilo Castelo Branco, São Paulo, SP, Brazil
[3]Professor of Oral and Maxillofacial Surgery, School of Dentistry, Department of Diagnostic and Therapeutics, Universidade Federal da Bahia, Salvador, BA, 40110-150,Brazil; Researcher, Institute of Research and Development (IP&D) Universidade Vale do Paraíba (UNIVAP) - São José dos Campos, SP, 12244-000, Brazil
[4]Professor and Chairman of Restorative Dentistry, School of Dentistry, Universidade de São Paulo, Ribeirão Preto, SP, Brazil

Introduction

Dental hypersensitivity has been studied for several years; it is reported as a strikingly painful condition that originates from the exposition of dentinal tubuli as a result of the reduction of thickness of the enamel or cement. Usually the exposed area is subjected to several kinds of stimuli, resulting in a rapid sharp acute pain. This painful condition makes eating and oral hygiene very difficult.[30] LLLT has been shown to have anti-inflammatory, analgesic and cellular effects in both hyperemic and inflammation of the dental pulp. The awareness of the disease and the use of correct parameters of LLLT are essential for treatment success. Among the several types of dental pain, this is the most frequent condition. It has a high prevalence among patients from the ages of 30 to 45 years old, and it occurs even among patients with outstanding oral hygiene.[10,16,24]There are several reports on how healthy teeth or the presence of a gingival retraction or small abrasion develop this condition. Several authors believe that the presence of inter-dentinal nervous fibers (18,000 to 40,000 tubes per mm^2) exposed to the oral environment and susceptible to local stimuli is what causes the symptoms.[21,29] (Fig. 1). Both animal and human studies on the innervation of teeth have established a relationship between sensitivity and dentin tubuli exposure. Reducing the number of open tubulis or decreasing their diameter would, therefore, be a treatment objective for sensitive teeth.[1,9,19,21] On the other hand Brannstrom et al.[3] proposed a hydrodynamic theory to explain the mechanism for the hypersensitivity associated with exposed dentin. The hypothesis is that movement of fluid in the dentin tubulis is capable of stimulating the pulp nerve tissue. Consequently, root surface areas with an increased number of exposed (or open) dentin tubulis should have an increased potential for dentin fluid flow and, therefore, dentin hypersensitiv-

ity. Brännstrom[4] assumes that further mechanisms, associated with psychological aspects, such as stress and neurological conditions, inducing morphological changes, may also be a cause for developing the disease.[3,4,8,19,20] Researchers more widely accept the Brännströn[3,4,5] theory. Brugnera, Jr.[5] classifies the main causes of hypersensitivity: 1) mechanical – caused by scaling; oral habits and abrasion 2) thermal – sudden temperature changes, especially cold stimulation 3) chemical – caused by dehydrating agents such as sugar or salt and bacterial products 4) Barotrauma or Barostress, which is the study of Barodontology – dental pain originating from pressure variations such as aboard airplanes and submarines and 5) Abfraction – oclusal hyperfunction or parafunction which may promote disruption of apatite crystals in the cervical regions of teeth. Other authors have classified these causes differently, but because of the importance of Barotrauma and Abfraction as causes of dentine hypersensitivity, we feel the need to emphasize these conditions.[8,12,13,15] The diagnosis of dentinal hypersensitivity has to consider the etiology and dental vitality and is what leads to the therapeutic choice and improves the possibility of the chosen treatment's success. Chemical treatments are mostly used, but they have limited efficiency in maintaining pain control and require periodical application of the chemical agent. This aspect led us to use LLLT in the treatment of dentinal hypersensitivity. The study's objective was to evaluate the efficiency of LLLT in the treatment of patients with dentinal hypersensitivity.

Materials and Methods: Clinical Application

This retrospective study reports the use of LLLT for treating patients suffering from dentinal hypersensitivity seen at the Laser Center of the Camilo Castelo Branco University; 1102 teeth of 388 patients were treated with LLLT (Laser Beam Company, Brazil) between 1995-2000. The Center treated 98 males and 290 females, 30 to 45 years old. All personnel involved in the study were well-trained graduates. Professors of the Laser Center oversaw all procedures and applications and safety procedures were respected.[22,23] Initial examination included an interview, assessment of tooth vitality with thermal stimuli (Endo-Frost®) (Fig. 2) and soft professional dental cleaning. An analogical visual scale assessed pain score and the tooth was dried with a cotton roll. LLLT was then applied perpendicular to the long axis of the tooth, CW, in a punctual manner. We chose 4 points of application in each tooth: 3 points in the vestibular surface of the incisors and canine teeth and 1 point in the lingual surface. In the premolar and molars: 2 points in the vestibular surface and 2 points in the lingual surface (Fig. 3). The pain score, again recorded as described previously, was repeated 7, 14, and 28 days after the last irradiation. If the patients no longer complained of pain after the first session the irradiation was not repeated, but they were reassessed up to 28 days after the first treatment. For LLLT, a diode laser was used at 780 nm, CW, 40 mW, elliptical area of the beam 2 mm^2, and exposure time per point 25 s. This corresponds to an equivalent dose of 50 J/cm^2 at each point (considering area of the spot). For a 1-cm^2 area, the total dose per tooth is 4 J/cm^2. With the diode laser 830 nm, CW, 50 mW, elliptical area of the beam was 2 mm^2, and the exposure time per point of 20 s, corresponding to an equivalent dose of 50 J/cm^2 at each point (considering area of the spot).

For a 1-cm^2 area, the total dose per tooth is 4 J/cm^2 (Fig. 4). Of the 1102 teeth, 58% were treated with 780 nm and 42% with 830 nm. All teeth were treated weekly with 4 J/cm^2. All lasers were certified and emission control was done every 6 months.

Results

Four aspects were considered in the analysis of the results: 1) the number of sessions required for reduction of the symptoms; 2) the number of treated teeth; 3) the most affected tooth; and 4) the number of sessions needed to observe improvement of the condition. Out of 1102, 403 (36.57%) required a single session for complete remission of the symptom; 255 (23.14%) needed two sessions; 182 (16.51%) three sessions; 107 (9.7%) four sessions; and 59 (5.35%) five sessions. Also, 96 (8.71%) did not respond to LLLT and the patients were reassessed and treatment changed (Table 1).

Table 1: Number of Sessions Required for Reduction of the Symptoms

NUMBER OF TEETH – 1102	100 %	NUMBER OF SESSION
403	36.57	01
255	23.14	02
182	16.51	03
107	9.70	04
59	5.35	05

The more affected tooth was lower premolar (301–27.4%), followed by lower molars (163–14.8%), upper premolar (149–13.5%), lower incisive (148–13.4%), upper canine (119–10.7%), upper incisive (108–9.9%), lower canine (62–5.6%), and upper molars (52–4.7%) (Table 2).

Table 2: Ratio of Hypersensitivity in Teeth Studied

GROUP OF TEETH	NUMBER OF TEETH	%
Lower premolar	301	27.4 %
Lower molars	163	14.8 %
Upper premolar	149	13.5 %
Lower incisive	148	13.4 %
Upper canine	119	10.7 %
Upper incisive	108	9.9 %
Lower canine	62	5.6 %
Upper molars	52	4.7 %
Total	1102	100 %

Previous Study: Histological Study

Previous studies were carried out by the authors[23] to evaluate histologically the reaction of the dentinal pulp in rats after LLLT was applied. Thirty-two upper molars from albinus rats with mechanically exposed dental pulps with standardized abrasion on the occlusal surface were treated with number 2 diamond burrs exposing dentinal tissues (~1 cm^2). The parameters of the laser were CW HeNe, 632.8 nm, 6 mW output, beam cross section 1.8 mm^2, and exposure time of 240 s in scanning mode each tooth, considering an occlusal area of approximately 1 cm^2. These were divided into 4 groups and were given weekly applications (Table 3).

Table 3: Classification of Groups, Number of Applications, Dose per Application, and Days Until Humanely Killed

GROUP	NUMBER OF APPLICATION PER TOOTH	DOSE APPLICATION PER TOOTH	DAYS FOR HUMANELY KILLED AFTER IRRADIATION
1	1	1.44 J/cm^2	7 days
1C	0	0	Same date as group 1
2	2	1.44 J/cm^2	7 days
2C	0	0	Same date as group 2
3	2	1.44 J/cm^2	14 days
3C	0	0	Same date as group 3
4	3	1.44 J/cm^2	14 days
4C	0	0	Same date as group 4

The results showed that irradiated animals presented an increased production of dentine and shutting of dentinal tubuli. On the other hand, non-irradiated subjects still showed signals of intense inflammatory reaction and even necrosis at the same experimental times. Irradiated teeth did not show cell degeneration. The LLLT was shown to be efficient in the stimulation of odontoblast cells, producing reparative dentin and closing dentin tubuli[6,28] (Figure 5).

Discussion

There is no previous report in literature with this number of teeth treated by LLLT. It is important to consider that only 388 (39.95%) of 972 patients referred to as suffering from dentinal hypersensitivity were properly diagnosed. Villa et al.[28] evaluated histologicaly the reaction of the dentinal pulp in rats after application of LLLT and results showed that irradiated animals presented an increased production of dentine and shutting of dentinal tubuli.
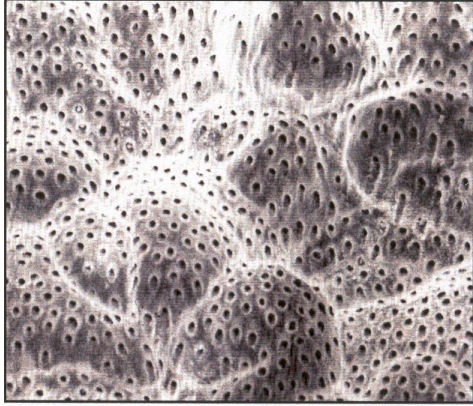
Figure 1: Human tooth, showing numerous dentin tubuli X 900. Courtesy Prof I. Watanabe. Scanning Electron Microscopy atlas of cells and tissue of the oral cavity, 1988.
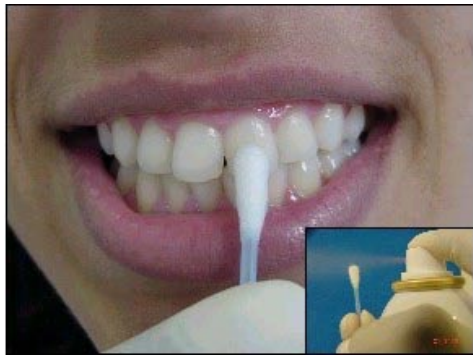
Figure 2: Assessment of the vitality of the tooth with thermal stimuli (Endo-Frost®).

Figure 3: Four points of application were chosen in each tooth. Three points in the vestibular surface of the incisors and canine teeth and one point in the lingual surface. In the premolar and molars: 2 points in the vestibular surface and 2 points in the lingual surface.

Figure 4: LLLT applied perpendicular to the long axis of the tooth, CW, in a punctual manner.
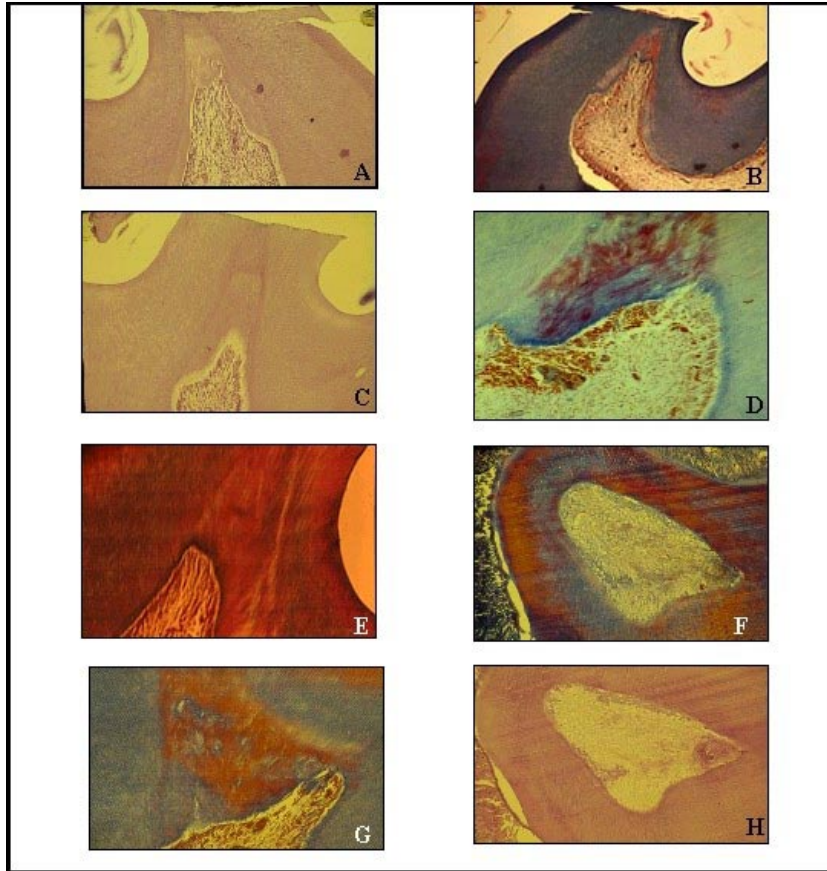
Figure 5: The intensity of the dentin neoformation in pictures 5A, 5C, 5E, 5G. The non-irradiated side in picture 5B and 5D showed intense inflamatory process. The non-irradiated side in picture 5F and 5H showed an intense degeneration evolving towards necrosis.
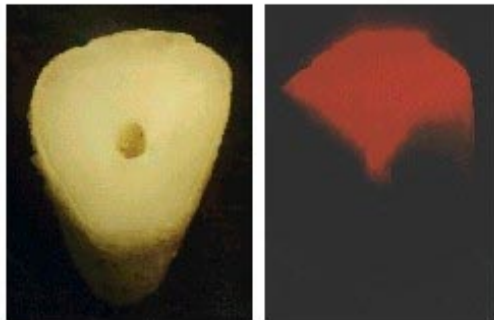
Figure 6: Transmission of laser beam into the tooth - Courtesy A.P. Sommer.

Matsumoto et al.[17] performed a histological study in monkeys with 64 teeth with exposed pulps (class V cavities). A 704-nm diode laser was used, CW, 30 mW, and exposure time of 30 s each tooth; 32 teeth were irradiated and all were controls. Histological analysis showed significant difference between the groups; irradiated ones were considered better than non-irradiated ones. In a clinical study, the same authors used a 780-nm diode Laser, 30 mW, with an exposure time of 30 s per tooth. They reported improvement in 85% when the irradiation was carried out directly over the dentine. In another group, the authors irradiated the tooth in the apical region; in these cases, the efficacy was about 60%, compared to other points of application. Matsumoto et al.[17], in another study, used an HeNe, CW, 6 mW, and exposure time of 60 s, beam cross sec-

tion 0.75 mm. In 90% of the cases, the treatment was considered effective when irradiation was carried out directly on the cervical area. When irradiation was carried out in other places, the effect was below 60% when compared to other sites of application. Direct irradiation of the pulp wall also favors an increased proliferation of odontoblasts and consequently higher dentine production. Aun et al.[2] showed a clinical study on the treatment of dentinal hypersensitivity using an HeNe laser, CW, 6 mW, beam cross section 1.8 mm^2, with an exposure time of 4 min per tooth in scanning mode on the vestibular area, test sample of 64 teeth. The patients received three applications with an interval of 7 days. The average pain duration under cold stimulation before and after irradiation was smaller. The initial duration of 6 s was reduced to close to 2 s immediately after the first application. After the second and third application, the average time was reduced to 1 s, a sixfold less value. It was also observed that between the first and second sessions (one week interval), the response time to stimuli was similar. Friedman's analysis showed a significant difference between the time before and after laser irradiation. These results confirmed that there was no pain between the sessions, demonstrating that improvement is long lasting. Brugnera, Jr. et al.[7] described the effect of laser therapy on hypersensitive dentinal which is divided into the following categories: 1) primary or immediate effect – remission of painful symptoms; and 2) secondary or late effect – intense cellular metabolic activity, profiling of odontoblast, production of reparative dentin and physiologic occlusion of the dentinal tube. According to Wakabayashi[27], the patient reports an immediate effect of LLLT directly after application of the same, in response to the increase in the nerve ending threshold of pain, attributed to the maintenance of the receptor membrane potential when not in use, by the suppression of the nerve ending fiber pulp potential. Kasai et al.[14] justifies the immediate analgesic effect as a consequence of the interruption of the nerve impulse path in the affected nerve fiber, concluding that the laser acts as a reversible suppressor directly on the neuronal activity. As Mezawa et al.[18] reported, the neuro-physiological mechanism responsible for the analgesic effect of the laser comes from the diminishing of the frequency of nerve ending stimuli observed in tests with electrodes on thermal nerve endings in cats' tongues after irradiation with the laser. LLLT interferes in the phenomenon of the transmission of peripheral nerve signals to the central nervous system, where these are interpreted. The maintenance of this analgesic state on the dentine comes from the sealing of dentinal tubuli, which impedes the internal communication of the pulp with the external – the oral fluids. The authors concluded that LLLT was effective on 97% of the cases. It was observed in the literature that several reports did not present all the parameters, which makes comparison even more difficult. One must consider that a recent study by Sommer[26] indicates that light energy density and intensity are biologically independent irradiation parameters, suggesting that LLLT's success or failure may be linked to the correct way to irradiate the application field with light. Many authors had questions as to whether the laser light really reached the dentine pulp. Sommer et al.[25] clarified this, as well as *how* the light reached the pulp. These authors also observed that laser light is focused toward the pulp by the inter-tubular dentine, respectively by the highly regular light conducting wave guide structure of the

dentin. Note that light travels parallel to, but not through, the tubuli.[11,25,26] The histological studies in Figure 6 demonstrate this directional light transmission phenomenon in human dentine (courtesy A.P. Sommer). This is an important finding which adds weight and credibility to the use of the laser on teeth.[11,25,26]

Conclusion

The result of the present investigation demonstrates indeed that LLLT, when based on the use of correct irradiation parameters, is effective in treating dentinal hypersensitivity as it quickly reduces pain and maintains a prolonged painless status. The authors concluded that the use of LLLT was effective on 91.27% of the cases.

References

1. Addy, M. and Urquhart, E. (1992). Dentine hypersensitivity: its prevalence, aetiology and clinical management. Dent Update, Dec; 19 (10): 407-8, 410-2. Review.

2. Aun, C.A.; Brugnera, A.J. and Villa, R.G. (1988). Raio Laser – Hipersensibilidade dentinária, Revista da APCD, 43 (2), 161-162.

3. Brännströn, M. (1986). The hydrodynamic theory of dentinal pain: sensation in preparations, caries and dentinal crack. J Endod., 12, 475-81.

4. Brännströn, M. (1965). The surface of sensitive dentine. Odont. Revy, 16, 293-9.

5. Brugnera Junior, A. (1998). Personal communication.

6. Brugnera Junior, A., Villa, R. Aun, CE.. (1992). Proceedings of the 3rd International Congress on Laser in Dentistry - Salt Lake City/USA. 126-128.

7. Brugnera Junior, A., Cruz, F.M., Zanin, F et al. (1998). Proceedings of the 6th International Congress on Laser in Dentistry. Hawai/USA. 157-159.

8. Coleman, T.A. and Kinderknecht, K.E. (2000). Cervical dentin hypersensitivity. Part I: The air indexing method. Quintessence Int. Jul-Aug; 31 (7): 466-73.

9. Cuenin, M.F.; Scheidt, M.J.; O´Neil, R.B.; Strong, S.L.; Pashley, D.H.; Horner, J.A. and Van Dyke, T.E. (1998). An in vivo study of dentin sensitivity: the relation of dentin sensitivity and patency of dentinal tubulis. J Periodontol, Nov; 62 (11):668-73.

10. Fischer, C.; Fischer, R.G.; and Wennberg. (1992). Prevalence and distribution of cervical dentine hypersensitivity in a population in Rio de Janeiro, Brazil. J. Dent. 20, 272-276.

11. Gente, M., Sommer, A. P. and Hoff, N., (2000), Light propagation in Dentin. 9th International Congress - Laser - No other alternatives, February 25-27, Frankfurt/Germany.

12. Goeth, W.H.; Bater, H. and Laban, C. (1989). Barodontalgia and barotraumas in the human teeth: findings in navy divers, frogmen and submarines of the Federal Republic of Germany. Mil Med; 154(10):491-5.

13. Holowatyj, R.E.(1996). Barodontalgia among flyers: a review of seven cases.J. Can Dent Assoc; 62(7):578-84.

14. Kasai S; Kono T; Yamamoto Y; Kotani H; Sakamoto T; Mito M. Effect of low power laser irradiation on impulse conduction in anesthetized rabbits. J. Clin Laser Med Surg, 1996; 14:107-13.

15. Kollmann, W.(1993). Incidence and possible causes of dental pain during simulated high altitude flights. J. Endod; 19(3): 154-9.

16. Liu, H.C.; Lan, W.H. and Hsieh, C.C. (1998). Prevalence and distribuition of cervical dentin hypersensitivity in a population in Tapei, Taiwan. J. Endod. Jan; 24 (11): 45-7.

17. Matsumoto, K.; Tomunari, H. And Bayashi, h. (1985). Study on the treatment of hypersensitive dentine by laser. Jap. J. Conservat. Dent., 28 (4), 208 ago.

18. Mezawa S; Iwata K; Naito K; Kamogawa H. The possible analgesic effect of soft-laser irradiation on heat nociceptors in the cat tongue. Archs Oral Biol, 1988; 33(9): 693- 4.

19. Pashey, D.H. (1979). The influence of dentin permeability and pupal blood flow on the pulp solute concentration. J Endod., 5(12) 355-356, Dec.

20. Pashley, D.H. (1992) Dentin permeability and dentin sensitivity. Proc Finn Dent Soc, 88, suppl I, 31-37.

21. Pécora, J.D. Complexodentina-polpa (http://www.forp.usp.br/restauradora/dentin.html) (2001).

22. Pinheiro, A.L.B. (1995). Normas de Segurança na utilização de lasers de CO_2. Rev. Bras. Med.,43 (11) 227-31.

23. Pinheiro, A.L.B. (1996). Normas de segurança na utilização de lasers em biomedicina. Rev. Bras. Med., 53 (11), 1133-6.

24. Renton-Harper, P. and Midda, M. (1992). Nd:YAG laser treatment of dentinal hypersensitivity. Br Dent J. Jan 11; 172 (1): 13-6.

25. Sommer, A. P. and Gente, M.(1999). Light-Induced Control of Polymerisation Shrinkage of Dental Composites by Generating Temporary Hardness Gradients. Biomed. Tech. 44 (10), 290-293.

26. Sommer, A. P., (2001) Personal communication.

27. Wakabayashi H; Hamba M; Matsumoto K; Tachibana H. Effect of irradiation by semiconductor laser on responses evoked in trigeminal caudal neurons by tooth pulp stimulation. Lasers Surg Med, 1993; 13:605-10.

28. Villa, R.; Brugnera Junior, A. and Aun, C. E. (1988). Estudo histologico da atuação do raio Laser He:Ne na neoformação dentinária em polpa de ratos. Proceedings of SBPqO, p.101.

29. Zanin, F; Brugnera Junior, A. (1998). In Brugnera Junior, A. & Pinheiro, A.Lasers na Odontologia Moderna, 297-306.

30. Zappa, U. (1994). Self-applied treatments in the management of dentine hypersensitivity. Arch Oral Biol. 39, Suppl: 107S-112S. Review.

THE USE OF NASA LIGHT-EMITTING DIODE NEAR-INFRARED TECHNOLOGY FOR BIOSTIMULATION

Harry T. Whelan

Medical College of Wisconsin, Milwaukee, WI
NASA Marshall Space Flight Center, Alabama, USA

Introduction

This work is supported and managed through the NASA Marshall Space Flight Center - SBIR Program. Studies on cells exposed to microgravity and hypergravity indicate that human cells need gravity to stimulate growth. As the gravitational force increases or decreases, the cell function responds in a linear fashion. This poses significant health risks for astronauts in long-term spaceflight. The application of light therapy with the use of NASA LEDs will significantly improve the medical care that is available to astronauts on long-term space missions. NASA LEDs stimulate the basic energy processes in the mitochondria (energy compartments) of each cell, particularly when near-infrared light is used to activate the color sensitive chemicals (chromophores, cytochrome systems) inside. Optimal LED wavelengths include 680, 730 and 880 nm and our laboratory has improved the healing of wounds in laboratory animals by using both NASA LED light and hyperbaric oxygen. Furthermore, DNA synthesis in fibroblasts and muscle cells has been quintupled using NASA LED light alone, in a single application combining 680, 730 and 880 nm each at 4 Joules per centimeter squared. Muscle and bone atrophy are well documented in astronauts, and various minor injuries occurring in space have been reported not to heal until landing on Earth. An LED blanket device may be used for the prevention of bone and muscle atrophy in astronauts. The depth of near-infrared light penetration into human tissue has been measured spectroscopically. Spectra taken from the wrist flexor muscles in the forearm and muscles in the calf of the leg demonstrate that most of the light photons at wavelengths between 630-800 nm travel 23 cm through the surface tissue and muscle between input and exit at the photon detector. The light is absorbed by mitochondria where it stimulates energy metabolism in muscle and bone, as well as skin and subcutaneous tissue. Long-term spaceflight, with its many inherent risks, also raises the possibility of astronauts being injured performing their required tasks. The fact that the normal healing process is negatively affected by microgravity requires novel approaches to improve wound healing and tissue growth in space. NASA LED arrays have already flown on Space Shuttle missions for studies of plant growth and the U.S. Food and Drug Administration (FDA) has approved human trials. The use of light therapy with LEDs can help prevent bone and muscle atrophy as well as increase the rate of wound healing in a microgravity environment, thus reducing the risk of treatable injuries becoming mission catastrophes.

Spaceflight has provided a laboratory for studying wound healing problems due to microgravity, which mimic traumatic wound healing problems here on Earth. Improved

wound healing may have multiple applications that benefit civilian medical care, military situations and long-term spaceflight. Enhancing the soldier's tissue responses to injury may lead to battlefield resilience and medical independence. Counter-measures to chemical, biological and radioactive weapons exposures, which are based on biostimulation of natural tissue regeneration mechanisms could be more universally safe and effective than conventional drugs and surgical modalities. Regeneration of wounded organs and limbs may also be possible if biostimulation could re-awaken molecular events leading to re-growth of tissue.

Central nervous system regeneration would be of particular benefit. Thus far, we have demonstrated that the best results for wound healing occur at wavelengths of 670 nm and 880 nm using energy densities 4-8 J/cm^2, applied at power intensities of approximately 50 mW/cm^2. However, studies to determine molecular mechanisms could lead to the optimization for current uses, as well as open up new applications.

Despite numerous reports on the benefits of near-IR on wound healing and rehabilitation over the last decade, the basic mechanisms of its action remain poorly understood. Britton Chance's group has reported that about 50% of near-IR light is absorbed by mitochondrial chromophores, such as cytochrome oxidase. However, the underlying cellular and molecular events are still unknown (Karu 1999, Sommer et al. 2001, Whelan et al. 1999, 2000, 2001).

Methods

In order to better understand the effects of LEDs on cell growth and proliferation, we have measured radiolabeled thymidine incorporation in vitro in several cell lines and animals treated with LED light at various wavelengths and energy levels, including 670, 730, 880 nm, 50 mW/cm^2, 4-8 J/cm^2. These data are important demonstrations of cell-to-cell contact inhibition, which occurs in vitro once cell cultures approach confluence. This is analogous, in vivo, to a healthy organism, which will regenerate healing tissue, but stop further growth when healing is complete. It is important to note that LED treatment accelerates normal healing and tissue regeneration without producing over-growth or neoplastic transformation. In addition, we have recently begun using NASA LEDs to promote healing of acute oral lesions in pediatric leukemia patients. A 4-J/cm^2, 50-mW/cm^2 dose of 670-nm light from LEDs was applied daily to the outside of each of 15 patients at the left cheek beginning on the day of bone marrow transplantation. The status of their oral mucosa, mouth, and throat pain were assessed three times a week by two calibrated dental clinicians. Throat pain was consistently higher than mouth pain, and because our light does not extend into this region, we have used this pain as our control. Although mouth and throat pain were initially similar, mouth pain peaked at 86% of throat pain on day 5 after transplant and subsequently fell to only 53% of reported throat pain by day seven. The greatest difference between throat and mouth pain was reported on day seven, when, surprisingly, oral mucosal ulceration is believed to be worst in untreated patients.

Military Special Operations are characterized by lightly equipped, highly mobile troops entering situations requiring optimal physical conditioning at all times. Wounds are an obvious physical risk during combat operations. Any simple and lightweight equipment that promotes wound healing and musculoskeletal rehabilitation and conditioning has potential merit. An LED array with 3 wavelengths combined in a single unit (670, 720, and 880 nm) was delivered to Naval Special Warfare Group-2 (SEALS) in Norfolk, VA. Treatment was 4 J/cm^2, 10 mW/cm^2.

Results and Discussion

Near infrared (IR) light has documented benefits promoting wound healing in human and animal studies. Our preliminary results have also demonstrated two to five-fold increases in growth-phase-specific DNA synthesis in normal fibroblasts, muscle cells, osteoblasts, and mucosal epithelial cells in tissue cultures treated with near-IR light. Our animal models treated with near-IR have included wound healing in diabetic mice and ischemic bipedical skin flap in rats. Near-IR induced a thirty percent increase in the rate of wound closure in these animal models. Dose- and time-dependent increases in vascular endothelial growth factor (VEGF) and fibroblast growth factor (FGF-2) occurred in animals treated with near-IR. Human studies have included the use of near-IR to prevent ulcerative mucositis resulting from high doses of chemotherapy and radiation. Widely published reports, including those from our laboratory, described accelerated recovery from musculoskeletal injuries, hypoxic-ischemic wounds, burns, lacerations, radiation necrosis, and diabetic ulcers with the use of near-IR. Lasers have some inherent characteristics, which make their use in a clinical setting problematic, including limitations in wavelength capabilities and beam width. The combined wavelengths of light optimal for wound healing cannot be efficiently produced, and the size of wounds which may be treated by lasers is limited. Light-emitting diodes (LEDs) developed for NASA crewed spaceflight experiments offer an effective alternative to lasers. These diodes can be made to produce multiple wavelengths, and can be arranged in large, flat arrays allowing treatment of large wounds.

Conclusion

We are now investigating new collaborations with the Defense Advanced Research Projects Agency (DARPA) for military applications of LED wound healing technology in military medicine. Several uniquely military situations and indications could be addressed, optimizing near-IR parameters for wound healing via LEDs during extended missions under conditions separated from medical personnel. These include burns, chemical agents, radiation, biological agents and highly infected flesh-eating wounds (with and without extended burns) typical for the hygienic conditions occurring in battle fields, also infectious diseases and external wounds occurring in environments with no solar irradiation, low oxygen and high carbon dioxide (submarines). The dramatic results with use of near-IR LED light to prevent digestive mucosal lesions (mucositis) and pain in cancer patients, after high-dose chemotherapy and radiation, suggest the potential for

military use of near-IR light to treat U.S. troops exposed to chemical and radioactive warfare agents in the field. These examples illustrate the many possible military uses for this technology. These life-saving applications require especially accelerated wound healing, rapid reduction of infections and pain modulation. Regeneration of muscles in amphibians has also been produced by near-IR therapy. The potential for regeneration of human tissue also deserves study.

Lasers have some inherent characteristics, which make their use in a clinical setting problematic, including heat, limitations in wavelength capabilities and beam width. The combined wavelengths of the light for optimal wound healing cannot be efficiently produced. The size of wounds which may be treated is limited (due to laser production of a narrow beam of light; a fact inconsistent with treating large areas), heat production from the laser light itself can actually damage tissue, and the pin-point beam of laser light can damage the eye. NASA-developed LEDs offer an effective alternative to lasers. NASA's interest is dependent on chronic care due to tissue breakdown in microgravity for spaceflight. Military research with these LEDs, in contrast, will be directed to new LED technology aimed at rapid battlefield wound repair. These diodes can be configured to produce multiple wavelengths, can be arranged in large, flat arrays (allowing treatment of large wounds), and produce no heat. It is also important to note that LED light therapy has been deemed to be a non-significant risk by the FDA.

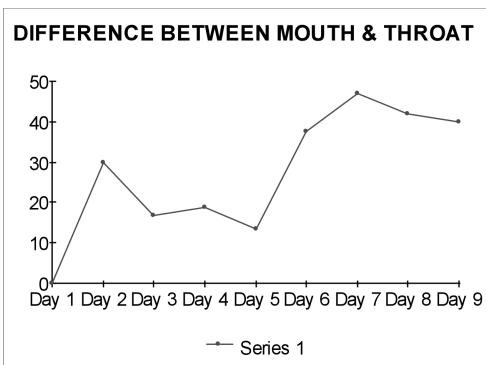**Figure 1**: The difference between LED-treated (mouth) and untreated control (throat) becomes more dramatic over time, with daily treatment using NASA LED at 670 nm, 50 mW/cm^2, 4 J/cm^2.

Figure 2: Cumulative results of data from 11 patients (SEALS) showing improvement in range of motion, pain, and girth reported as % change from chronic, unimproving injured baseline after LED treatment at 4 J/cm^2, 10mW/cm^2
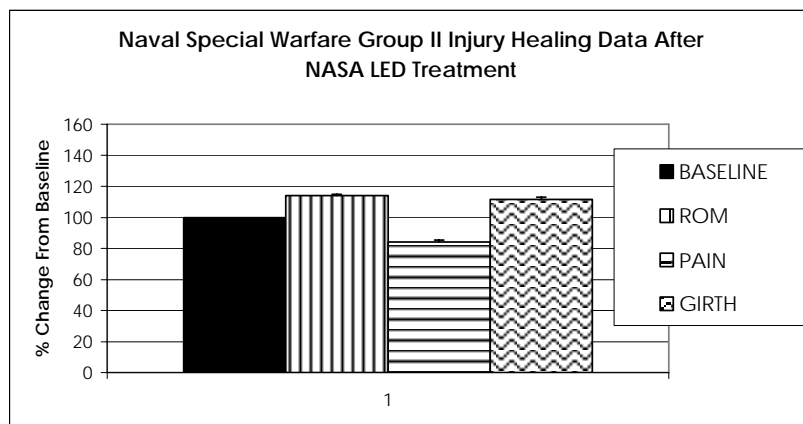
Group	Day 1	Day 3	Day 7	Day 12	Day 17
Control	100	73.5 ± 7.9	41.4 ± 8.4	20.4 ± 3.8	12.4 ± 2.9
LED only	100	69.2 ± 5.7	33.2 ± 6.2	14.1 ± 3.7	8.1 ± 2.0

Figure 3: Percent of original wound area in experimental controls and LED treated rats.
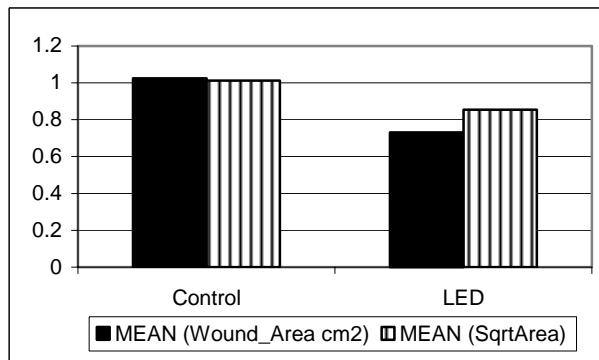
Figure 4: Type II Diabetic Mice with excisional skin wounds treated with 3 LED wavelengths, 50 mW/cm^2, 4 J/cm^2. The square root of wound area is used in the dependent variable in the analysis. This transformation was needed to correct for non-constant error in the General Linear Model. SqrtArea could be interpreted as being proportional to the radius of a circular wound.
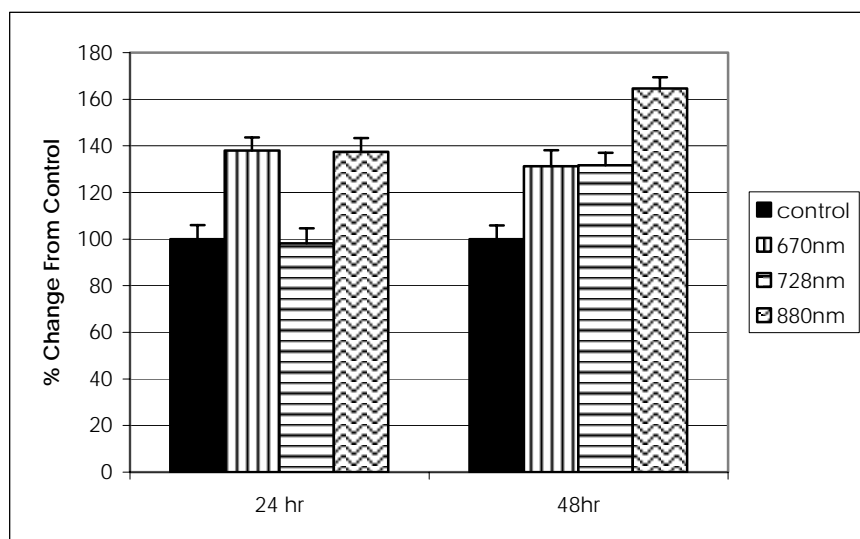
Figure 5. 3T3 Fibroblast DNA Synthesis 8 J/cm^2, 50 mW/cm^2, individual wavelengths. 24- and 48-hour ^{3}H thymidine incorporation.

Figure 6. 3T3 Fibroblast DNA synthesis 3-hour incubation; LED 50 mW/cm^2; 4, 8, 12 J/cm^2.
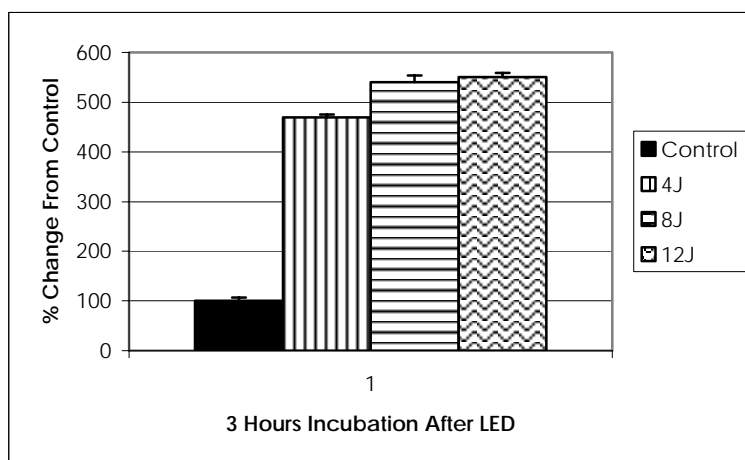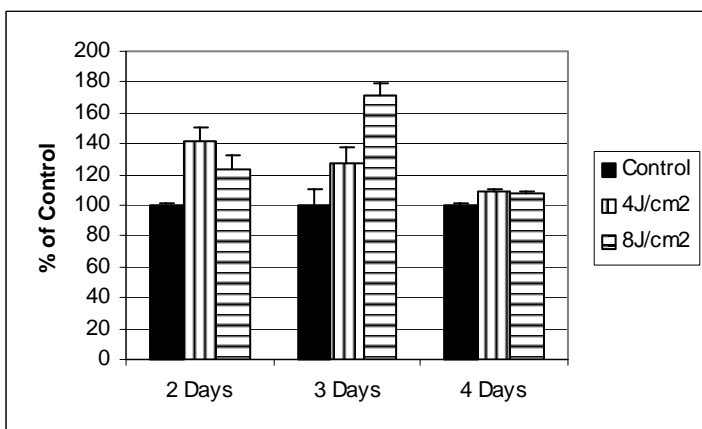
Figure 7: Growth phase specificity of 3T3 fibroblasts; combined wavelengths; 50 mW/cm^2; 4 J/cm^2 vs. 8 J/cm^2.

Figure 8: Growth phase specificity of L-6 cells treated at 50 mW/cm^2; 8 J/cm^2.
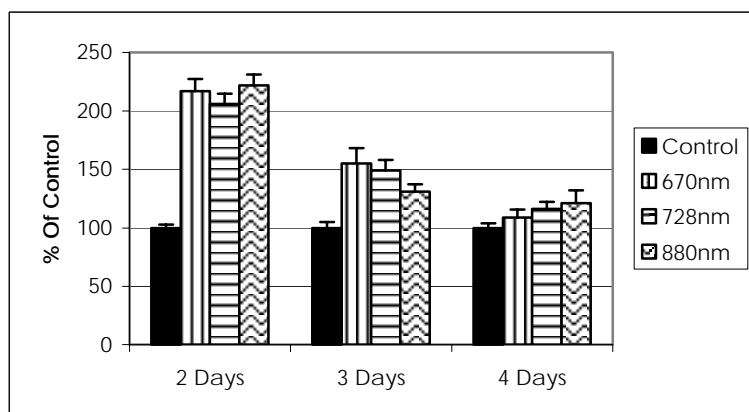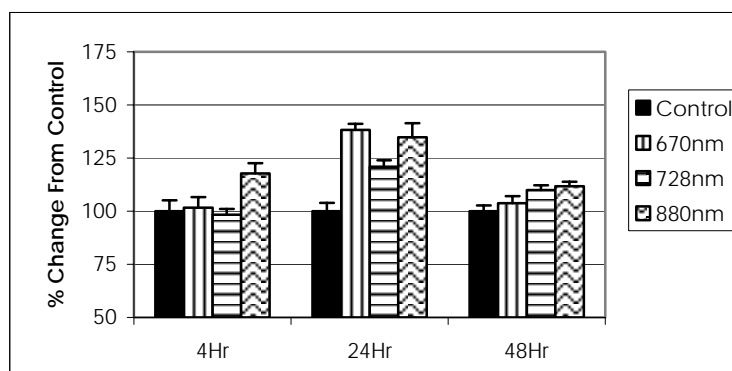
Figure 9: Growth phase specificity of osteoblasts; individual wavelengths; 50 mW/cm^2, 8 J/cm^2.

Figure 10: Growth phase specificity of HaCAT epithelial cells treated with individual wavelengths at 50 mW/cm^2, 8 J/cm^2.
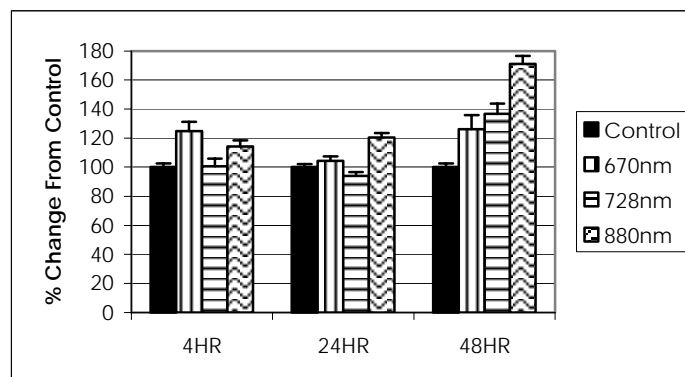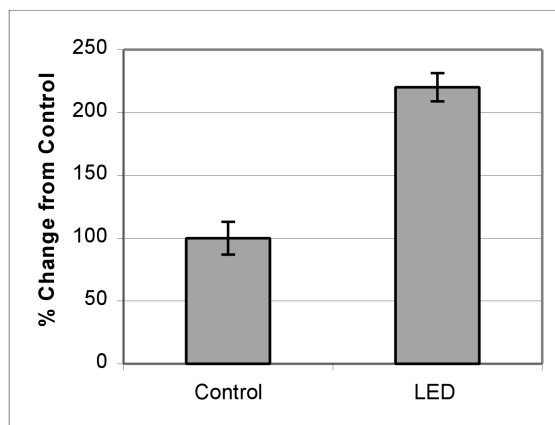
Figure 11: HaCAT epithelial cell collagen synthesis 50 mW/cm^2, 8 J/cm^2, 670 nm. 24-hour ^{3}H proline incorporation.

Figure 12: Change in wound size in rat ischemic wound model vs. time (days).
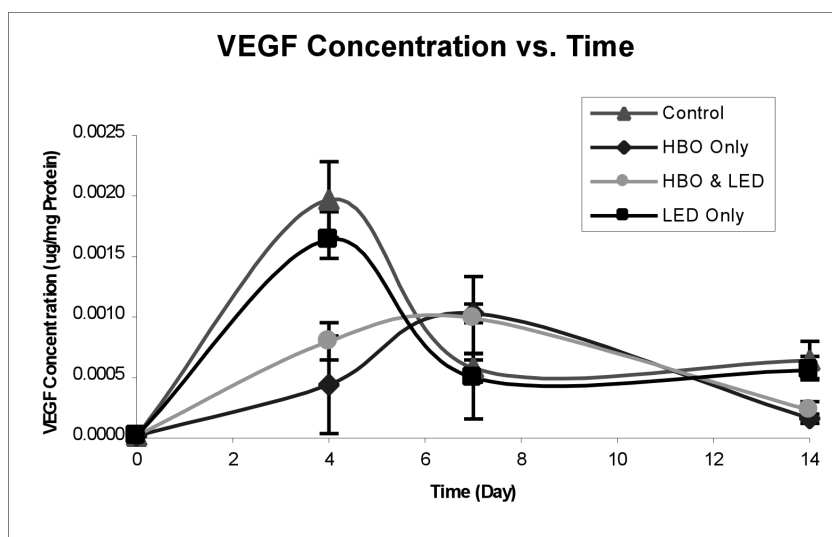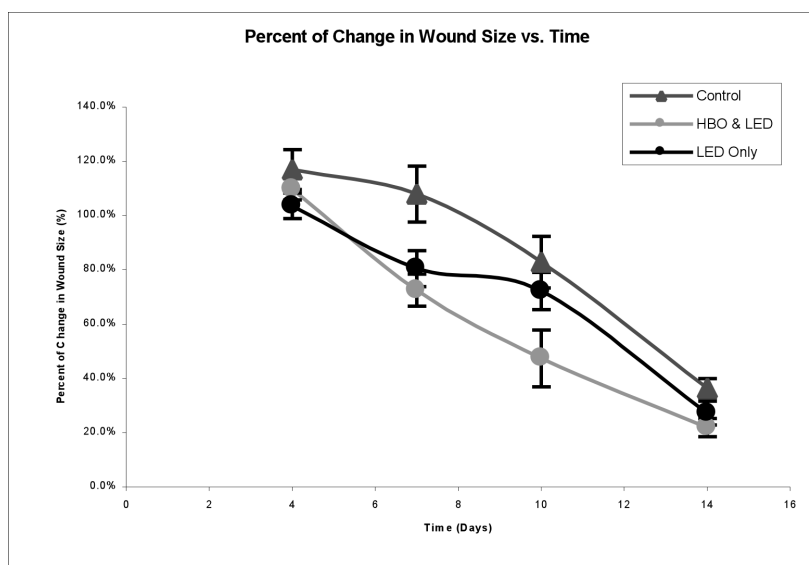
Figure 13: Change in vascular endothelial growth factor (VEGF) concentration (μg/mg protein) vs. time (days) in rat ischemic wound model.
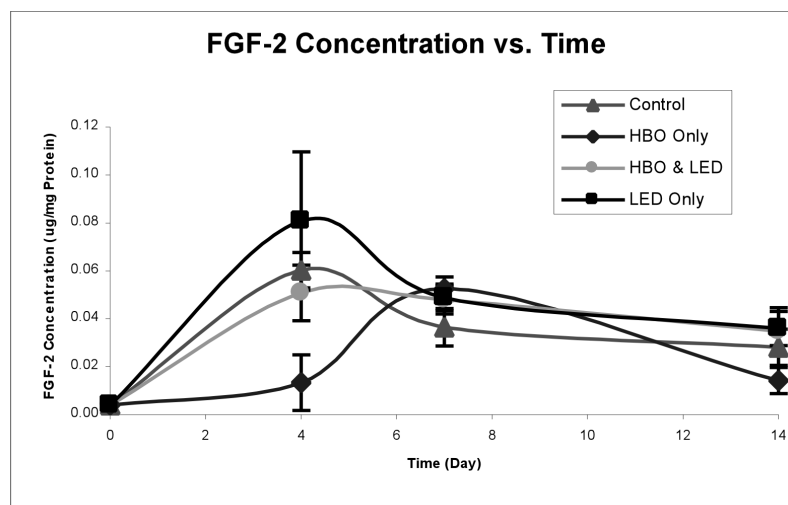
Figure 14: Change in basic fibroblast growth factor (FGF-2) concentration (µg/mg protein) vs. time (days) in rat ischemic wound model.

References

Karu T., "Primary and secondary mechanisms of action of visible to near-IR radiation on cells." *J. Photochem. Photobiol. B. Biol.* 49,1-7 (1999*).*

Sommer A.P., Pinheiro A.L., Mester A.R., Franke R.P., Whelan H.T. "Biostimulatory windows in low intensity laser activation: Lasers, scanners and NASA's light emitting diode array system." *Journal of Clinical Laser Medicine & Surgery* 19, 27-33 (2001).

Whelan H.T., Houle J.M., Donohoe D.L., Bajic D.M., Schmidt M.H., Reichert K.W., Weyenberg G.T., Larson D.L., Meyer G.A., Caviness J.A., "Medical Applications of Space Light-Emitting Diode Technology-Space Station and Beyond." *Space Tech. & App. Int'l. Forum* 458, 3-15 (1999).

Whelan H.T., Houle J.M., Whelan, N. T., Donahue, D. L., Cwiklinski, J., Schmidt, M. H., Gould, L., Larson, D. L., Meyer, G. A., Cevenini, V., and Stinson, H."The NASA Light-Emitting Diode Medical Program- Progress in Space Flight and Terrestrial Applications." *Space Tech. & App. Int'l. Forum* 504, 37-43 (2000).

Whelan H.T., Buchmann E.V., Whelan N.T., Turner S.G., Cevenini V., Stinson H., Ignatius R., Martin T., Cwiklinski J., Meyer G.A., Hodgson B., Gould L., Kane M., Chen G., Caviness J. "NASA light emitting diode medical applications: From deep space to deep sea." *Space Tech. & App. Int'l Forum* 552, 35-45 (2001).

Whelan HT, Smits RL, Buchmann EV, Whelan NT, Turner SG, Margolis DA, Cevenini V, Stinson H, Ignatius R, Martin T, Cwiklinski J, Philippi AF, Graf WR, Hodgson B, Gould L, Kane M, Chen G, Caviness J: Effect of NASA Light-Emitting Diode (LED) Irradiation on Wound Healing. *Journal of Clinical Laser Medicine and Surgery*. 19, 305-314 (2001)*.*

Acknowledgments

EFFECT OF 670-NM LIGHT-EMITTING DIODE LIGHT ON NEURONAL CULTURES

Margaret T.T. Wong-Riley[1] and Harry T. Whelan[2]

[1]Department of Cell Biology, Neurobiology and Anatomy
[2]Department of Neurology,
Medical College of Wisconsin, Milwaukee, Wisconsin, USA

Introduction

Light close to and within the near infrared range has documented benefits for promoting wound healing in human and animal studies (Conlan et al., 1996; Yu et al., 1997; Sommer et al., 2001). Our preliminary results using light-emitting diodes (LEDs) in this range have also demonstrated two- to five-fold increases in growth-phase-specific DNA synthesis in normal fibroblasts, muscle cells, osteoblasts, and mucosal epithelial cells in tissue cultures (Whelan et al., 2001). However, the mechanisms of action of such light on cells are poorly understood.

Britton Chance's group reported that about 50% of near-infrared light is absorbed by mitochondrial chromophores such as cytochrome c oxidase (Beauvoit et al., 1994), which is the terminal enzyme of the electron transport chain (Wikstrom et al., 1981). Karu's extensive review (1999) indicated that cytochrome oxidase is a key photoacceptor when cells are irradiated with monochromatic red to near-infrared radiation. Cytochrome oxidase is an integral membrane protein and contains four redox active metal centers and has a strong absorbance in the red to near-infrared range detectable in vivo by near-infrared spectroscopy (Cooper and Springett, 1997).

Cytochrome c oxidase (EC 1.9.3.1) is the terminal enzyme of the electron transport system of all eukaryotes, oxidizing its substrate cytochrome c and reducing molecular oxygen to water. It is an important energy-generating enzyme critical for the proper functioning of almost all cells, especially those of highly oxidative organs such as the brain. The level of energy metabolism in neurons is closely coupled to their functional activity, and cytochrome oxidase has proven to be a sensitive and reliable marker of neuronal activity (reviewed in Wong-Riley, 1989).

We hypothesized that the therapeutic effects of such light result from the stimulation of cellular events associated with increases in cytochrome oxidase activity. As a first step in testing our hypothesis, we subjected primary neuronal cultures to impulse blockade by tetrodotoxin (TTX), a voltage-dependent sodium channel blocker, and applied LED light at 670 nm to determine if it could partially or fully reverse the reduction of cytochrome oxidase activity by TTX. The wavelength and parameters were previously tested to be beneficial for wound healing (Whelan et al., 2001).

Methods

Primary neuronal cultures from postnatal day 3-4 rat visual cortex were grown on coverslips inverted onto a glial feeder layer; the two were separated from each other by small wax spheres (Zhang and Wong-Riley, 1999; modification of Goslin and Banker, 1991). The replication of non-neuronal cells was inhibited by cytosine arabinoside, a DNA synthesis blocker. Three culture age groups were used at the start of the experiments: early (5th to 6th day of culture), middle (11th to 12th day), and late (15th to 16th day) groups. The purpose was to determine if the effects observed were age-dependent. Within each age group, cultures were subdivided into a) Control; b) TTX exposure for 6 days; c) TTX exposure for 6 days and LED treatment once per day for the last 5 of the 6 days; and d) LED treatment without TTX, once per day for 5 days. For the early group, we also tested for the effect of one-time LED treatment on the last day of TTX exposure. All experiments were repeated six times.

We used a GaAlAs light emitting diode (LED) array of 670 nm wavelength (bandwidth of 25-30 nm at 50% power), power intensity of 50 mW/cm^2, and energy density of 4 joules/cm^2 when applied for 1 minute and 20 seconds. The wavelength and parameters were previously determined to be beneficial for wound healing.

Cytochrome oxidase reactions were performed as described previously (Wong-Riley, 1979; Zhang and Wong-Riley, 1999). Reaction product of cytochrome oxidase activity was measured by optical densitometry via a Zeiss Zonax MPM 03 photometer. Multiple, two-micron spot-size readings were taken from the cytoplasm of each cell. Between 150-300 cells were measured from each group, using a 25x objective lens. The background was subtracted by setting zero over a blank area (without cells) in each slide, and all lighting conditions, magnifications, and reference points were kept constant. Two-tailed Student's t test for paired comparisons and analysis of variance (ANOVA) for group comparisons were used to analyze differences between treated and untreated groups. Results were expressed as mean ± SEM. A probability of 0.01 or less was considered significant.

Results and Discussion

Results indicated that primary neurons in culture were heterogeneous in size, shapes, and levels of cytochrome oxidase activity. They were classified into three metabolic cell groups: dark, moderate, and lightly reactive for cytochrome oxidase. TTX caused a significant reduction in enzyme levels of all neurons examined, without causing detectable changes in cell size, shape, or viability. This is in agreement with our previous findings (Zhang and Wong-Riley, 1999). In the presence of six days of TTX, 670 nm LED light treatment at 1 min 20 sec per day for five days led to a reversal of the TTX effect, such that cytochrome oxidase levels in all cells reached control levels (Fig. 1). Comparable results were obtained in all three age groups examined: early, middle, and late.
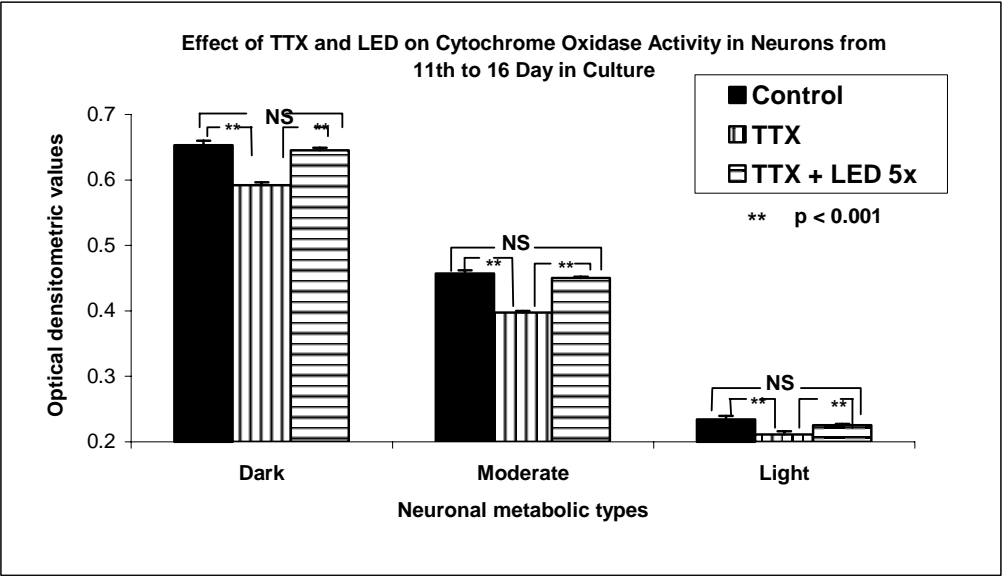
Figure 1

LED treatment alone for five days without the presence of TTX induced an up-regulation of cytochrome oxidase activity that was significantly higher than that of control sister cultures (Fig. 2). To our surprise, a single treatment of LED on control neurons or neurons that had been inactivated by TTX for 5 days brought about a significant increase in cytochrome oxidase activity in darkly reactive neurons, though not in moderately or lightly reactive neurons. This increase, however, did not reach control levels, indicating an incomplete reversal.
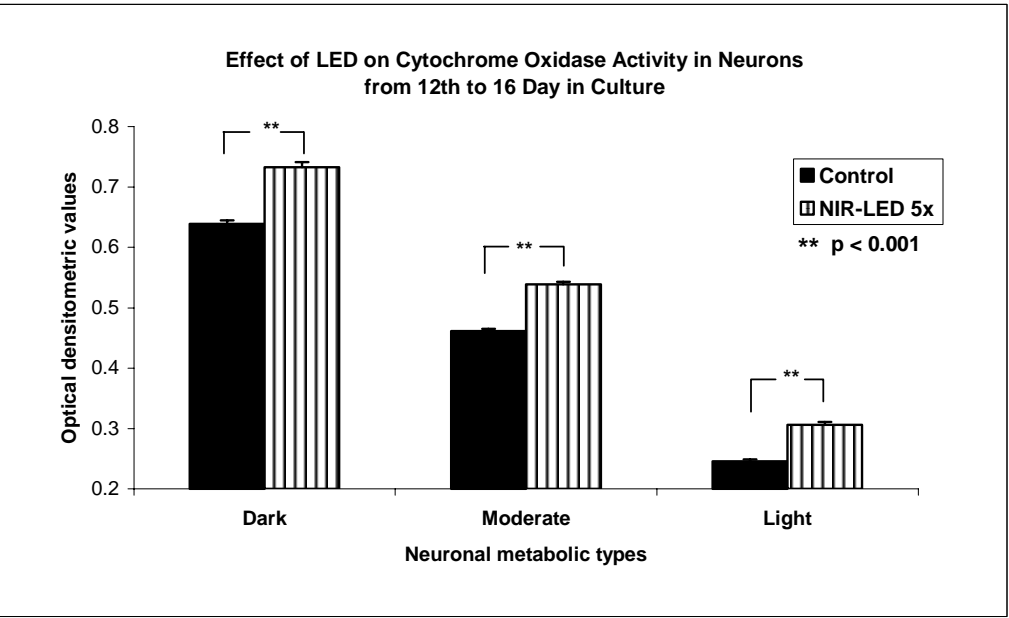
Figure 2

42

The fact that LED applications of only 1 minute and 20 seconds over a 24 hour period was able to activate and sustain elevated levels of cytochrome oxidase activity during that period indicates that a cascade of events must have been triggered by the initial activation of the enzyme. These events may include the activation of immediate early genes, transcription factors (Zhang and Wong-Riley 2000a), cytochrome oxidase subunit gene expressions (Zhang and Wong-Riley 2000b), subunit protein synthesis, and other metabolic pathways. Future studies will be directed at testing other wavelengths with LED arrays and probing the molecular mechanisms underlying the activation of cytochrome oxidase in neurons by LED.

References

Beauvoit B, Kitai T and Chance B. Contribution of the Mitochondrial Compartment to the Optical Properties of the Rat Liver: A Theoretical and Practical Approach, Biophys J 67, 2501-2510 (1994).

Conlan MJ, Rapley JW and Cobb CM. Biostimulation of Wound Healing by Low-Energy Laser Irradiation, J Clin Periodont 23, 492-496 (1996).

Cooper CE and Springett R. Measurement of cytochrome oxidase and mitochondrial energetics by near-infrared spectroscopy. Philos Trans R Soc Lond B Biol Sci 352, 669-676 (1997).

Goslin K and Banker G. "Rat hippocampal neurons in low-density culture". In Banker G and Goslin K, eds. Culturing nerve cells. Cambridge: The MIT Press, 1991:251-281.

Karu T. Primary and secondary mechanisms of action of visible to near-IR radiation on cells, J Photochem Photobiol B: Biol 49, 1-17 (1999).

Sommer AP, Pinheiro ALB, Mester AR, Franke RP and Whelan HT. Biostimulatory windows in low intensity laser activation: lasers, scanners and NASA's light emitting diode array system. J Clin Laser Med Surg 19, 29-33 (2001).

Whelan HT, Buchmann EV, Whelan NT, Turner SG, Cevenini V, Stinson H, Ignatius R, Martin T, Cwiklinski J, Meyer GA., Hodgson B, Gould L, Kane M, Chen G, and Caviness J. NASA light emitting diode medical applications: From deep space to deep sea. Space Tech. & App Int'l Forum 552, 35-45 (2001).

Wikstrom M, Krab K and Saraste M. Cytochrome Oxidase. A Synthesis. Academic Press (1981).

Wong-Riley M. Changes in the visual system of monocularly sutured or enucleated cats demonstrable with cytochrome oxidase histochemistry. Brain Res. 171, 11-28 (1979).

Wong-Riley MTT. Cytochrome oxidase: an endogenous metabolic marker for neuronal activity. Trends Neurosci 12, 94-101 (1989).

Yu W, Naim JO, and Lanzafame RJ. Effects of Photostimulation on Wound Healing in Diabetic Mice. Lasers Surg Med 20, 56-63 (1997).

Zhang C and Wong-Riley M. Expression and regulation of NMDA receptor subunit R1 and neuronal nitric oxide synthase in cortical neuronal cultures: Correlation with cytochrome oxidase. J Neurocytol 28, 525-539 (1999).

Zhang C and Wong-Riley M. Depolarization stimulation upregulates GA-binding protein in neurons: a transcription factor involved in the bigenomic expression of cytochrome oxidase subunits. Eur J Neurosci 12, 1013-1023 (2000a).

Zhang C and Wong-Riley M. Synthesis and degradation of cytochrome oxidase subunit mRNAs in neurons: Differential bigenomic regulation by neuronal activity. J Neurosci Res 60, 338-344 (2000b).

Acknowledgments

A MULTI-DIMENSIONAL PLATFORM TECHNOLOGY FOR NON-INVASIVELY ASSESSING TISSUE FUNCTION: NEAR INFRARED FREQUENCY DOMAIN SPECTROSCOPY

William W. Mantulin

Laboratory for Fluorescence Dynamics
University of Illinois at Urbana/Champaign, Urbana, Illinois, USA

Abstract

Near infrared (near IR) light penetrates deep into human tissue thereby permitting non-invasive examination of interior regions of the anatomy. Researchers have exploited this fact to advance methods in optical imaging of tissues (for example, optical biopsies for breast cancer detection) and a quantitative, functional assessment of tissue viability and tissue oxygenation (such as in peripheral vascular disease and sleep apnea). As the near IR light enters the tissue it is highly scattered and the photons follow a circuitous path, modeled as photon diffusion, before emerging from the tissue. Contrast in the collected near IR data arises from differences in the recorded optical signals corresponding to oxy- and deoxy-hemoglobin. We have devised instrumentation, which is now commercially available, that operates in the frequency domain and permits quantitative measurement of the optical properties of tissues in terms of both scattering and absorption coefficients. These measurements also provide assessment of tissue oxygenation, tissue function as measured through oxygen consumption and measures of tissue viability; all collected, processed and displayed in real time. We have performed many types of tissue oxygenation measurements, and examples of applications to brain function, sleep apnea, peripheral vascular disease, sports medicine, breast cancer imaging and several other cases will be provided. (Supported by NIH, NCI, and NCRR).

LASER EYE INJURY ON THE MODERN BATTLEFIELD: CLINICAL, RESEARCH AND MILITARY ISSUES

Jeremiah Brown, Jr., Harry Zwick, Steven Schuschereba, David J Lund, Bruce E. Stuck

US Army Medical Research Detachment,
Walter Reed Army Institute of Research, Brooks AFB, Texas 78235

Introduction

The military use of lasers has expanded dramatically over the past 30 years. Military applications range from low power laser training tools to devices such as rangefinders, target designators, optical countermeasures, and optical communications. High-energy lasers are also being developed for theatre ballistic missile defense systems and lasers will also be used in chemical/biological detection. Furthermore, threat nations have developed laser systems that can produce ocular injury at tactical ranges. The potential exists for large numbers of soldiers, aircrew and seamen sustaining laser retinal injuries. Experience with past laser injuries has shown that retinal injuries may result in permanent visual loss. The goals of treating these injuries include reducing scar formation and protecting the viability of injured photoreceptors.

One challenge in the treatment of laser eye injuries is their varied presentation. Laser injuries may create an isolated retinal burn, or may result in intravitreal, intraretinal, or subretinal hemorrhage. Secondary events such as intraretinal scarring and macular holes may occur (Powell et al.; Pollack et al.; Custis et al.; Stuck et al.; Brown et al.). Furthermore, many soldiers may be expected to have bilateral injuries if their fixation is directed toward a distant source. The development of treatments for the varied types of laser retinal injuries is a priority for the Department of Defense.

Background

Laser bioeffects are dependent upon the energy, pulse duration, retinal location, retinal spot size and wavelength of the laser. For example, a continuous wave Argon green laser with a pulse duration of milliseconds can cause a thermal burn resulting in full thickness retinal injury. Energy absorption by retinal pigment epithelial (RPE) cells results in thermal denaturation of RPE and photoreceptor cellular proteins. With longer duration pulses of moderate intensity, rupture of Bruch's membrane (which separates the retina from the underlying choroidal blood supply) may occur; however, this occurs less commonly than with lesions created by q-switched lasers (see below). Following the injury, inflammatory cells infiltrate the lesion site and begin a process of scarring. In the absence of hemorrhage, the lesions resolve with retinal atrophy, hypertrophy of RPE cells and little fibrovascular scarring.

Alternatively, Nd:YAG q-Switched Lasers deliver energy in a shorter duration (nanoseconds) and produce a primarily photodisruptive lesion at the level of the retinal pigment epithelium. If the energy is sufficient, the basement membrane of the RPE cell (Bruch's membrane) is disrupted allowing blood from the underlying choriocapillaris and choroid to enter the subretinal, retinal and vitreous spaces. Blood in the retina is toxic to photoreceptors and also plays a role in scar formation. There may be thermal injury to the overlying retina as well. Damaged cells release toxic substances that lead to further injury in the surrounding tissue. In response to the injury, inflammatory cells migrate to the site. Inflammatory cells cause further tissue destruction and lead to scar formation. The result is disorganization of photoreceptor outer segments, intraretinal scarring, iron toxicity to photoreceptors, and scarring of the choriocapillaris. Late events may also include macular hole formation and the growth of abnormal vessels from the choroid into the retina (choroidal neovascularization). To date, most of the accidental laser retinal injuries have involved q-switched Nd:YAG lasers (Stuck et al.; Thach et al.). Increased use of continuous wave lasers in future battlefield situations is expected.

The process of scarring evolves over several months. Laser induced retinal injuries may result in a visual impairment that gradually worsens. A macular hole may form in the fovea due to the initial injury or due to progressive retinal traction from epiretinal and intraretinal scar contraction (Ciulla and Topping; Tso and Fine). Subretinal neovascularization may develop leading to hemorrhage, exudation and further visual loss months or years after the initial injury (Roider et al.; Ishibashi et al.).

Goals

One goal of an effective treatment for laser induced retinal injuries is to reduce the retinal scarring that occurs following the injury. Ophthalmologists have used steroidal medications for decades to reduce the scarring that occurs in response to ocular infectious or autoimmune inflammatory conditions (Beck et al.; Shah et al.). A second strategy is to use a medication that will protect the surrounding minimally injured retina from oxidative damage. Neuroprotection strategies attempt to preserve as many normal retina cells around the injury site as possible and thereby limit visual loss. The National Spinal Cord Injury Study showed that high dose corticosteroids can improve neurologic outcome (Bracken et al.). Corticosteroids exhibit neuroprotective features such as an ability to limit lipid peroxidation, stabilize lysosomal membranes and limit the release of arachidonic acid (Hall and Braughler). Attempts at the use of other neuroprotective compounds in animal models have been unsuccessful (Lanzino et al.; Rosner et al.; Hickenbottom and Grotta).

The use of corticosteroids deserves further discussion as many clinicians have employed these medications for the treatment of laser injuries. The use of corticosteroids in animal models for laser induced retinal injuries has met with mixed success. The difficulty in evaluating the literature is the variation in dosage and experimental design. Studies have demonstrated a limited treatment benefit rat and primate models of laser injury

(Lam et al.; Rosner et al.; Takahashi et al.). A rabbit model showed an adverse effect when the animal was treated with steroids prior to injury (Schuschereba et al. 2001; Schuschereba et al. 1997). Several experimental designs have employed a brief burst of steroids followed by abrupt cessation. This dosage regimen can result in rebound inflammation. Other designs have failed to follow the progression of the retinal pathology long enough to fully evaluate post-injury scar contraction. Some patients have been treated with steroids with good resulting visual acuity (Zwick et al.). However, other patients without treatment have had both good and poor outcomes.

Consequently, there is no accepted treatment plan for patients that suffer laser induced retinal injuries (Schuschereba and Scales; Thach et al.). Our laboratory is currently conducting a long-term study looking at the use of corticosteroids and nonsteroidal medications for laser retinal injuries due to continuous wave and q-switched lasers.

New therapies for laser retinal injury should be targeted to specific wound healing processes. Corticosteroids introduce numerous effects, some of which are beneficial while others may be detrimental to wound healing. As we learn more about the components of the wound healing response in the retina, we hope to be able to develop more directed therapies.

The use of low-level phototherapy to enhance wound healing is receiving increased attention (Iwase et al.; Whelan et al.; Sommer et al.). A recent report of reduction of ischemic damage in central nervous system tissue following treatment with low level laser therapy is very encouraging. Furthermore, Anders has reported the effect of low power laser irradiation to stimulate regeneration of facial nerve tissue in a rat model. Phototherapy may enhance beneficial aspects of neuronal wound healing without stimulating fibrosis and scarring. It is critical that we learn as much as possible about the mechanism of the therapeutic effect and the light parameters that are more successful for stimulating neuronal tissue. The use of low level phototherapy to stimulate retinal tissue healing deserves to be investigated.

Summary

The military applications for lasers are steadily increasing. As the applications increase, the potential exists for large numbers of soldiers sustaining laser eye injuries. Review of current accident cases reveal that the injury process evolves over weeks to months. This may result in a full thickness retinal burn, intraretinal scarring, retinal and vitreous hemorrhage or a macular hole. Despite anectodotal use of steroids to reduce retinal scarring, there is no generally accepted therapy for these injuries. Future research into the mechanism of action of low-level phototherapy to enhance wound healing in nervous system tissue may yield useful data with applications for laser retinal injury.

References

Beck RW, Cleary PA, Anderson MM Jr., et al. A randomized, controlled trial of corticosteroids in the treatment of acute optic neuritis. The Optic Neuritis Study Group. N Engl J Med 1992;326:581-8.

Bracken MB, Shepard MJ, Collins WF, et al. A randomized, controlled trial of methylprednisolone or naloxone in the treatment of acute spinal-cord injury. Results of the Second National Acute Spinal Cord Injury Study. N Engl J Med 1990;322:1405-11.

Brown J, Zwick H, Schuschereba ST, Stuck BE. Clinical features of laser-induced macular holes as imaged by optical coherence tomography (OCT). SPIE 2001;4246:10-19.

Ciulla TA and Topping TM. Surgical treatment of a macular hole secondary to accidental laser burn. Arch Ophthalmol 1997;115:929-30.

Custis PH, Gagliano DA, Zwick H, et al. Macular hole surgery following accidental laser injury with a military range finder. SPIE 1996;2674:166-174.

Hall ED, Braughler JM. Glucocorticoid mechanisms in Acute Spinal Cord Injury: A review and therapeutic rationale. Surg Neurol 1982;18:320-7.

Hickenbottom SL, Grotta J. Neuroprotective therapy. Semin Neurol 1998;18:485-92.

Ishibashi T, Miller H, Orr G, Sorgente N, Ryan SJ. Morphologic observations on experimental subretinal neovascularization in the monkey. Invest Ophthalmol Vis Sci 1987;28:1116-30.

Iwase T, Hori N, Morioka T and Carpenter DO. Low power laser irradiation reduces ischemic damage in hippocampal slices in vitro. Lasers in Surgery and Medicine 1996;19:465-70.

Lam TT, Takahashi K, Fu J, Tso MOM. Methylprednisolone therapy in laser injury of the retina. Graefe's Arch Clin Exp Ophthalmol 1993;231:729-36.

Lanzino G, Kassell NF, Dorsch NW, et al. Double-blind, randomized, vehicle-controlled study of high-dose tirilazad mesylate in women with aneurysmal subarachnoid hemorrhage. Part I. A cooperative study in Europe, Australia, New Zealand, and South Africa. J Neurosurg 1999;90:1011-7.

Pollack A and Korte GE. Repair of retinal pigment epithelium and choriocapillaries after laser photocoagulation: correlations between scanning electron, transmission electron and light microscopy. Ophthalmic Res 1997;29:393-404.

Powell JO, Tso MO, Wallow IH, Frisch GD. Recovery of the retina from argon laser radiation: clinical and light microscopic evaluation. Ann Ophthalmol 1974;6:1003-6, 1009-12.

Roider J, Buesgen P, Hoerauf H, et al. Macular injury by a military range finder. Retina. 1999;19(6):531-5.

Rosner M, Solberg Y, Turetz J, Belkin M. Neuroprotective therapy for argon-laser induced retinal injury. Exp Eye Res 1997;65:485-95.

Schuschereba ST, Brown J., Stuck BE, Marshall J. Untoward effects of high dose methylprednisolone therapy on blood-retinal barrier closure, retinal hole repair, and long-term scarring. SPIE 2001;4246:1-9.

Schuschereba ST, Cross MT, Pizarro JM et al. Pretreatment with hydroxyethyl starch-deferoxamine but not methylprednisolone reduces secondary injury to retina after laser irradiation. Lasers and Light 1997;8:1-14.

Schuschereba ST, Scales DK. Current therapy for laser-induced retinal injury: overview of clinical and experimental approaches. SPIE 1997;2974:171-88.

Shah GK, Stein JD, Sharma S, et al. Visual outcomes following the use of intravitreal steroids in the treatment of postoperative endophthalmitis. Ophthalmology. 2000;107:486-9.

Sommer AP, Pinheiro ALB, Mester AR et al. Biostimulatory windows in low-intensity laser activation: lasers, scanners, and NASA's light-emitting diode array system. Journal of Clinical Laser Medicine & Surgery 2001;19:29-33.

Stuck BE, Zwick H, Molchany JW, et al. Accidental human laser retinal injuries from military laser systems. SPIE 1996;2674:7-20.

Takahashi K, Lam TT, Fu J, Tso MOM. The effect of high-dose methylprednisolone on laser induced retinal injury in primates: an electron microscopic study. Graefe's Arch Clin Exp Ophthalmol 1997;235:723-32.

Thach AB, Lopez PF, Snady-McCoy LC et al. Accidental Nd;YAG laser injuries to the macula. Am J Ophthalmol 1995;119-767-73.

Tso MO, Fine BS. Repair and late degeneration of the primate foveola after injury by argon laser. Invest Ophthalmol Vis Sci 1979;18:447-61.

Whelan HT, Smits RL, Buchmann EV, et al. Effect of NASA light-emitting diode (LED) irradiation on wound healing. Journal of Clinical Laser Medicine & Surgery 2001, in press.

Zwick H, Stuck BE, Dunlap W et al. Accidental bilateral q-switched neodynium laser exposure: treatment and recovery of visual function. SPIE 1998;3254:80-9.

APATITE BIOFILM FORMING AGENT: NANOBACTERIA AS A MODEL SYSTEM FOR BIOMINERALIZATION & BIOLOGICAL STANDARD FOR NOA – A PRELIMINARY STUDY

E. Olavi Kajander[1], Katja Aho[1], and Vardit Segal[2]

[1] Department of Biochemistry, University of Kuopio, Finland
[2] Leonard & Diane Sherman Center for Research in Biomaterials,
Department of Biomedical Engineering, Technion-Israel Institute of Technology, Israel

Introduction

Since 1985 we have detected and cultured an agent in human blood that mediates apatite nucleation and crystal growth under terrestrial conditions simulating blood and urine (Kajander et al, 1997; Kajander & Ciftcioglu 1998). The agent is passageable and has been continuously cultured in the laboratory, with monthly passages for 10 years. It grows in mammalian cell culture media and does not need mammalian cells or serum for growth. However, growth is more rapid when supplemented with serum or with a growth factor preparation produced by the nanobacteria itself into its growth medium, and by Bacillus sp. (Ciftcioglu & Kajander 2000). We named the agent, autonomously replicating biological particles alias nanobacteria, to separate it from common bacteria in the 1990 timeframe. Independently from us, other mineral-associated nanosized possible microorganisms have been detected. Tiny coccoid particles were found in sedimentary rocks using scanning electron microscopy (SEM) after acid etching of samples and were named as nanobacteria (Folk 1993). Possible fossils of nanobacteria were detected with SEM in a Martian meteorite (McKay et al, 1996) and nano-organims in deep Australian sandstone (Uwins et al., 1998). The latter ones, named as nanobe, could also be cultured.

Nanobacteria are unconventional bacteria-like agents that can replicate new apatite-forming units. Typically they are coccoid particles having a diameter of 80-250 nm. Thus their size is about 100-fold smaller than that of common bacteria. For this reason, their direct observation via conventional optical microscopes is extremely difficult. They can produce carbonate apatite biofilms and stones in vitro and apparently in vivo in human body (Ciftcioglu et al., 1998; 1999). A small study has indicated that Koch's postulates can be fulfilled for nanobacteria causing kidney stones (Garcia Cuerpo et al., 2000). Nanobacteria have been detected in human aortic plaques and thus they may have a role in atherosclerosis (Puskas 2001). It thus appears that they may have medical significance in pathological states, but may also reveal how normal bodily calcification processes work. Mechanisms for bone formation and other calcifications remain poorly understood.

Nanobacteria appear to be too small for being living organisms on currently accepted criteria for packing and operating a DNA-based genome. However, they have many, if not

all, properties of a parasitic organism (Kajander et al., 1999). They have been cultured successfully in many laboratories (Burton & Lappin-Scott, 2000; Garcia Cuerpo et al., 2000; Puskas 2001; Hjelle et al., 2000; Vali et al., 2001). Cisar et al. (2000) could also culture nanobacteria-like particles from human saliva. They put forward an alternative hypothesis for particule formation involving apatite nucleation by phospholipids and apatite itself. It is obvious that apatite can nucleate in supersaturated solutions abiogenically on such nidi. However, nanobacteria are able to do that in nonsaturated solutions (Kajander et al., 2001). Nanobacteria show susceptibility to antibiotics and gamma irradiation, which apatite does not. Replication of nanobacteria particules, measured by turbidometry or uridine incorporation, can be stimulated several fold by a short exposure to low level light at certain wavelengths (EO Kajander and A Sommer, unpublished data; H Whelan, personal communication). Stimulation of growth by light is a phenomenon common to many living organisms including human cells (Sommer et al., 2001). Apparently, nonbiogenic synthetic apatite and nanobacteria are very different.

Apatite formation induced by nanobacteria is a biogenic process since it takes place in a biomatrix around the agent. Nanobacteria form small spherical units of apatite in nanoscale crystal size that are very resistant toward acid hydrolysis and can be formed under non-saturating medium levels of calcium and phosphate (Kajander et al., 1998). The apatitic biofilm formation is dependent on the presence of oxygen, and can be prevented with several antibiotics and antimetabolites and with high gamma irradiation at sterilizing doses (Kajander et al., 1997). Ultraviolet-light at doses detrimental to most organisms does not affect their growth and proliferation (Bjorklund et al., 1998). Most importantly, the nanobacteria-mediated calcification can proceed in human samples cultured under cell culture conditions. Samples mediating such calcifications have been isolated from kidney stones, prostate microliths and urine or serum of such patients (see Kajander et al., 2001). The agent can also exist intracellularly. It transports apatite via kidney cells into urine. It can survive and grow in urine. Calcified nanobacteria are not only very resistant to chemical disinfection, heat, UV and gamma irradiation, but can also survive in lyophilized state for extended periods of time (Bjorklund et al., 1998; Kajander & Ciftcioglu, 2000). Thus, their elimination from urinary stones, or catheters and stents is an extremely difficult, but potentially a beneficial task. Highly desirable is therefore a deep understanding of physicochemical processes occurring at the nanobacteria/substrate-interface. Understanding apatitic biofilm formation may help to resolve the mechanisms of bone formation remodelling and osteoporosis. Furthermore, nanobacteria may be regarded as a model of primordial life (Kajander & Ciftcioglu, 2000); it carries a self-replicating system involving mineral and metal components, possibly catalysts, immobilized and protected under apatite mineral coat. Understanding how nanobacteria adhere, colonize and operate, may help understanding how life started on Earth and Mars.

Methods

Small stainless steel plates were coated with the following organic polymers: (a) pyrrole, in 0.1 M KNO_3; (b) 3-aminophenylacetic acid, in 0.1 M H_2SO_4; and (c) tyramine, in 0.3 M NaOH.

In addition, we have also studied a sample coated with poly(tyramine), to which an enzyme – alpha-chymotrypsin – was chemically attached using glutaraldehyde. All steel coatings were made by Vardit Segal, Technion, Israel. Detailed procedures will be described in her thesis. The steel plates were stored dry at ambient temperature before use. Initially they were inspected and photographed using Philips XL30 environmental scanning electron microscope (ESEM). Thereafter, the steel plates were immersed in gentamycin solution, 10 mg/ml, overnight for disinfecting. After washing with DMEM, the plates were placed in Petri dishes with DMEM, nanobacteria were added and cultures were incubated for one day at +37°C in a cell culture incubator.

Nanobacteria were cultured initially in 10% FBS-DMEM (Gibco, Life Tehnologies, Paisley, UK) as previously described (Kajander & Ciftcioglu, 1998). Continuous culture was maintained by 1:10 passage every 4 weeks into fresh medium. For initiating the experiment above, 4.5 ml of 3-week-old culture was harvested by centrifugation at 13 200xg for 20 minutes and the pellet washed twice with filtered (0.1 micron pore-size) PBS. The pellet was thereafter suspended into 1 ml of DMEM and added to a cell culture dish containing a steel plate sample in 4 ml DMEM.

After incubation, culture medium was removed and plates were washed twice with particle-free PBS. Before ESEM the plates were rinsed with particle-free pharma-ceutical grade water. The plates were examined and photographed with ESEM mode.

Results and Discussion

To study relevant mechanisms, particularly the adhesion of the nanobacteria to chemically and/or topographically different surfaces, we have started collaboration with Technion/Israel (design and preparation of the polymer samples), ENSOMA/University of Ulm/Germany (NOA) and investigation of the interaction of nanobacteria with the samples in Kuopio. The interaction of nanobacteria with the metal samples coated with different polymers has been under investigation since February 2001. The samples were prepared at Technion by electrochemical polymerization, using stainless steel as support. The monomers used and the pertinent polymerization media were: (a) pyrrole, in 0.1 M KNO_3; (b) 3-aminophenylacetic acid, in 0.1 M H_2SO_4 ; and (c) tyramine, in 0.3 M NaOH. In addition, we have also studied a sample coated with poly(tyramine), to which an enzyme - alpha-chymotrypsin - was chemically attached using glutaraldehyde.

Figure 1A shows that the stainless steel surface was smooth and no nanobacteria-sized particles were observed. After a 1-day exposure to nanobacteria the surface was covered with nanobacteria, seen as pale diplococci-like particles, indicating that nanobacetria could adhere easily on stainless steel surfaces. The polypyrrole-coated surface showed large granules of the polymer (Fig 2A). Nanobacteria do adhere on this coating as shown on Fig 2B. The polytyramine and polytyramine-alpha-chymotrypsin coatings appeared smooth (Figs 3A and 4A). Nanobacteria could adhere on both coatings effectively as shown in Figs 3B and 4B. The poly-3-aminophenylacetic acid coating repelled

nanobacteria, because the exposed surface (Fig 5B) showed no adhered nanobacteria particles and was similar to the non-exposed surface (Fig 5A).

The studied coating materials are extremely interesting because of two practical reasons: first, they represent a simple set of test-surfaces allowing investigation and optimization of the surface chemistry and the local topography in order to obtain – depending on what is intended – a maximum or a minimum adhesion of nanobacteria on solid surfaces; second, the coating materials could be prepared in a gel-like form, allowing the nanobacteria to survive on such surfaces under conditions similar to cell culture media. This point is expected to be especially relevant in experiments carried out in space under microgravity conditions.

An ideal non-invasive optical method for investigation of nanobacteria – serum free and in vitro – is near-field optical analysis (NOA). Recent nanoscale images of nanobacteria obtained by Andrei P. Sommer via NOA at ENSOMA are encouraging. Preliminary results indeed suggest that these nanoscopic bioparticles having several aspects in common with the hard tissues of the human body (dentine, enamel, bone), could be used as a "biological standard" for NOA (see A. Sommer, these proceedings). During the first international NOA conference, it was postulated that mineralized nanobacteria biofilms, respectively nanobacteria colonies protected by crystalline apatite shells, might have survived extreme conditions in space allowing them to travel on the surface of meteorites (Kajander 2001). Nanobacteria could also be an important model for early lifeforms for another reason: nanobacteria are self-replicating particles where immobilized minerals and metals could function to support life by providing scaffold for metabolic pathways and organized compartments. Immobilized synthetic systems and compartments are regarded as essential for synthesis of macromolecules in prebiotic time before real 'life' occurred (Ferris et al., 1996). Finally, nanobacteria could also offer a model to study calcification under microgravity, disorders of which are limiting long human spaceflights.

Conclusions

Nanobacteria are self-replicating particles that provide a culturable model to study primordial life strategies. In this study, we showed that nanobacteria do adhere rapidly and effectively on stainless steel and on several, but not all, organic polymer coatings. Such coatings are powerful tools to control nanobacterial biofilm formation. These findings have direct applications in planning reactors to study nanobacterial biofilms and mineralization, both under 1g and in microgravity. Such experiments should atract astrobiologists, geologists, and those from the biomaterial science and medicine disciplines. Improved coatings/matrixes might prevent pathological calcification, or improve deficient calcification in a controlled manner.
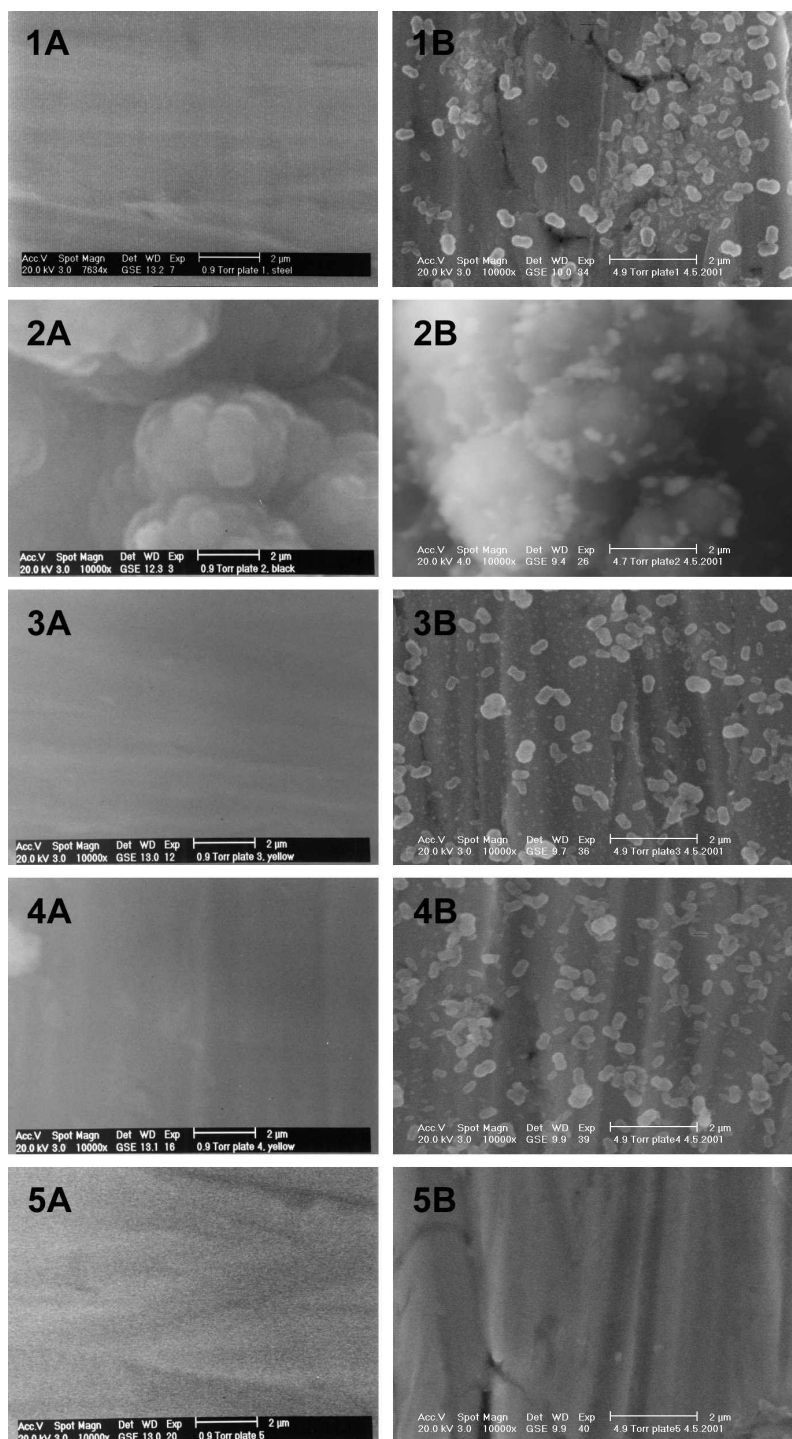
Figures 1-5: ESEM pictures showing metal plates with different coatings before (left side) and after the incubation with nanobacteria in plain DMEM medium (right side). Magnification is approximately 10,000x, see the bar of 2 μm. **Figures 1A** and **1B** show uncoated stainless steel plate, before and after the incubation with serum-free nanobacteria. **Figures 2A** and **2B** show stainless steel plate coated with polypyrrole, **3A** and **3B** with polytyramine, **4A** and **4B** with poly tyramine linked to a-chymotrypsin, and **5A** and **5B** with poly-3-aminophenylacetic acid before and after the incubation with nanobacteria, respectively.

References

Bjorklund M, Ciftcioglu N, Kajander EO (1998); Extraordinary survival of nanobacteria under extreme conditions, Proc SPIE Int Soc Opt Eng 3441:123-129.

Burton S, Lappin-Scott HM (2000); Nanobacteria; Environmental survey and development of detection methods, Proceedings of Am Soc Microbiol General Meeting; 21-25 May 2000, Los Angeles: abstract R19.

Ciftcioglu N, Bjorklund M, Kajander EO (1998); Stone formation and calcification by nanobacteria in human body, Proc SPIE Int Soc Opt Eng 3441:105-111.

Ciftcioglu N, Björklund M, Kuorikoski K, Bergström K, Kajander EO (1999); Nanobacteria: An infectious cause for kidney stone formation, Kidney Int 56:1893-1898.

Ciftcioglu N, Kajander EO (2000); Nanobacterial growth factor, Proc SPIE Int Soc Opt Eng 3755: 113-119.

Cisar JO, Xu D-Q, Thompson J, Swaim W, Hu L, Kopecko DJ (2000); An alternative interpretation of nanobacteria-induced biomineralization, Proc Natl Acad Sci 97:11511-11515.

Ferris JP, Hill AR Jr, Liu R, Orgel LE (1996); Synthesis of long prebiotic oligomers on mineral surfaces, Nature 381:59-61.

Folk RL (1993); SEM imaging of bacteria and nannobacteria in carbonate sediments and rocks, J Sediment Petrol 63:990-999.

Garcia Cuerpo E, Kajander EO, Ciftcioglu N, Lovaco Castellano F, Correa C, Gonzalez J, Mampaso F, Liano F, Garcia de Gabiola E, Escudero Barrileiro A (2000); Nanobacteria. Un modelo de neo-litogenesis experimental, Archivos Espanoles de Urologia 53:291-303.

Hjelle JT, Miller-Hjelle MA, Poxton IR, Kajander EO, Ciftcioglu N, Jones ML, Caughey RC, Brown R, Millikin PD, Darras FS (2000); Endotoxin and nanobacteria in polycystic kidney disease, Kidney Int 57:2360-2374.

Kajander EO (2001); Apatite biofilm forming agent: Nanobacteria, Proc. Of the 1st International Conference on Near-Field Optical Analysis, Castle Reisenburg, Germany, Nov 4-7, 2000, Sommer AP (ed), J Clin Laser Med & Surg 19:111.

Kajander EO, Björklund M, Ciftcioglu N (1998); Mineralization by nanobacteria, Proc SPIE Int Soc Opt Eng 3441:86-94.

Kajander EO, Bjorklund M, Ciftcioglu N (1999); Suggestions from observations on nanobacteria isolated from blood, In: Size limits of very small microorganisms, Proceedings of a Workshop, National Academy Press, Washington DC, pp.50-55.

Kajander EO, Ciftcioglu N (1998); Nanobacteria: An alternative mechanism for pathogenic intra- and extracellular calcification and stone formation, Proc Natl Acad Sci 95:8274-8279.

Kajander EO, Ciftcioglu N (2000); Nanobacteria as extremophiles, Proc SPIE Int Soc Opt Eng 3755:106-112.

Kajander EO, Ciftcioglu N, Miller-Hjelle MA, Hjelle JT (2001); Nanobacteria: controversial pathogens in nephrolithiasis and polycystic kidney disease, Curr Opin Nephrol Hypertens 10:445-452.

Kajander EO, Kuronen I, Akerman K, Pelttari A, Ciftcioglu N (1997); Nanobacteria from blood, the smallest culturable autonomously replicating agent on Earth, Proc SPIE Int Soc Opt Eng 3111:420-428.

McKay DS, Everett KG Jr, Thomas-Keprta KL, Vali H, Romanek CS, Clemett SJ, Chillier XDF, Maechling CR, Zare RN (1996); Search for past life on Mars: Possible relic biogenic activity in Martian meteorite ALH840001, Science 273:924-930.

Puskas L (2001); Detection of nanobacteria in human atherosclerotic plaques, International Nanobacteria Minisymposium, Kuopio March 8th, 2001, Abstract book, University of Kuopio Publication Series, in press. Also available at www.nanobac.com.

Sommer AP, Pinheiro ALB, Mester AR, Franke R-P, Whelan HT (2001); Biostimulatory windows in low-intensity laser activation: Lasers, scanners and NASA's light-emitting diode array system, J Clin Laser Med & Surg 19:29-30.

Uwins PJR, Webb RI, Taylor AP (1998); Novel nano-organisms from Australian sandstones, American Mineralogist 83:1541-1550.

Vali H, McKee MD, Ciftcioglu N, Sears SK, Plows FL, Chevet E, Ghiabi P, Plavsic M, Kajander EO, Zare RN (2001); Nanoforms. A new type of protein associated mineralization, Geochim Cosmochim Acta 65:63-74.

BASIC PATHOPHYSIOLOGICAL MECHANISMS OF HOST RESPONSES

Marti Jett[1], Rina Das[1], Christanio Cummings[1], Chanaka Mendis[1], Roger Neill[1], COL David Hoover[1], Luther Lindler[1], Chrysanthe Paranavitana[1], Xiaozhe Huang[1], George Ludwig[2], COL Erik Henchal[2], David C.H Yang[3]

[1]Department of Molecular Pathology, Walter Reed Army Institute of Research, Silver Spring, MD
[2]USAMRIID, Frederick, MD
[3]Chemistry Department, Georgetown University, Wash. DC

Abstract

In our changing world, there has been a significant increase in both the nature and degree of the threat posed by the use of biological agents. Studies for many years have focused on rapid detection of known biological threat agents using structural-based probes designed and directed toward features of the pathogenic agent. However, concerns relating to unidentifiable pathogens that could result from either deliberate or natural mutation processes have prompted studies to find alternative approaches. Our thesis was that an exposed individual would show gene expression responses unique to the pathogenic agent and before onset of the full illness. Therefore this study focused on using peripheral blood mononuclear cells (PBMC) as a readily accessible reservoir of historical information for developing a library of host gene expression responses to known biological threat agents. The gene responses seen in this accessible tissue would be a compilation of both primary and secondary effects on PBMC and would present a signature pattern of a specific biological threat agent. In this study, we establish a library of host responses to pathogenic agents for use to a) predict the course of impending illness especially for unidentifiable pathogens so that appropriate therapeutic intervention can be initiated, b) to characterize the degree of individual exposure in order to assist health personnel to rapidly differentiate those who will become seriously ill from "the worried well" individuals and c) reveal new therapeutic targets that can be initiated even in late-stage illness caused by biological threat agents.

Introduction

Identifying pathogenic agents using structural-based probes directed at specific pathogen properties has been the classic approach for rapid detection of biological threat agents. Situations exist in which that system could need a supplemental approach. The obvious scenario would be pathogenic agents that are unidentifiable due to deliberate or natural mutations. In addition to that unique situation, even for identifiable bacterial pathogens, the extent of individual exposure would be limited by detection thresholds. This relates to findings that some toxins are sequestered into target tissues and unavailable for identification in blood samples or bacterial pathogens require time to

undergo sufficient growth to reach detection threshold levels. For example, detection of bacterial products in human blood samples after exposure to B. anthracis have been found 2-3 days post exposure; by that time, the pathogen had undergone extensive proliferation, manifesting serious illness. Similarly, for staphylococcal enterotoxin (SE) B, the toxin disappears from the peripheral circulation and is sequestered in the kidney (~70%) and other organs within 30 min of exposure. Actual toxin/fragments in blood or urine are not identified unless blood samples were taken just after exposure.

The approach we have pursued relies on gene expression responses to biological threat agents using PBMC of the exposed individual. We are accumulating a library of these responses to infectious and biological threat agents. Although PBMC may not be the primary target for a particular pathogenic agent, they can respond to a combination of primary and secondary effects and they reflect information in the form of secreted products as well as gene responses related to encountered stimuli. Gene discovery technology allows us to examine large numbers of genes simultaneously for the various biological threat agents, both in vitro and in PBMC from an animal exposed to the threat agents. Certainly, structural-based probes to identify biological threat agents allow us to test environment/personnel externally for an obvious exposure and an identifiable pathogen. In contrast, the gene library we are developing will relate gene profiles with subsequent illness patterns to characterize natural or deliberately modified pathogenic agents and initiate appropriate countermeasures to ameliorate or prevent serious illness. In addition, examples of mass accidental exposures throughout the world can result in chaos at medical care facilities, due in part to panic (1). Gene array technology offers the potential to determine the degree of individual exposure (and perhaps susceptibility), to separate the "worried well" from the seriously ill. This technology is undergoing phenomenal advances relating to devices that automatically process blood samples to isolate RNA in minutes, and newly described technology to reduce PCR-based analysis of gene arrays to 30 min. Based on the developing library of gene responses to biological threat and other pathogenic agents, our ultimate objective is to design gene chips containing relatively few genes (hundreds rather than thousands) that could concisely predict the likely pathogenic agent or modified version of such, the degree of individual exposure and the course of impending illness. We aim to provide a tool to defend against biological threats so that resultant panic, morbidity, mortality can be reduced and targets identified for even late-stage treatment modalities.

Methodology Employed in This Study

<u>Overview</u>. For 14 years, our laboratory has been carrying out in vitro and in vivo studies of host responses to staphylococcal enterotoxins as biological threat agents, centering on signal pathways (2-6), cell mediators (5-8), and evaluation of gene expression responses(5). For the latter studies, we have specifically used differential display (DD) - PCR (5) and gene array analysis technology (9) to determine cellular responses to *B.*

anthracis, B. melitensis, Y. pestis, staphylococcal enterotoxins (SEs), cholera toxin (CT) and a number of other threat and infectious agents.

Gene discovery technology. There are numerous reports describing the use of global gene analysis to identify critical changes in expression of a few selected genes indicative of specific illnesses. For example, identification of the gene coding for Fetuin was reduced by 45% in liver cirrhosis (10). In some cases specific genes disappeared, such as i) Annexin VI expression in melanoma progression (11) or ii) MIF (macrophage migration inhibitory factor) in metastatic prostate cancer patients (12). These are just a few examples of the utility of gene array analysis to identify surrogate markers for a disease state and provide avenues for therapeutic intervention.

Gene microarrays. In the studies we describe in this article, we have utilized gene arrays/microarrays to define gene expression patterns for diagnosis as well as to identify potential new approaches for targeting therapy. Our first approach was to use large commercial screening arrays so that we could design inexpensive custom microarrays to define pathogens in terms of kinetics and dose responses. For in vitro studies, blood was drawn from healthy volunteers and PBMC were obtained by elutriation (13). PBMC were exposed to each biological threat agent (or control) for the designated time period, RNA extracted and purified, RT carried out and the resulting product hybridized onto the gene arrays according to standard procedures (9). Specialized computer programs determined the differences in gene expression between control and test for each gene. The data were subjected to various software packages for statistical and cluster analysis (for genes within a time period and threat agent) aimed for these huge data sets (14, 15). Self-organizing maps and other analytical tools were applied to determine patterns of gene expression similarities and differences for each biological threat agent and these analyses also correlated information according to exposure time periods. For in vivo studies, blood was drawn, as described previously (16, 17), from exposed or control monkeys (other of our studies have used piglet models of SE-induced lethal shock) at the designated time periods. In these studies, PBMC were isolated and purified and the same procedure followed as for the in vitro experiments. This approach has provided information in an efficient manner and will facilitate development of a library of genes involved in pathogenesis for each agent examined.

Pathogens. PBMC exposure to each of the pathogens was carried out in the laboratory of the person who is the expert for each biological threat agent. The following is a list of the expert associated with each pathogen. George Ludwig (B. anthracis), David Hoover (B. meletensis), Luther Lindler (Y. pestis), Neill/Jett (SEs), and Yang (cholera toxin). The cell exposures were carried out using exposure concentrations/doses and other conditions that had been established in their laboratory. For in vitro exposures, the useful time frame ranged from 2-12 hours. In vivo, the time periods reflected the time course of the progression of illness, but blood samples were drawn prior to onset of illness, since gene patterns would be expected to precede the display of illness.

Results and Discussion

Our laboratories have been carrying out gene expression profiling of the host response to numerous infectious and biological threat agents, however this manuscript will be limited to discussions of studies with anthrax, SEs, LPS, plague, Brucella and cholera toxin. The initial screening used commercial gene arrays studying the host immune response in vitro using elutriated human peripheral blood mononuclear cells (PBMC). We have also carried out experiments to compare in vitro and in vivo results by utilizing PBMC obtained from non-human primates challenged with the specific biological threat agent.

Our initial work with global gene analysis studies was directed to determine the extent of the similarities and differences in PBMC responses in vitro to two classical shock-inducing toxins, staphylococcal enterotoxin B vs lipopolysaccharide (LPS), the smallest active unit of endotoxin (5, 9, 18). For these two toxins, the progression of illness is quite similar but we know from the volumes of studies on each toxin that there are some specific differences in production of mediators throughout the course of the illness. Indeed we found certain common patterns in gene expression profiles, especially for sets of genes relating to production of subgroups of inflammatory mediators and their accessory molecules, but the confluence of responses showed high correlation between the two toxins for genes relating to the common eventual lesions, such as pulmonary distress and loss of regulation of vascular tone. Figure 1 shows an example of SEB or LPS-induced changes (relative to controls) in expression of a gene that codes for a protein regulator of vascular tone. It is an example of genes showing similar responses to both toxins and this expression pattern also was observed in monkeys challenged with SEB. It is essential to carry out these experiments observing gene alterations at increasing exposure time periods since many genes show time-dependent expression patterns. The kinetic changes in gene expression are especially critical in vivo. An example is that genes coding for cytokines usually display up-regulation at early time periods and the expression levels frequently disappear as time progresses. That is not an unexpected finding, since cytokine production can be seen for brief periods of time following exposure to toxins (5, 9, 16-19).

In contrast to the similarities in gene expression just described, clear differences were seen in response to SEB vs LPS for expression levels of genes coding for numerous cytokines and their accessory molecules, many of the signaling cascade molecules and a variety of other surface adhesion molecules, etc. This probably represents the differences in initial cellular receptors and their linked signal transmission cascades. This study pointed out to us that gene expression changes could show differences in patterns for each agent, but also show similarities relating to common eventual lesions, such as loss of regulation of vascular tone, the hallmark of lethal shock. The unique and common patterns of gene expression were confirmed in SEB-challenged monkeys.
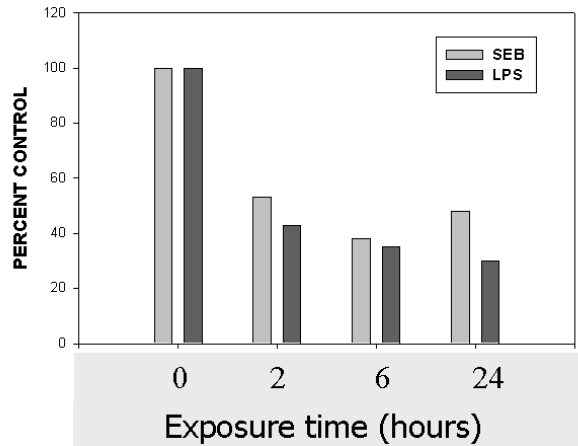
61

Figure 1: Changes in gene expression in response to two shock-inducing toxins. Gene coding for a protein involved in regulating vascular tone shows the example of similarities that result from exposure of PBMC to SEB or LPS in vitro. Expression of this gene was also down-regulated in monkeys challenged with SEB. Although for this particular gene, the kinetics of gene expression was similar over the 24-h time period, that is frequently not the case. Therefore, study of gene responses in a time-dependent manner is essential, especially for in vivo studies, in order to understand the useful time frame for intervention aimed at potential therapeutic targets.

Of course, these studies obviously identify new therapeutic intervention sites and, furthermore, predict the time period during which that approach could be usefully targeted. This information provided the foundation for the current study of multiple biological threat agents, since identification of course of impending illness (such as loss of regulation of vascular tone, vascular leakage, pulmonary or renal distress, etc.) could provide key information should there be exposures to unidentifiable agents. Gene expression responses occur prior to production of their corresponding proteins, and there is frequently a time lag for the concerted action of the causative proteins to result in the demonstration of the lesion. Therefore, gene expression studies offer an early glimpse into the course of the impending illness and shows in a time-dependent manner when a specific therapy regimen might be effective.

Creation of a library of gene expression responses to biological threat agents. The studies with SEB vs LPS showed that unique gene patterns resulted from exposure to each toxin, but common genes, very few of which had previously been described for these toxins, showed associations predictive of the eventual lesions known to be induced by both toxins. Therefore, we carried out experiments, first in vitro in human PBMC, to determine the pattern of gene expression in response to exposures to B. anthracis, Y. pestis, B. meletensis, SEB and cholera toxin (CT). We chose the latter toxin to interpret the data and to compare with the other biological threat agents, since much information exists about biochemical pathways and their relationship to lesions for CT. For studies with the 5 pathogens listed above, we accumulated the gene expression response patterns and began to mine from the data examples of pathogen-specific changes in host immune response gene profiles and identified unique genes that could potentially be used as diagnostic markers and serve

as therapeutic targets. The data amassed in this study are voluminous. Figure 2 is a condensation of results that shows patterns of gene alterations common to more than one agent and other changes that are unique to a particular agent. This is but a small set of gene expression changes and they are sorted according to the listed functional activities. In this table, there are numerous examples of specific genes that respond to one of these toxic agents, while there are other examples of genes that are altered in response to most or all of the pathogens (see interleukins). As a group, genes coding for cytokines/chemokines were altered by multiple biological threat agents, although specific mediator receptors frequently showed individual responses. In Figure 2, time dependency is shown for all of the pathogenic agents except cholera toxin). The kinetics of gene expression responses is especially important, as pointed out previously, since it reveals potential therapeutic targets that may provide effective intervention at specific time periods during late stages of illness.
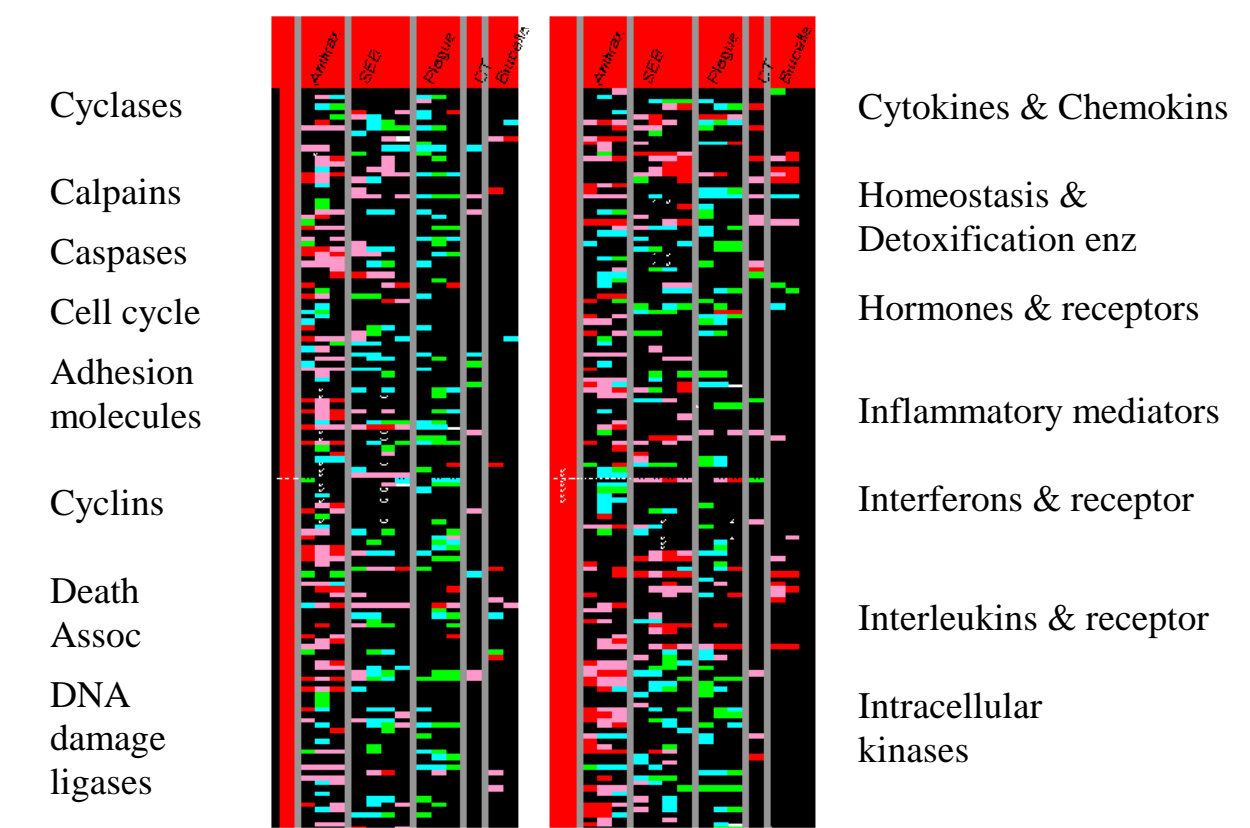

Figure 2: Gene array analysis of PBMC treated with biological threat agents. Each agent was studied at different time periods, usually 2,4,8 hr and for SEB, an additional time period of 18 h. CT was studied at 16 h. Red/pink indicates up-regulated genes while green/blue shows down-regulated genes relative to control samples. The kinetics of gene responses for each different agent provide important information for possible late-stage therapeutic targets. Some gene classes show responses with most of these pathogenic agents (interleukins) while a host of other genes show patterns that could distinguish one pathogenic agent from another.

<u>NHP-challenge: B. anthracis</u>. We have verified numerous changes in gene expression in non-human primates exposed to B. anthracis at T=0, 24, 48, 72 h post-exposure. We again found, in general, that cytokines appeared primarily at T=24 h while genes involved in apoptosis and cell death were up-regulated at 48-72 h. Many unanticipated changes in gene response have provided potential therapeutic targets for late treatment.

Summary

We found a series of gene alterations in PBMC from monkeys challenged with SEB that confirm the gene pattern observed in vitro. In cells from the challenged monkeys, we have defined a series of genes, the expression of which was altered in the pattern typical of SEB, not LPS or other shock-inducing toxin by 30 min post exposure. Since onset of illness begins at approximately 3 h post exposure for SEB, early detection of the gene pattern could permit initiation of appropriate countermeasures prior to, or at least in the early stages of illness. In the case of B. anthracis, by 48-72 h, gene patterns from challenged monkeys show resemblances of the "lethal shock" profile that was seen at early time periods with SEB. Indeed, anthrax infection eventually proceeds to lethal shock. One of the purposes of relating gene alterations with a course of illness is that exposure to unknown or genetically altered agents could be "categorized" as to expected lesions and can provide the opportunity to initiate preventive therapy prior to onset of severe illness.

Acknowledgments

References

1.   Carmo, L. d., Cummings, C., and Jett, M. Characterization of staphylococcal enterotoxin-induced illness in accidental contamination of food products, Molecular Biology of the Cell. *11:*, 2000.

2.   Yan, Z., Yang, D. C., and Jett, M. Cholera toxin induces tumor necrosis factor alpha production in human monocytes, Mol Cell Biol Res Commun. *2:* 124-30, 1999.

3.   Yan, Z., Yang, D., and Jett, M. Cholera Toxin Induces TNF production by human monocytes via cAMP Independent pathways, FASEB Journal. *10:* 2746, 1997a.

4.   Yan, Z., D. Yang and Marti Jett (1997b).   , Protein Kinase C is involved in SEB induced TNF-a production., FASEB Journal. *10:* 1922., 1997b.

5.   Mendis, C., Das, R., Yang, D., and Jett, M. Effects of SEB on Stress-Induced Signal Transduction Pathways in Human Lymphoid System, J. Biol Chem, Submitted.

6.   Das, R., Kodsi, N., and Jett, M. Cross talk between the MAP kinase and the Arachidonic Acid pathway in signal transduction of growth factor in breast cancer cells, Int. J. Cancer, 1997.

7.   Boyle, T., Lancaster, V., Hunt, R., Gemski, P., and Jett, M. Method for simultaneous isolation and quantitation of platelet activating factor and multiple arachidonate metabolites from small samples: analysis of effects of Staphylococcus aureus enterotoxin B in mice, Anal Biochem. *216:* 373-82, 1994.

8.   Campbell, W. N., Fitzpatrick, M., Ding, X., Jett, M., Gemski, P., and Goldblum, S. E. SEB is cytotoxic and alters EC barrier function through protein tyrosine phosphorylation in vitro, Am J Physiol. *273:* L31-9, 1997.

9.   Das, R., Mendis, C., Yan, Z., Neill, R., Boyle, T., and Jett, M. Alterations in Gene Expression Show Unique Patterns in Response to Toxic Agents. *In:* Proceedings. Army S 1998, pp. FP-9.

10.   Forestier, M., Reichen, J., and Solioz, M. Application of mRNA Differential Display to Liver Cirrhosis: Reduced Fetuin Expression in Bilary Cirrhosis in the Rat., Biochem. Biophys. Res. Commun. *225:* 377-383, 1996.

11.   Francia, G., Mitchell, S. D., Moss, S. E., and Hanby, A. M. Identification by Differential Display of Annexin-VI, a Gene Differentailly Expressed during Melanoma Progression., Cancer Res. *56:* 3855-3858, 1996.

12.   Meyer-Seigler, K. and Hudson, P. B. Enhanced expression of macrophage migration inhibitory factor in prostatic adenocarcinoma metastases., Urology. *48:* 448-452, 1996.

13.   Jett, M., Neill, R., Welch, C., Boyle, T., Bernton, E., Hoover, D., Lowell, G., Hunt, R. E., Chatterjee, S., and Gemski, P. Identification of staphylococcal enterotoxin B sequences important for induction of lymphocyte proliferation by using synthetic peptide fragments of the toxin, Infect Immun. *62:* 3408-15, 1994.

14.   Banfield, J. D. and Raftery, A. E. Model-based Gaussian and non-Gaussian clustering., Biometrics. *49:* 803-822, 1992.

15.   Eisen, M. B., Spellman, P. T., Brown, P. O., and Botstein, D. Cluster analysis and display of genome wide expression patterns., Proc Natl Acad Sci U. S. A. *95:* 14863-14868, 1998.

16.   Hunt, R. E., Johnson, A. J., Jett, M., J.Tseng, Komisar, J., Wilhelmsen, C., Pitt, L., and Ruble, P. SEB-induced lesions in challenged monkeys. *In:* The New Frontiers 17th Army Science Conference, The Woodlands, TX, 1993.

17.   Jett, M., Hunt, R. E., Pitts, L., Johnson, A. J., and Gemski, P. Staphylococcal enterotoxins B aerosol challenge in Monkeys: Early production of PAF, TNF and arachidonate metabolites was predictive of illness or death. 7th International Symposium on Staphylococci and Staphylococcal Infections, pp. 160-161. Stockholm: Karolinska Press, 1992.

18.   Mendis, C., Das, R., and Jett, M. Additive effect of LPS on staph enterotoxin B-induced signal transduction pathways in human lymphoid cells., FASEB J. *12:* A1485, 2001.

19.   Jett, M., Brinkley, W., Neill, R., Gemski, P., and Hunt, R. Staphylococcus aureus enterotoxin B challenge of monkeys: correlation of plasma levels of arachidonic acid cascade products with occurrence of illness, Infect Immun. *58:* 3494-9, 1990.

REGENERATION STUDIES IN THE MRL MOUSE

Ellen Heber-Katz

Professor, The Wistar Institute

Introduction

Traumatic injury in higher organisms induces two broad classes of healing: wound repair and regeneration. Wound repair involves fibroblast migration to the wound site, formation of granulation tissue, and accumulation of collagen in a disorganized fashion and the formation of scar tissue. The tissue that remains is not as strong and never completely replaces what was there before. On the other hand, regeneration involves the gross replacement and restoration of tissue mass with normal architecture and function and in the extreme case full organs. The capacity for tissue regeneration in mammals is limited or nonexistent, when compared to the chick and amphibians, where entire limbs can be regenerated after amputation. This apparent lack of mammalian regenerative capacity has largely directed the focus of study toward wound repair, the common response to injury in mammals (3,5,10).

We have recently described the ability of the mouse strain, MRL/MpJ, to heal a through-and-through ear hole wound (2), a phenomenon also seen in other mammals (5). The method used to reveal this phenotype, ear hole punching, is actually a standard technique for identifying mice by number in the animal colony. In our experience, no other mouse strain tested, besides a derivative strain, the LG mouse, is capable of healing this mark. What is remarkable in rabbits and MRL mice is that their ear hole closures not only display full scar-free healing, but also show the recovery of normal architecture, collagen structure, angiogenesis, the appearance of hair follicles and sebaceous glands and cartilage. In many ways, the closure resembles what is seen in mammalian development and neonatal wounding more than it resembles adult wound healing. Since mice are available as inbred strains making breeding/segregation studies easy to carry out, we generated a large population and did a complete genome-wide screen using available microsatellite markers. These studies led to identifying at least 7 loci (7). Most recently, we have carried out F2 crosses using different nonhealers and generated congenic mice, which will allow us to narrow the loci for the eventual identification of the genes involved in the regenerative process.

In the present paper, we will discuss the extent of regeneration in the MRL mouse, the role of scarring in regeneration, and possibly extending this type of healing to other mammals.

Methods

Ear hole phenotyping. We made a 2-mm through-and-through hole in the center of the cartilagenous part of both ears of 6-week-old mice using a metal ear punch (Fisher Scientific, Pittsburgh, cat # 01-337B). The holes were measured at the time of wounding and followed for wound closure using a grid-etched reticle (Bausch and Lomb, 7x) (ref 2).

<u>Cryoinjury to the right ventricle of the heart</u>. Myocardial injury was cryogenically induced trans-diaphagmatically as previously described (6,11), without puncturing the diaphragm, on the right ventricular surface of the heart as follows: A 6-8 mm incision was made through the skin on the ventral surface of the abdomen below the rib cage. The diaphragm was exposed and the right atrial surface of the heart could be visualized as adjacent to the diaphragm. Myocardial injury was accomplished by applying a 2mm blunt probe directly on the diaphragm after cooling in liquid nitrogen.

Results and Discussion

After a 2-mm through-and-through hole is made in the cartilagenous part of the ear of a mouse, a healing process takes place. The kinetics of this ear hole closure can be seen in Figure 1. Early on, the nonregenerating strain (C57BL/6) begins to show closure but the hole scars over and closure stops. The regenerating strain (MRL), on the other hand, shows a change in the rate of closure around day 5 and closes at about 3 weeks. After closure takes place, the cartilage begins to grow and shows extensive filling in of the wound area at 3 months (2).

What is happening around day 5 and why does the cartilage grow, an event rarely seen in mammals? Examination of the matrix protein laid down at the wound site indicates that the MRL can reduce the amount of such protein which blocks cell interactions, specifically between epithelial and mesenchymal cell types (4). We propose that this reduction in protein, which essentially makes up the new basement membrane between epidermis and dermis leads to the formation of the blastema and rapid growth of cells, including cartilage. The presence of increased levels of MMPs, in both the pro-forms and active forms, in the MRL healing ear is consistent with this matrix breakdown.

Though the ear hole problem is a fascinating one, it was important to extend this work to another tissue that is even more generally considered a nonregenerating tissue in mammals. The current dogma is that adult cardiomyocytes are terminally differentiated and therefore do not proliferate and that the heart is lacking in stem cells or satellite cells like other muscle (1, 8). We therefore focused on wound healing in the heart. Cardiac wounds were created in mice trans-diaphragmatically against the right ventricle of the heart. We observed that by day 60, the MRL mouse showed near normal restoration of cardiac tissue, with clear evidence of cardiomyocyte proliferation using BrdU labeling. On the other hand, the wound in the C57BL/6 mouse showed extensive scarring by day 15 and remained that way at day 60. The MRL mice, in addition to showing normal histology, showed significant improvement in function through echocardiograhic studies. These hearts appeared completely normal after 3 months (6).

We analyzed matrix protein changes by examining the accumulation of hydroxyproline (as an indicator of collagen accumulation). Surprisingly, the amount of collagen in the normal MRL hearts was greater than the C57BL/6 hearts. Upon injury, the amount of collagen continued to go down in the MRL, supporting the idea that a protease response was induced

and continued up to at least day 60. On the other hand, the C57BL/6 response looked like a typical scar response with increasing amounts of collagen after wounding (ref 6) (Fig. 2).
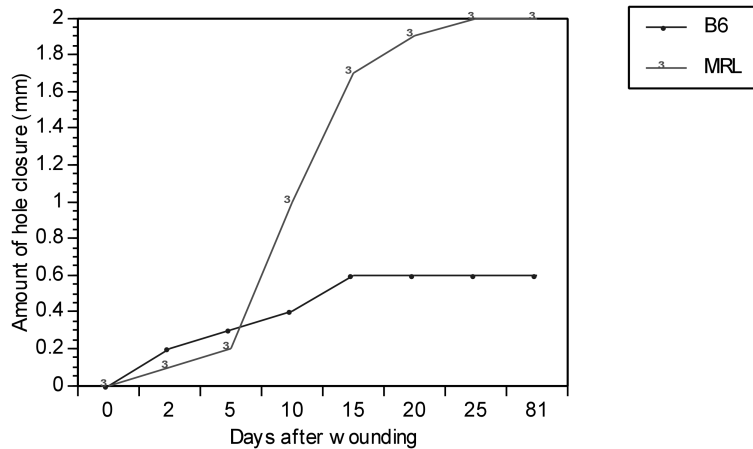

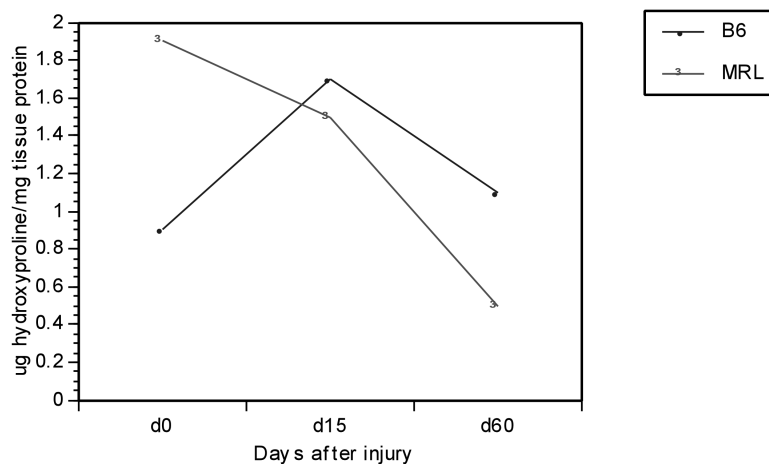**Figure 1**: The kinetics of ear hole closure in MRL and C57BL/6 mice.

Figure 2: Hydroxyproline content in MRL and C57BL/6 mice after cardiac injury.

Conclusion

It seems clear from these two studies and from others not reported here, including spinal cord injury, that there is something unusual about this mouse that appears to be able to regenerate and that one component of this is the scar response. Of course, the question remains: can one replicate this in a non-regenerating strain? As-yet unpublished studies from our laboratory using the C57BL/6 mouse have shown that a complete transection of the spinal cord but without cutting of the dura mater essentially leaves the injury site with a reduced amount of scar tissue (9). This allows the regrowth of axons through the injury site and also allows the recovery of function.

We propose that elimination of this scar tissue or prevention of scar formation will allow the normal re-growth of tissue and organs. One possible approach to elimination of scar tissue

is the treatment of wounds with light at wavelengths that suppress or avoid the generation of the scar. Evidence was presented at this meeting indicating that rapid healing takes place using lasers or LEDs (12). We have begun to test the ability of such light sources to enhance the regenerative response of the MRL mouse and also to test the regenerative capacity of a nonhealer mouse such as the C57BL/6 using the model systems discussed above. The results have been quite interesting and warrant further study.

References

1. Carbone,A, Minieri,M, Sampaolesi,M, Fiaccavento,R., De Feo,A., Cesaroni,P, Peruzzi,G., Di Nardo, P. (l995). Hamster Cardiomyocytes: a model of myocardial regeneration? *Annals of the New York Academy of Sciences.* 752: 75-71.

2. Clark, L., Clark, R., and Heber-Katz, E. (1998) A new model for mammalian wound repair and regeneration. Clin. Imm. and Immunopath. 88: 35-45.

3. Clark, R.A.F. (l996). Wound Repair: Overview and general consideration. in *The Molecular and Cellular Biology of Wound Repair.* ED. R.Clark. (Plenum Press, NY). pp.3-35.

4. Gourevich,D, Samulewicz, SJ, Clark,L, and E. Heber-Katz. 2002. Protease activity correlates with blastema formation in the regenerating ear hole model. In preparation.

5. Gross, J. (1996). Getting to mammalian wound repair and amphibian limb regeneration: a mechanistic link in the early events. Wound Repair and Reg. 4:190 202.

6. Leferovich, J, Bedelbaeva, K, Samulewicz, S, Xhang, X-M, Zwas, DR, Lankford, EB, and Heber-Katz, E (2001) Heart regeneration in adult MRL mice. Proc. Ntl. Acad. Sci. USA, 98: 9830-9835.

7. McBrearty, B.A., Desquenne-Clark, L., Zhang, X-M, Blankenhorn, E.P., and Heber-Katz, E. (1998) Genetic analysis of a mammalian wound healing trait. Proc. Natl. Acad. Sci. USA, 95: 11792–11797.

8. Nadal-Ginard,B. (l978). Committment, fusion, and biochemical differentiation of a myogenic cell line in the absence of DNA synthesis. *Cell.* 15:855-864.

9. Seitz, A., Aglow, E and Heber-Katz, E. (2001) Recovery from spinal cord injury: a new transection model in the C57BL/6 mouse. J. Neuroscience Research 67: 337:345.

10. Stocum, DL. (l996). Tissue restoration: approaches and prospects. Wound Repair and Regeneration. 4: 3-15.

11. Taylor, D.A., Atkins, B.Z., Hungspreugs, P., Jones, T.R., Reedy, M.C., Hutcheson, K. A., Glower, D.D. and Kraus, W.E. (1998) Regenerating functional myocardium: improved performance after skeletal myoblast transplantation. Nature Medicine, 4: 929-933

12. Whelan, HT, Buchmann, EV, Whelan, NT, Turner, SG, Cevenini, V, Stinson, H., Ignatius, R., Martin, T., Cwiklinski, J., Meyer, GA, Hodgson, B., Gould, L, Kane,M, Chen, G, Vainess, J. (2001) NASA light emitting diode medical applications – From Deep Space to Deep Sea. Space Tech and App Int'l Forum 552:35-45.

LASERS IN WOUND HEALING

Farouk A.H. Al-Watban

Laser Medicine Section, Biological and Medical Research,
King Faisal Specialist Hospital & Research Centre, Saudi Arabia

Introduction

Lasers are now used in different medical applications that supersede traditional methods of healing and diagnosis. Several types of medical lasers fit almost all of these needs. Each kind of laser exhibits optical beam properties making it suitable for specific medical applications that depend on the laser light's interaction with tissue. High-power lasers, whether continuous or pulse, are used in surgical treatments to cut, vaporize, coagulate and/or weld tissues, depending on their thermal effects. Also, high-energy pulse lasers in the near ultraviolet region of the spectrum are used to ablate tissues through uncoupling of molecular bonds. Several low power lasers modify biological materials through the photochemical effects of laser photons with the tissue, a non-thermal process that is called Biostimulation or Low Level Laser Therapy (LLLT). Over the past decade, LLLT has become widely used for the treatment of a variety of conditions, including the promotion of wound healing, the reduction of edema, and the relief of pain of various etiologies (1). Many studies in animals (2-4) and clinical observation (5) have demonstrated that biostimulation has a beneficial effect on wound healing. Other research groups, however, have been unsuccessful in achieving the same effects (6-9). The most utilized system for low power laser therapy has been the helium-neon (He-Ne) laser. In contrast, comparison of the effects of wound healing using different kinds of laser wavelengths on rats has not been investigated extensively. The present study was carried out in continuation with previous studies (10-13), comparing the effects of wound healing on rats (i.e. wavelength dependency), observing the inhibitory effect (i.e. dose dependency) and the influence of treatment schedule on wound healing, and calculating the actual dose for the purpose of clinical treatment.

Materials and Methods

<u>Animals</u>. A number of male Sprague-Dawley rats, 27 weeks old, 372 to 488 gm, were used in this study. The animals were originally imported from Charles River Co., UK, in 1984. Now they are bred and provided by the Animal Facility of King Faisal Specialist Hospital & Research Centre (KFSH & RC). After anesthesia with Ketamine (up to 50 mg/kg) and Xylocaine (up to 20 mg/kg) I.P. injection, the surgical site was shaved and applied with hair removing lotion for a few minutes to clean the skin of remaining hair to minimize reflection losses. The hairless area was disinfected with alcohol swabs. A 0.39-cm^2 (1.26-cm^2 for study of treatment schedule) elliptic full thickness skin wound was created aseptically with a scalpel on the shaved back of the animal in the gluteus maximus. All animals with this wound were divided randomly into treated groups and control groups on the basis of the process designed.

70

Laser Systems. The study used HeCd, λ=442 nm (Liconix 4240NB), Argon laser, λ=488-514 nm (Coherent 800), He-Ne laser, λ=632.8 nm (Spectra-Physics 127), GaAlAs lasers, λ=786 and 829 nm (Navital GALA System) and CO_2 lasers, λ=10,600 nm (Coherent System 451). A system of reflectors for the HeCd and CO_2 lasers, fiber optics for the Argon laser and expanders for He-Ne laser and GaAlAs lasers delivered the laser beam. Liconix 45PM, Molectron MAX5200, Coherent 210 power meters and Laser Guide integrating sphere power meters continuously measured the output power. The dose (J/cm^2) is the energy density of the laser beam, calculated as the measured power in mW, multiplied by the treatment time in seconds and divided by the area in cm^2 of the laser spot directed on the wound. The dose rate (mW/cm^2) is the power density of the beam, measured as the power in mW, divided by the laser spot size in cm^2. We used different incident doses up to 140 J/cm^2 (calling it incident dose to differentiate it from the actual dose where we subtract the skin reflection and cage material reflection) on a schedule of three-times/ week for comparing the effects of wound healing using different lasers and wavelengths. We observed and localized the spot size in the infrared laser with a Find-R-Scope (FJW optical systems, Inc.). All spot sizes were calculated as a circular beam, apart from the diode lasers that were calculated as elliptic with the use of a digital planimeter (Planix 7P).

Experimental Treatments. The laser beam was irradiated to cover the entire wound area including the boundaries with a margin of 5 mm. The rats were restrained in a Plexiglas cage without anesthesia during the laser irradiation period. The control group carefully received similar manipulation except for the laser exposure. The wounds were measured several times every other day with a caliper, digital planimeter and with a digital camera attached to a computer, until complete wound closure. A complete separation of assessment and treatment process was adopted. The elliptical wound area was calculated as follows: Area = (L/2 x W/2) π (cm^2), where L and W and the length and width of the wound in centimeters, respectively. The relative percentage of overall wound healing (RWH) was calculated as follows: % RWH = [1 – A(n) / A(z)] x 100(%), where A(n) is wound area on postoperative days and A(z) is the wound area on day zero. The percentage acceleration of wound healing will be referred to as acceleration in wound healing days or size reduction, wherever applicable. The percentage acceleration of wound healing days (AccD) relative to the control was calculated as follows: AccD = [1 – TA / CA] x 100(%), where TA and CA are wound areas of treated and control animals, and 80% wound healing is reached on the former (this avoids large variation in measurements after 80% wound healing).

To detect the possible inhibitory effect of wound healing, we used differing dosages up to 140 J/cm^2 three times/week. The dose rate was changed to 80 mW/cm^2 for dosages higher than 70 J/cm^2 for treatment time and convenience. We used treatment schedules of up to 10 times/week at 10 J/cm^2 and 20 J/cm^2 for observing the influence of treatment schedule.

The mean days and/or size reduction required for 80% wound healing in several groups were calculated and expressed as graphs, Figures 1 to 4.
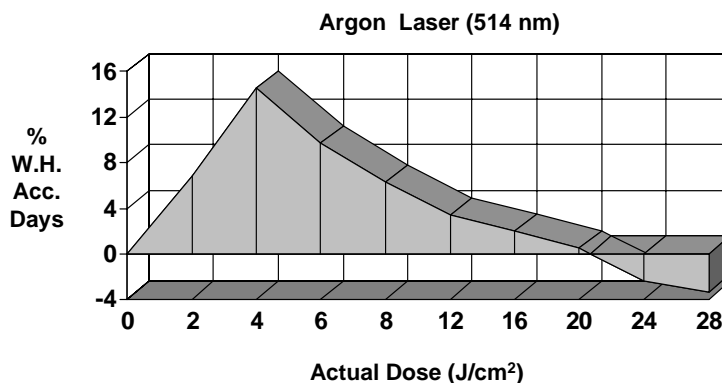

Figure 1: Dose dependency of the acceleration in wound healing days (%) as a function of the computed actual doses of Argon laser (514 nm).

Loss Rate From Plexiglas Cage and Laser Distribution Within Rat's Skin. We determined the loss rate from the Plexiglas cage, which was used to restrain the rats during the experiment, using the different laser wavelengths used in this study, except for the CO_2 laser (10,600 nm) experiment, where laser photons could not transmit through the Plexiglas. (In this case, a special Plexiglas cage with a hole was aligned to the wound area during treatment.) We measured the rate of laser transmission on the rat's skin. A full thickness skin sample was on the outside rim of the integrating sphere power meter, the transmitted power was measured and when the skin was at the base of the integrating sphere, the refection power was measured. We calculated percentages of transmission, reflection, and absorption relative to the incident power and in accordance with the energy conservation principal.

The Actual Dose Calculated for Clinical Laser Treatment. The actual dose D(AC) after correction from incident dose was calculated as follows: D(AC) = D(IN) – D(GL) – D(SR), where D(IN), D(GL), and D(SR) are the incident dose, Plexiglas cage loss dose and skin reflection dose, respectively (Figure 5). The CO_2 laser (10,600nm) calculation for actual dose was calculated as follows: D(AC) = D(IN) – D(SR).

Results and Discussion

The study has indicated that LLLT at the appropriate dosimetric parameters can provide the effect of promoting wound healing. The effect of wound healing acceleration was dependent on the dose, treatment schedule and the wavelength used (Figs. 1, 2 and 3, respectively). The optimum stimulative dose was 4.8 J/cm^2 (computed actual doses are from 3.64 up to 6.21 J/cm^2) (Fig. 4).
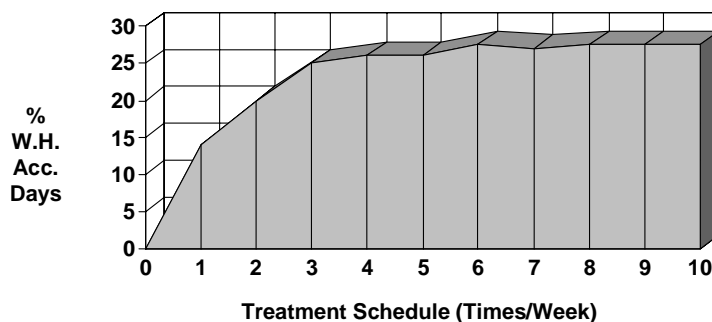
Figure 2: The percentage of acceleration in wound healing days as a function of the treatment schedule for HeNe laser (632 nm).
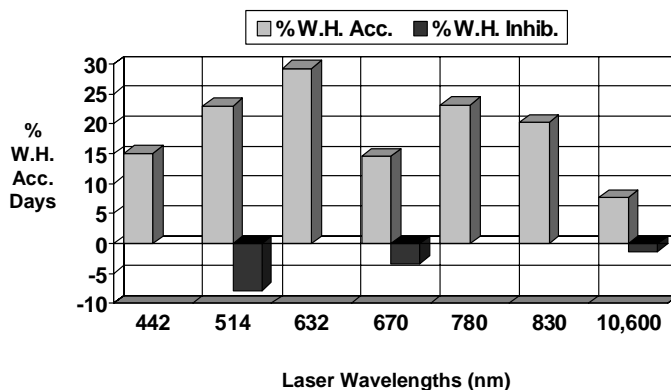

Figure 3: The acceleration percentage in healing days that exemplify wound healing wavelength dependency. Wavelengths 514 nm, 670 nm and 10,600 nm exhibit stimulation and inhibition effects, while 442 nm, 632 nm, 780 nm and 830 nm lasers were not able to reach inhibitory doses due to their low output power, making the treatment time too long and inconvenient.
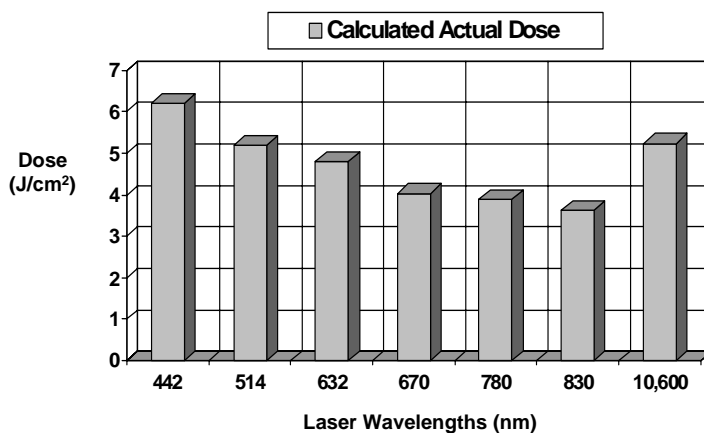

Figure 4: The calculated optimal actual doses for each wavelength for wound healing treatment in rats.

The purpose of computing the actual doses of the various lasers is to show how calculations were done for the purpose of clinical treatment (Fig. 5). Comparing the effects from different lasers showed that the HeNe laser, 632 nm, was the most effective in LLLT for wound healing in rats (Fig. 3) and was also found effective in a human diabetic ulcer (Fig. 7). A study

comparing the HeNe laser, 632.8 nm, with pharmacological agents, Solcoseryl[TM] and Poly-gen[TM] showed that the laser used at 4.8 J/cm^2 actual dose was the best single treatment modality. That is equivalent in its efficacy to the combined laser + Solcoseryl[TM] or laser + Poly-gen[TM] treatment in the enhancement of wound healing in the normal rat (14).

Wound healing acceleration increases with dose until it reaches an optimum actual dose of 4 J/cm^2 (Argon Laser, 514 nm), then a reduction in the stimulatory effect appears, reaching zero-bioactivation at 20 J/cm^2 actual dose, thereafter reaching optimum inhibitory dose of 28 J/cm^2 (Fig. 1). The optimum treatment schedule is 3 times/week, higher appears to show a saturation effect and lower reduces the acceleration in healing days. This may indicate that in-vivo wound healing has no cumulative dosage effect as compared to in-vitro where cumulative laser doses cause bio-stimulation, zero bio-activation then inhibition (15).

The dosimetry of any laser treatment must be considered in two parts. First, the external dosimetry that involves light quantities that are directly controlled by the operator. Second, the internal dosimetry, which involves an attempt to a) determine the light distribution within the tissue, and b) evaluate the relationship between the laser tissue penetration and the effect of wound healing. The rates of transmission and reflection in rat skin were determined using similar lasers. Our results indicate that the laser tissue penetration were dependent on the laser wavelength but were out of proportion to the effects of wound healing (Fig. 3) (16). The reason is unclear why HeNe (632 nm) is the most effective in promoting wound healing, apart from the fibroblast absorption (17) that is highest at this wavelength compared to other wavelengths used in this experiment. There may be additional mechanisms affecting the biostimulative effects of LLLT.

Conclusion

This study has shown that lasers in wound healing is dose-, wavelength-, and treatment schedule-dependent, and that laser tissue penetration was dependent on the laser wavelength but out of proportion to its effect on wound healing.

It has been proposed by Basford (4) that the stimulating mechanism must be a result of properties unique to the laser, i.e. coherency (wavelength in phase) and monochromaticity (single wavelength). The lack of adequate knowledge of how lasers enhance wound healing could delay general acceptance of laser biostimulation in clinical medicine. Wound healing acceleration in rats, Figure 6, and in humans was observed (Fig. 7), together with increases in the rate of ATP (18), DNA, and RNA synthesis (19-20), fibroblast proliferation (21), and collagen synthesis (22) by low power lasers. It is imperative to do more studies to elucidate the mechanisms and foundations of laser biostimulation, particularly at the level of molecular biology and associated research.
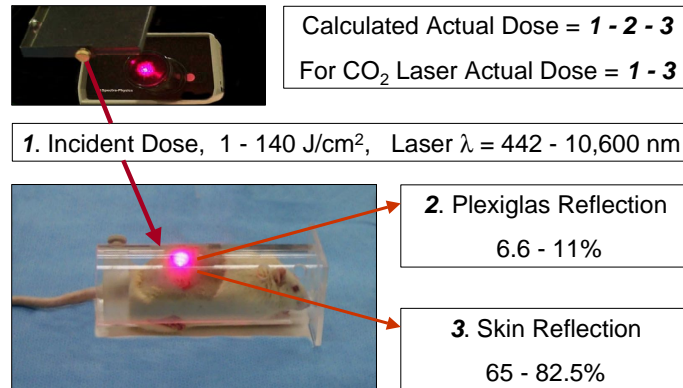
Calculated Actual Dose = **1 - 2 - 3**

For CO_2 Laser Actual Dose = **1 - 3**

1. Incident Dose, 1 - 140 J/cm², Laser λ = 442 - 10,600 nm

2. Plexiglas Reflection
6.6 - 11%

3. Skin Reflection
65 - 82.5%

Figure 5: How the calculations for optimal actual doses for each wavelength were achieved.

Actual Dose: 4.8 J/cm²   Treatment Schedule: 3 times/week
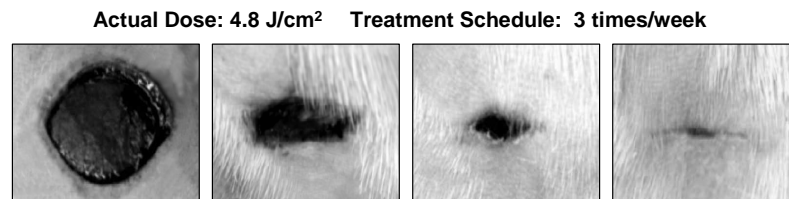

Figure 6A. Oval full-thickness rat wound, 0.39 cm2 at day 1 post wounding.
Figure 6B. Wound contraction at day 4.
Figure 6C. Wound healing at day 8. He-Ne laser-treated group reached 80% wound healing at
7.72 (±0.1) days, while the control group at 10.77 (±0.18) days.
Figure 6D. He-Ne-treated wound closure almost completed at day 12.

Figure 6: The wound healing of 0.39 cm² full thickness rat wound with HeNe laser (632 nm) treatment of 4.8 J/cm², 3 times/week, giving 80% wound healing at 7.72 (±0.18) days while the control at 10.77 (±0.18) days.

Actual Dose: 4 J/cm²   Treatment Schedule: 5 times/week

Figure 7A. The patient was hospitalized for 26 days, but the wound was not responsive to conventional treatment.
Figure 7B. LLLT was initiated using He-Ne laser (632 nm) at 4 J/cm² laser dose and 5 times/week treatment schedule. Granulation tissue is shown to cover the wound from the perimeter toward the center after 15 days of laser treatment.
Figure 7C. Complete wound closure was observed at day 30. *(With permission from Dr. Ali Abaci)*

Figure 7: The wound healing of human diabetic foot ulcer treated with 4 J/cm², 5 times/week with HeNe laser (632nm). Figure 7A shows a diabetic wound ulcer unresponsive to conventional wound healing treatment for 26 days. Figure 7B shows granulation tissue covering the peripheral wound after 15 days of laser treatment. Figure 7C shows full recovery after 30 days.

References

1. Baxter GD, Bell AJ, Allen JM, Ravey J (1991). Low Level Laser Therapy: Current Clinical Practice in the Northern Ireland, Physiotherapy, 77:171-178.

2. McCaughan JS, Bethel BH, Johnston T, Janssen W (1985). Effect of Low-Dose Argon Irradiation on Rate of wound Closure, Lasers Surg Med, 5:607-614.

3. Cummings JP (1985). The Effect of Low Energy (He-Ne) Laser Irradiation on Healing Dermal Wound in an Animal Model, Phys Ther, 65:737.

4. Basford JR, Hallman HO, Sheffield CG, Mackey GL (1986). Comparison of Cold Quartz Ultraviolet, Low-Energy Laser and Occlusion in Wound Healing in Swine Model, Arch Phys Med Rehab, 67:151-154.

5. Mester E, Mester AF (1989). Wound Healing: Laser Therapy, 1:7-15.

6. Surinchak JS, Alago ML, Bellamy RF, Stuck BE, Belkin M (1983). Effects of Low-Level Energy Lasers on the Healing of Full Thickness Skin Defects, Lasers Surg Med, 2:267-274.

7. Jongsma FHM, Bogoard AE, Gemert MJ, Henning GP (1983). Is Closure of open skin Wound in Rats Accelerated by Argon Laser Exposure? Lasers Surg Med, 3:75-80.

8. Hunter J, Leonard L, Wilson R, Snider G, Dixon J (1984). Effects of Low-Energy Laser on Wound Healing in a Porcine Model, Lasers Surg Med, 3:285-290.

9. Colver GB, Priestley GC (1989). Failure of a Helium-Neon Laser to Affect Components of Wound Healing In-vitro, Br Med J, 121:178-189.

10. Al-Watban FAH, Zhang XY (1993). Towards Optimum Dosimetric Parameters for the Effect of Laser Therapy on Wound Healing. Lasers Surg Med, supplement 5:10.

11. O'Kane S (1993). Review of the Biostimulation Session of the 13th Annual Meeting of the ASLMS, Laser Therapy, 6:181-184.

12. Al-Watban FAH, Zhang XY (1994). Laser Biostimulator and Bioinhibitor, Lasers Surg Med, supplement 6:9.

13. Al-Watban FAH, Zhang XY (1995). Stimulative and Inhibitory Effects of Low Power Argon Laser on Wound Healing, Laser Therapy, 7,1.

14. Al-Watban FAH, Andres BL (2000). Effect of He-Ne Laser (632.8 nm) and Polygen on CHO Cells, J Clin Laser Med Surg, 18(3):145-150.

15. Al-Watban FAH, Zhang XY (2000). The Acceleration of Wound Healing is not Attributed to Laser Skin Transmission, Laser Therapy, 1-6.

16. Van Breugel H, Bar P (1992). Power Density and Exposure Time of He-Ne Laser Irradiation are More Important Than Total Energy Dose in Photo-Biomodulation of Human Fibroblasts In-Vitro, Lasers Surg Med, 12: 528-537.

17. Basford JR (1986). Low-Energy Laser Treatment of Pain and Wounds: Hype, Hope or Hokum? Mayo Clin Proc, 61:671.

18. Karu TI, Piatibrat LV, Kalendo GS, Serebriakov NG (1993). Changes in the Amount of ATP in HeLa Cells Under the Action of He-Ne Laser Radiation, Biull Eksp Biol Med, 115: 617-618.

19. Fava G, Marchesini R, Melloni E, et al. (1986). Effect of Low Energy Irradiation by He-Ne Laser in Mitosis Rate of HT-29 Tumor Cells in Culture, Lasers Life Sci, 1:135:141.

20. Karu TI, Kalendo GS, Lebokhov VS, Lobko JJ (1984). Biostimulation of HeLa Cells by Low Intensity Visible Light: Stimulation of DNA and RNA synthesis in a Wide Spectral Range. Il Nuovo Cimento, 3:309-318.

21. Boulton M, Marshall J (1986). He-Ne Laser Stimulation of Human Fibroblast Proliferation and Attchment in Vitro, Lasers Life Sci, 1:125-134.

22. Lam TS, Abergel RP, Meeker CA, et al. (1986). Laser stimulation of Collagen Synthesis in Human Skin Fibroblast Cultures, Laser Life Sci, 1:61-77.

NEAR-FIELD OPTICAL ANALYSIS (NOA) VIA HYDROPHOBIC OPTICAL ELEMENTS AND LOW-INTENSITY LIGHT-ACTIVATED BIOSTIMULATION EFFECT OF NOA

Andrei P. Sommer

University of Ulm, Dept. of Biomaterials, ENSOMA Laboratory,
Ulm, Germany

Introduction

Near-field optical analysis (NOA) is a potentially inoffensive method, predicted to provide time-resolved morphological mappings of soft cell surfaces with resolutions on the nanoscale level (Sommer, 2001). The performance of NOA in imaging unlabeled biosystems with continuous liquid/solid-boundary variations was recently demonstrated at the ENSOMA Laboratory in living cells attached to titanium discs. NOA via near-field scanning optical microscopy (NSOM) has produced the highest optical resolution ever achieved – a method exploiting the energy transfer from the tip of an optical element (tip diameter ≥ 20 nm) oscillating within the characteristic range of the energy transfer ($\sim$10 nm) in the near-field of the sample to be analyzed. Irradiation-induced energy transfer between excited molecules (emitter) and receptor molecules (acceptor), positioned in the proximity of the emitter molecules via spacer molecules, has been confirmed experimentally (Kuhn, 1970). Specific irradiation-induced energy transfer is common to a number of biosystems. In mitochondria, cytochrome c oxidase, a photo-acceptor for monochromatic red to near-IR light (Karu, 1999), could provide energy transfer, discussed as one possible mechanism in low level laser therapy (LLLT). Biostimulatory effects achieved in various biosystems by using non-monochromatic light indicate, however, the action of some unspecific photobiological energy transfer mechanism within these systems.

Methods

In NOA, a molecular assembly is monitored by visible light with a spatial resolution far below the wavelength of visible light. It is important to realize the principal difference between the existing NSOM techniques which could, in principle, be reduced to two basic modes: tapping mode, with tip-oscillations normal, and shear force mode, with tip-oscillations parallel to the surface of the substrate. Both modes have their specific advantages and disadvantages. In biological systems, however, where scanning in a liquid environment is prevalent (e.g. cell cultures) elongated optical elements non-invasively operated in the shear force mode could have some explicit advantages when compared to the contact mode systems. While tapping mode NSOM provides satisfactory nanoscale images even on solid surfaces covered with millimeters of liquids, the performance of shear force mode NSOM is presently largely confined to the investigation of dry sample surfaces exposed to normal atmospheric humidity. NOA of surfaces substantially covered with aqueous liquids, investigated with conventional shear force

mode sensors (optical elements), required the adjustment of the physicochemical interaction parameters (Q-factor adjustment) between sensor and the surrounding liquid medium (Sommer and Franke, 2002). Using hydrophobically coated sensors, topography and NOA images of biological sample surfaces could be obtained – of soft sample surfaces with temporally and spatially variable viscosity gradients in an aqueous milieu, and of rough sample surfaces at air, with resolutions on the nanoscale level.
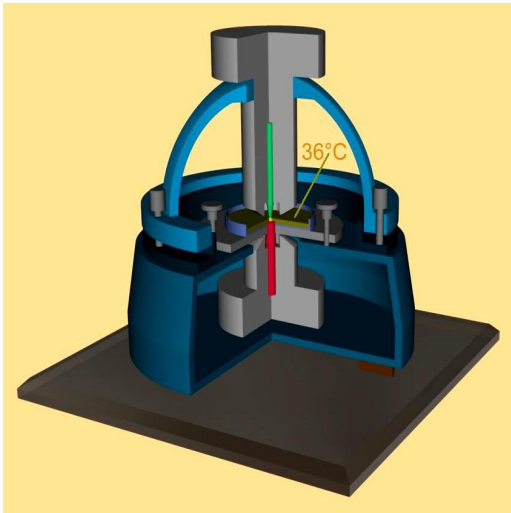

Figure 1: Heart of NOA instrument for in vitro study via 488 nm laser and LILAB via 670 nm laser.
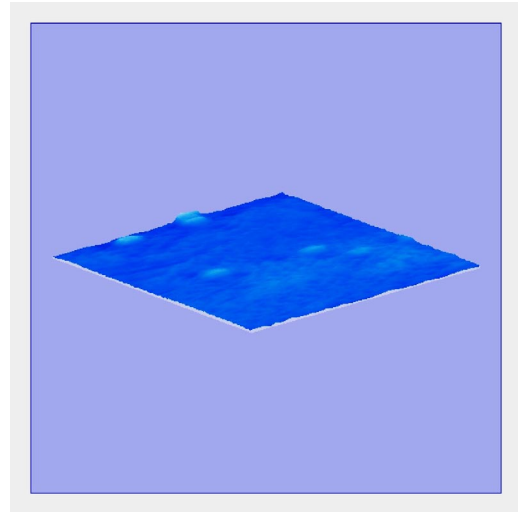

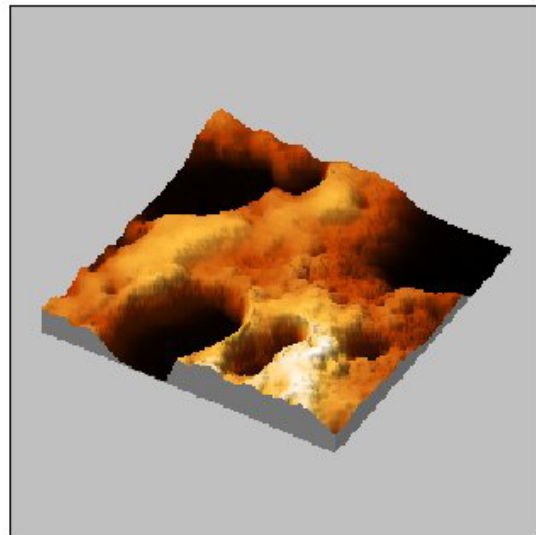**Figure 2**: Nanobacteria isolated by O. Kajander. Scan 8 x 8 μm (NOA).
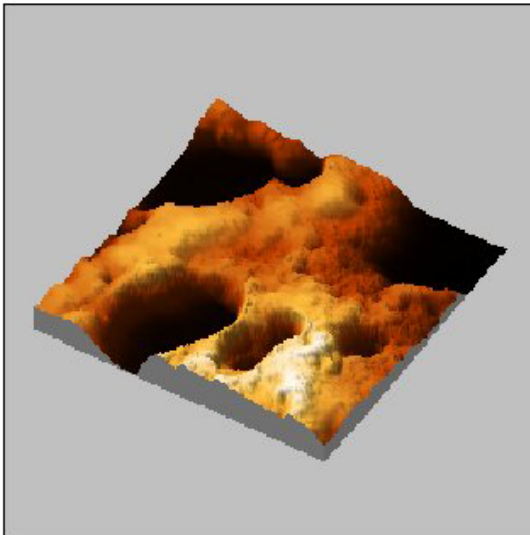

Figure 3: Human dentine; two subsequently scanned 8 x 8 μm areas of the same surface.

Results and Discussion

One of the major results of the present study is the quantitative estimation of the biological effect associated with NOA. NOA of living cells in translucent aqueous media, also in combination with additionally administered light stimulation (Fig. 1) and irradiation parameters adjusted conform to the low-intensity, light-activated biostimulation (LILAB) equation (Sommer et al., 2001), is now expected to facilitate our direct access to the photobiological energy transfer mechanisms of accelerated wound healing processes observed in LLLT, cell functionality, nanoscale characterization of cell/biomaterial-interactions determining biocompatibility in vitro and to the online imaging of light induced biomineralization processes in nanobacteria (Fig. 2) – under terrestrial conditions and possibly in space – a multifaceted field, motivating and reflecting the multidisciplinary composition of the conference.

According to our present knowledge, the performance of shear force mode operations, even on dry samples exposed to air (normal atmospheric humidity), depends on the presence of a liquid like water layer coating and protecting the sample surface to be analyzed (nanoscopic liquid like molecular mask). The protection includes both sides, the fragile tip of the optical element and the sensitive biological substrate beneath (Fig. 3).

NOA requires that laser irradiation coupled into an optical element ending in a nanoscopic tip is transferred in the form of an evanescent field to the molecules at the surface of the sample during scanning at a stable tip/sample-distance of the order of the near-field (~10 nm). Within this range, the radiation field increases sensitively with decreasing tip/sample-distance. It is interesting to estimate the order of the principal irradiation parameters, energy density, and local intensity, for the simplest situation in NOA. The biological impact of NOA on biosystems examined has never been quantified in terms of biological threshold parameters, as done in the LILAB equation (Sommer et al., 2001). With the LILAB-equation, verified to be valid in photobiostimulation in general and in LLLT in particular, we are now in the advantageous position to evaluate possible photobiological effects triggered by the process of observation in NOA. This could be essential in optimizing irradiation parameters (wavelength, intensity and energy density) for biological NOA operations, potentially stimulating the development of biologically harmless nanoscale resolution inspection instruments.

Light/tissue-effects could be divided into several categories, depending on the energy density of the irradiation delivered into the biological target volume. The lowest light/tissue-interaction level is described for 'cold' laser applications in photobiostimulation (Sommer et al., 2001). In contrast to scanner-based LILAB (Sommer, 2000), the cellular surface being scanned for NOA receives near-field irradiation locally only once per scan. Thus, the local light intensity is of central interest. It is instructive to assess possible biological effects of the laser irradiation on the investigated cells versus the thermal effects of the light on the optical element itself. In metal-coated optical elements, the factor limiting the laser power coupled into the optical element is the temperature increase of the metal (e.g. aluminum).

Several reports exist describing a melting of the metal coating. These observations do not necessarily contradict reports of no evident damage in biological samples investigated via NSOM (Betzig et al., 1993). The estimated local intensity (I_{noa}) stemming from near-field light in NOA is about 10^3 higher than the local light intensity (I_{stim}) values applied in LLLT (Sommer et al., 2001). For optical elements with a tip diameter of about 30 nm, the associated linear scan velocity v_s ($v_s \sim 10$ µm/s) allows an estimate of the local duration of the light stimulus Δt delivered by the tip of the optical element onto the sample: $\Delta t \sim 3$ms. Surprisingly, the corresponding activating energy density value is with $(E/a)_{act} \sim 4 \times 10^4$ J/m^2 well within the accepted Arndt-Schultz-range. The primary light parameter potentially influencing the temperature of the sample is the actual energy density and not the local intensity. Here again, we could profit from the LLLT experiences, where practically no temperature effects have been reported for doses of the order of 4×10^4 J/m^2.

Establishing contact between LLLT and NOA (Sommer, 2001) could be fruitful for the reversed situation too, offering a novel route to the explanation of photobiological mechanisms assumed to occur in LLLT. Reproducible biostimulatory effects achieved in various biosystems using one solitary wavelength, the synergistic cooperation of two wavelengths, or non-monochromatic light for activation indicated, however, the action of some unspecific photobiological energy transfer mechanism in these systems. Interestingly, the energy transfer mechanism observed to occur in molecular systems (Kuhn, 1970), which has been successfully converted into NOA technologies, could represent one original mechanism for processes in which visible to near-IR light is coupled into biosystems – in primordial submicroscopic manifestations of life and in more complex forms containing mitochondria. Considering mitochondria, nanostructured molecular clusters within the organized membranes, or matrix components, having the proper size and dielectric structure, could serve as unspecific antennas (far-field acceptors) for propagating light penetrating locally at intensities required for the transfer of energy and activation of specific photoreceptors within the near-field of the far-field acceptors. In analogy to the radiation transfer in molecular systems, the light energy (hν) transferred in biosystems is expected to depend sensitively on the particular distance between the correlated receptors: the unspecific antennas and specific photoreceptors in their near-field. Thus, different light wavelengths could induce approximately the same quantity of energy, as suggested by laboratory experiments in which biosystems responded with identical reactions to their stimulation with different laser wavelengths. The proposed biophysical radiation transfer mechanism does not represent a paradigm change; it offers, complementary to existing photonic models, a simple explanation for the observed spectral insensitivity of a significant body of biosystems, presumably also accounting for the recent results of light-induced proliferation of nanobacteria.

Conclusion

NOA in vitro requires understanding the physicochemical interaction between the optical elements and the nanoscopic liquid-like molecular mask coating the surface of the

cells, and the estimation of the biological impact of the near-field light coupled into the cells. Regarding the first problem, we have made one considerable step forward by implementing hydrophobic optical elements in combination with biostandards for validation (dentin and nanobacteria). We could resolve the second problem by adjusting the irradiation parameters for NOA in vitro to the parameters employed in the LILAB-equation, exploiting valuable photobiological data presented at this conference. LLLT is clearly separating between the photobiological thresholds, activating energy density and local intensity. The quantitative interplay of these parameters, as described by the LILAB-equation, appears to be relevant for understanding and performing NOA in living biosystems, allowing minimizing possible disturbances induced by the process of observation. NOA in vitro, focusing on the nanoscale characterization of cell responses to different stimuli, including additionally applied photobiostimulation, has started now at the ENSOMA Laboratory. Apparently, the combination NOA–LLLT is bilaterally beneficial: while LLLT could stimulate optimization of the irradiation parameters in NOA, the physical energy transfer mechanism which facilitated NOA technologies could apply to photobiological processes in different forms of life. It is worth noting that, for billions of years, all aerobic forms of terrestrial life have been exposed to solar irradiation of an intensity of the order of ~ 1000 W/m^2. Observing that systems as different as nanobacteria and those containing mitochondria react to photobiostimulation, the hypothesis of a common photobiological mechanism appears promising. The hypothesis receives additional support from the observation that the most pronounced biostimulatory effects could be realized in nanobacteria with irradiation parameters (intensity, dose) in the order of the variables found to be effective in clinical light applications, e.g. wound healing. The therapeutic potential of reliable photobiological mechanisms is enormous, reaching from the predictability of novel indications to advance and an improved level of acceptance in LLLT. Little is known about the precise nature of unspecific emitter/receptor-systems: multidisciplinary collaborations working on the physical, chemical, and biological identification and on the modeling of nanostructured photoreceptors in photosensitive biosystems are recommended. Starting here could be favorable to stimulate the progress in the field.

References

Betzig, E., Chichester, R.J., Lanni, F., and Taylor, D.L., (1993); Near-Field Fluorescence Imaging of Cytoskeletal Actin, Bioimaging, 1, 129-135.

Karu, T., (1999); Primary and secondary mechanisms of action of visible to near-IR radiation on cells, J. Photochem. Photobiol. B, 49 (1), 1-17.

Kuhn, H., (1970); Classical Aspects of Energy Transfer in Molecular Systems, J. Chem. Phys. 33 (1), 101-108.

Sommer, A.P., (2001); Components for Near-Field Optical Analysis of Biosystems at Nanoscale Resolution, Proc. 1st International Conference on Near-Field Optical Analysis, Castle Reisensburg, Germany, Nov. 4-7, 2000, Sommer, A.P., (ed), J. Clin. Laser Med. & Surg., 19 (2), 112.

Sommer, A.P., (2000); Beam distributor for lasers, Patent Nr. 4308474, Germany, March 1993.

Sommer, A.P., and Franke, R.P., (2002); Hydrophobic Optical Elements for Near-Field Optical Analysis (NOA) in Liquid Environment – a preliminary study, Micron 33, 227-231.

Sommer, A.P., Pinheiro, A.L.B., Mester, A.R., Franke, R.P., and Whelan, H.T., (2001); Bio-stimulatory Windows in Low-Intensity Laser Activation: Lasers, Scanners, and NASA's Light-Emitting Diode Array System, J. Clin. Laser Med.& Surg., 19 (1), 29-33.

EFFECT OF NASA LIGHT-EMITTING DIODE ON WOUND HEALING ABOARD SUBMERGED SUBMARINES

Jim Caviness[1], Julio Esquilin[2], Harry Whelan[3]

[1]Undersea Medical Officer, U.S. Navy Submarine Squadron Eleven
[2]Hospital Corpsman First Class, U.S. Navy USS Salt Lake City SSN 716
[3]M.D., Medical College of Wisconsin

Introduction

It is an accepted condition of service aboard U.S. Navy submarines that wounds, burns, and lacerations heal more slowly during submerged operations at sea than they would normally heal if not on board the submarine. This phenomenon is not understood, nor has it been studied. The submarine environment is complex, but differs significantly from normal atmosphere in several key areas. The total atmospheric pressure is typically elevated, but at times may actually be reduced, the partial pressure of oxygen is reduced, while the partial pressure of carbon dioxide is elevated, and there is the complete absence of sunlight. Additional confounding variables are the numerous atmospheric contaminants produced by the various mechanical and electrical systems on board. Similar anecdotal reports of delayed wound healing aboard U.S. spaceflights demonstrate that the environment of an artificial atmosphere alters the role of wound healing. Space differs from the undersea environment do to the absence of gravity, but otherwise the atmospheric conditions are similar with respect to sunlight, O2, and CO2. Our supposition is that the decreased amount of oxygen and increased amount of carbon dioxide result in a delay in the normal progression of wound healing.

Research has shown that hypoxia actually plays a role in the stimulus of initial wound healing (Anderson 1995), but recently it has been shown that the initial upregulation of proalpha collagens decreases after continued hypoxic exposure past the initial 24 hours (Steinbrech 1999, Yamanaka 2000). Chronic hypoxia resulted in inhibition of epithelial and connective tissue elements, as well as suppression of collagenogenesis in skin (Khomullo 1986). Using a rabbit model, hypoxic wounds were shown to heal more quickly at SUBatmospheric pressures. (Fabian 2000). Also using a rabbit model, Stillman demonstrated decreased rate of wound healing for hypoxia, increased wound healing for hyperoxia, using inspired oxygen of 14, 21, and 41% (all normobaric). Kivisaari et al. demonstrated that breathing 11% O2 resulted in retardation of collagen, decreased capacity for glucose utilization, decreased oxygen consumption, and lower levels of ADP and ATP (Kivisaari 1975).

Based on prior research by Harry Whelan, the NASA light-emitting diode (LED) dramatically increased the rate of wound healing in a rat model under normal atmospheric conditions (Whelan 2001). Based on our observations of wounds aboard submarines, the differences in atmospheric conditions aboard the submarine, and the demonstrated

ability of the LED to speed the rate of healing, we hypothesized that using the LED for wounds aboard the submarine would increase the rate of healing.

Methods

Two submarines were selected to test our hypothesis. The first, USS Jefferson City, would serve as control. All wounds, burns, and lacerations would be digitally photographed (set focal point or with ruler adjacent to wound to enable comparison of wound surface area as the wound closed) and would be given standard care for wounds – debridement, irrigation, suturing, topical antibiotic, dressings, as indicated. The second submarine, USS Salt Lake City would serve as the experimental group. Wounds would receive the same standard care, and digital photography, but additionally receiving daily $4J/cm^2$ LED treatment of the wound. The LED device, produced by Quantum Devices, produces non-thermal light at 670, 735, and 880 nm. The protocol was to include all wounds that occurred when the submarine was submerged for at least 10 days following the wound. Exposure to normal atmosphere – whether by arrival at port or simply travelling on the surface of the ocean, rather than submerged, would terminate a given trial of LED use.

Results and Discussion

During the 6 months the NASA LED was on board, there were few injuries to personnel, and only one that met the required 10-day period of being submerged. This wound corresponded nicely in size and location to a similar control wound. Two other wounds did not meet the 10-day period, but again had similar control wounds for comparison. Digital photos were analyzed by the laboratory of Harry Whelan, using NIH image scan. Photos were analyzed for decrease in wound surface area over time, increase in granulation tissue over time, and percent of complete wound edge approximation and epithelialization over time in the case of lacerations. Two other lacerations were followed for 3 days, but then the submarine returned to normal atmospheric conditions, and the LED use was terminated. They were still compared to a control laceration of similar size for that initial 3-day post-injury period. Computer analysis of the digital photos indeed demonstrated enhanced healing in the LED group. The observation made by the hospital corpsman on board, who has made several 6 month deployments on submarines, was that the LED markedly increased the rate of wound healing for injuries suffered while submerged. The actual analysis of the photographs showed 40% faster healing for the injury treated for 10 days, but due to the low number of cases (1), this is not statistically significant.

Tables 1, 2, and 3 show the atmospheric values for both the control and experimental group (LED) submarines, for the days that wounds were photographed. Figures 1-28 show the side-by-side comparison of the LED versus control wound over the treatment period.

Table 1: Atmosphere Data Case 1

	LED			CONTROL		
	ATM	O2	CO2	ATM	O2	CO2
Day 1	712	142	3.6	750	150	3.7
Day 2	717	139	2.7	800	150	3.9

Figure 1: Case 1 Day 1 LED patient.

Figure 2: Case 1 Day 1 control wound.

Figure 3: Case 1 Day 2 LED patient.

Figure 4: Case 1 Day 2 control wound.

Figures 1-4: Case 1 LED and control wounds treated for 2 days before exposure to ambient air and sunlight.

Table 2: Atmosphere Data Case 2

	LED			CONTROL		
	ATM	O2	CO2	ATM	O2	CO2
Day 1	719	142	3.6	750	150	3.7
Day 2	717	139	2.7	800	150	3.9

Figure 5: Case 2 Day 1 LED patient.

Figure 6: Case 2 Day 1 control wound.

Figure 7: Case 2 Day 2 LED patient.

Figure 8: Case 2 Day 2 control wound.

Figures 5-8: Case 2 LED and control wounds treated for 2 days before exposure to ambient air and sunlight.

Figure 9: Case 3 Day 1 LED patient.

Figure 10: Case 3 Day 1 control wound.

Figure 11: Case 3 Day 2 LED patient.

Figure 12: Case 3 Day 2 control wound.

Figure 13: Case 3 Day 3 LED patient.

Figure 14: Case 3 Day 3 control wound.

Figure 15: Case 3 Day 4 LED patient.

Figure 16: Case 3 Day 4 control wound.

Figure 17: Case 3 Day 5 LED patient.
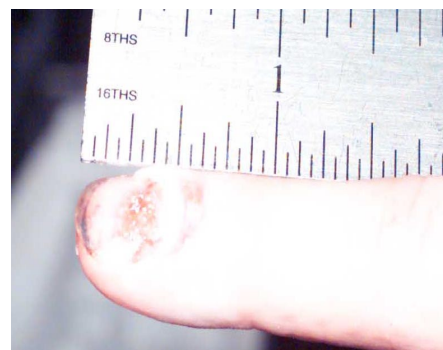
Figure 18: Case 3 Day 5 control wound.
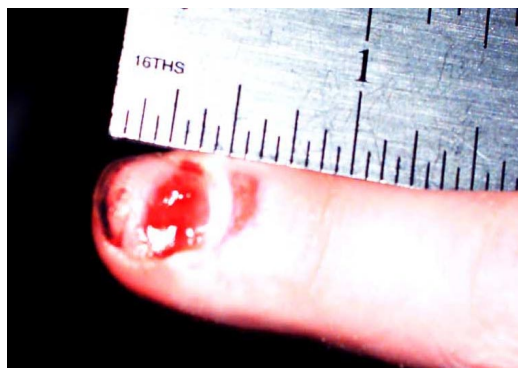
Figure 19: Case 3 Day 6 LED patient.

Figure 20: Case 3 Day 6 control wound.

Figure 21: Case 3 Day 7 LED patient.

Figure 22: Case 3 Day 7 control wound.

Figure 23: Case 3 Day 8 LED patient.
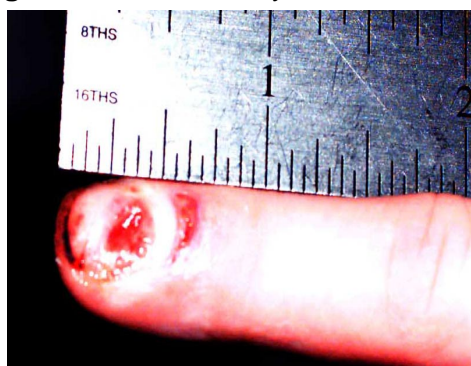

Figure 24: Case 3 Day 8 control wound.

Figure 25: Case 3 Day 9 LED patient.

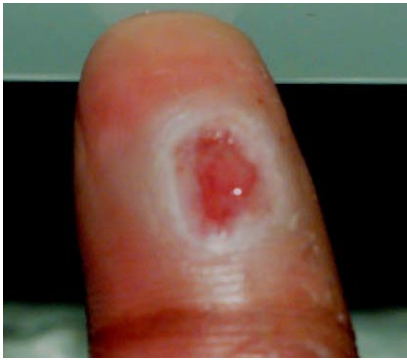**Figure 26**: Case 3 Day 9 control wound.

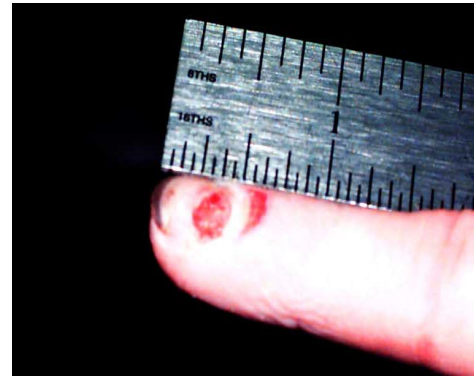**Figure 27**: Case 3 Day 10 LED patient.

Figure 28: Case 3 Day 10 control wound.

Figures 9-28: Case 3 LED and control laceration of similar size and location treated daily.

Table 3: Atmosphere Data Case 3

	LED			CONTROL		
	ATM	O2	CO2	ATM	O2	CO2
Day 1	710	144	3.4	759	145	4.2
Day 2	675	136	2.8	778	148	4.1
Day 3	710	143	4.1	773	147	3.0
Day 4	705	142	3.6	767	145	4.3
Day 5	735	142	3.6	763	143	3.1
Day 6	674	132	2.7	760	159	1.0
Day 7	706	132	3.2	760	159	1.0
Day 8	740	140	3.5	760	159	1.0
Day 9	706	131	3.0	760	159	1.0
Day 10	761	155	1.5	760	159	1.0

Conclusion

We did not have enough injuries to constitute a group of sufficient size to demonstrate statistical significance. Anecdotally, the effect of the LED on wound healing was noticeable to the submarine's hospital corpsman. The delay in wound healing aboard submarines has been widely observed but not studied. Replicating the submarine environment for animal model wound healing experiments would be cost-prohibitive. Technology cannot currently eliminate the differences in environmental conditions that exist aboard submarines, which means sailors injured at sea will continue to have slower healing. Further evaluation of the LED aboard deployed submarines is warranted to determine if this technology should be a routine piece of submarine medical equipment.

References

Kivisaari J, Niinikoski J. "Effects of hyperbaric oxygenation and prolonged hypoxia on the healing of open wounds." Acta Chir Scand 1975; 141(1): 14-19.

Kivisaari J, et al. "Energy metabolism of experimental wounds at various oxygen environments." Ann Surg 1975 Jun; 181(6):823-8.

Fabian TS, et al. "The evaluation of subatmospheric pressure and hyperbaric oxygen in ischemic full-thickness wound healing." Am Surg 200 Dec; 66(12): 1136-43.

Steinbrech DS, et al. "Fibroblast response to hypoxia: the relationship between angiogenesis and matrix regulation." J Surg Res 1999 Jun 15: 84(2): 127-33.

Yamanaka M, Ishikawa O. "Hypoxic conditions decrease the mRNA expression of proalpha (I) and (III) collagens and increase matrix metalloprotienases-1 of dermal fibroblasts in three-dimensional cultures." J Dermatol Sci 2000 Nov; 24(2): 99-104.

Anderson GR, et al. "The anoxic fibroblast response is an early-stage wound healing program." J Surg Res 1995 Dec; 59(6): 666-74.

Khomullo GV, et al. "Effect of hypoxia on DNA synthesis and collagen levels in regenerating skin." Kosm Biol Aviakosm Med 1986 May-Jun; 20(3): 57-61.

Whelan HT, Smits RL, Buchmann EV, Whelan NT, Turner SG, Margolis DA, Cevenini V, Stinson H, Ignatius R, Martin T, Cwiklinski J, Philippi AF, Graf WR, Hodgson B, Gould L, Kane M, Chen G, Caviness J: Effect of Light-Emitting Diode (LED) Irradiation on Wound Healing. Journal of Clinical Laser Medicine and Surgery. 2001;19:305-314.

REPORT DOCUMENTATION PAGE

Form Approved
OMB No. 0704-0188

1. AGENCY USE ONLY *(Leave Blank)*	2. REPORT DATE October 2002	3. REPORT TYPE AND DATES COVERED NASA Conference Publication

4. TITLE AND SUBTITLE
Second International CONFERENCE ON Nearfield Optical Analysis: Photodynamic Therapy & Photobiology Effects

5. FUNDING NUMBERS

6. AUTHOR(S)
Dennis Morrison

7. PERFORMING ORGANIZATION NAME(S) AND ADDRESS(ES)

Lyndon B. Johnson Space Center
Houston, Texas 77058

8. PERFORMING ORGANIZATION REPORT NUMBERS
S-896

9. SPONSORING/MONITORING AGENCY NAME(S) AND ADDRESS(ES)

National Aeronautics and Space Administration
Washington, DC 20546-0001

10. SPONSORING/MONITORING AGENCY REPORT NUMBER
CP-2002-210786

11. SUPPLEMENTARY NOTES

12a. DISTRIBUTION/AVAILABILITY STATEMENT

Available from the NASA Center for AeroSpace Information (CASI)
7121 Standard
Hanover, MD 21076-1320   Subject Category: 54

12b. DISTRIBUTION CODE

13. ABSTRACT *(Maximum 200 words)*

The International NASA/DARPA Photobiology Conference held at the Johnson Space Center in Houston/TX demonstrated where low level laser therapy (LLLT), respectively low intensity light activated biostimulation (LILAB) and nanotechnological applications employing photobiomodulation techniques will presumably go in the next ten years. The conference was a continuation of the 1st International Conference on Nearfield Optical Analysis organized by Andrei Sommer (ENSOMA Lab, University of Ulm, Germany) in November 2000 at Castle Reisensburg, Germany, which started with a group of ten scientists from eight different countries. The 1st conference was co-sponsored by the American Chemical Society to evaluate the molecular mechanism of accelerated and normal wound healing processes. The 2nd conference was co-sponsored by DARPA, NASA-JSC and the Medical College of Wisconsin. Despite the short time between events, the 2nd conference hosted 40 international experts from universities, research institutes, agencies and the industry. The materials published here are expected to become milestones forming a novel platform in biomedical photobiology. The multidisciplinary group of researchers focused on LLLT/LILAB-applications under extreme conditions expected to have beneficial effects particularly in space, on submarines, and under severe battlefield conditions. The group also focused on novel technologies with possibilities allowing investigating the interaction of light with biological systems, molecular mechanisms of wound healing, bone regeneration, nerve regeneration, pain modulation, as well as biomineralization and biofilm formation processes induced by nanobacteria.

14. SUBJECT TERMS

biostimulation; photbiology; laser therapy; nanotechnology; nanobacteria; biomineralization; biofilm; biological systems; molecular; biology

15. NUMBER OF PAGES

105

16. PRICE CODE

17. SECURITY CLASSIFICATION OF REPORT	18. SECURITY CLASSIFICATION OF THIS PAGE	19. SECURITY CLASSIFICATION OF ABSTRACT	20. LIMITATION OF ABSTRACT
Unclassified	Unclassified	Unclassified	Unlimited